Isolation and identification of secondary metabolites from the fungus *Phomopsis* spp., a pathogen responsible for vine excoriosis

Thèse présentée à la Faculté des Sciences
Institut de Chimie
Université de Neuchâtel

Pour l'obtention du grade de docteur ès sciences
Par

Nicolas MOTTIER

Chimiste diplomé de l'Université de Genève

Acceptée sur proposition du jury:

Prof. Raffaele Tabacchi, directeur de thèse	Université de Neuchâtel
Dr. Eliane Abou-Mansour	Université de Neuchâtel
Dr. Brigitte Mauch-Mani	Université de Neuchâtel
Dr. Andrew Marston	Université de Genève
Dr. Olivier Viret	Agroscope Changins

Soutenue le 19 Août 2005

Université de Neuchâtel
2005

Isolement et identification de métabolites secondaires du champignon *Phomopsis* spp., un pathogène responsable de l'excoriose de la vigne

Thèse présentée à la Faculté des Sciences
Institut de Chimie
Université de Neuchâtel

Pour l'obtention du grade de docteur ès sciences
Par

Nicolas MOTTIER

Chimiste diplomé de l'Université de Genève

Acceptée sur proposition du jury:

Prof. Raffaele Tabacchi, directeur de thèse	Université de Neuchâtel
Dr. Eliane Abou-Mansour	Université de Neuchâtel
Dr. Brigitte Mauch-Mani	Université de Neuchâtel
Dr. Andrew Marston	Université de Genève
Dr. Olivier Viret	Agroscope Changins

Soutenue le 19 Août 2005

Université de Neuchâtel
2005

Université de Neuchâtel

IMPRIMATUR POUR LA THESE

Isolation and identification of secondary metabolites from the fungus *Phomopsis* spp., a pathogen responsible for vine excoriosis

Nicolas MOTTIER

UNIVERSITE DE NEUCHATEL

FACULTE DES SCIENCES

La Faculté des sciences de l'Université de Neuchâtel,
sur le rapport des membres du jury

Mmes B. Mauch-Mani, E. Abou-Mansou,
MM. R. Tabacchi (directeur de thèse),
O. Viret (Changins)
et A. Marston (Genève)

autorise l'impression de la présente thèse.

Neuchâtel, le 14 novembre 2005

Le doyen :

J.-P. Derendinger

Faculté des Sciences
■ Rue Emile-Argand 11 ■ CP 2 ■ CH-2007 Neuchâtel
■ Téléphone : +41 32 718 21 00 ■ Fax : +41 32 718 21 03 ■ E-mail : secretariat.sciences@unine.ch ■ www.unine.ch

Remerciements

Je voudrais remercier le Prof. R. Tabacchi pour m'avoir donner l'opportunité d'accomplir ce travail de recherche dans son groupe et pour la liberté et la confiance qu'il m'a accordé.
Je voudrais aussi remercier les membres du jury le Dr B. Mauch-Mani, Dr E. Abou-Mansour, Dr A. Marston et Dr O. Viret pour avoir accepté de lire et réviser le présent travail et pour l'intérêt qu'ils y ont porté.
Je tiens à remercier aussi D. Christen pour nous avoir fourni les souches du champignon ainsi que le Dr. D. Job et son groupe pour m'avoir permis d'utiliser son laboratoire de l'institut de Biologie. Merci aussi à Mr. F. Fehr de l'Université de Fribourg pour avoir si bien fait les analyses de RMN 500 MHz et H. Bursian pour l'analyse des composés par RMN 400 Hz.

Un grand merci a Camille Perret qui m'a accueilli dans le groupe et qui a eu le temps et la patience pour m'apprendre à utiliser l'HPLC et la masse ainsi que pour sa gentillesse.
Merci aussi à Manuel Tharin pour ses bougonnements légendaires et grâce à qui j'ai pu découvrir les parties les plus secrètes des HPLC et qui m'a accueilli dans mon nouveau travail.
Un merci tout particulier à Eliane pour son aide, sa patience, sa disponibilité et ses conseils durant toute cette thèse.
Un grand merci aussi à Jules pour la bonne ambiance qu'il aura amené dans le labo, son aide et sa patience avec la RMN et les conseils pour les purifications ainsi que pour les explications sur les différents types de Zouk. Merci aussi à Marie-Lorène Goddard pour son travail précurseur sur le champignon.
Un grand merci aussi à Nathalie et David, Florence, Julie Brettar, Julie Lenoble, Sabine, pour leur encouragements et leur soutient et à Blaise pour les sorties à skis annuelles qui se sont toujours déroulées les moustaches frétillantes.
Un grand merci aux membres présent et passé du groupe, Emmanuel, Sandrine, Laura, Bernard, Mustapha, Josée, Mélanie, Sabine et à tous les membres de l'Institut, doctorants ou étudiants, trop nombreux pour tous les citer ici.

Un grand merci à ma famille, mes parents, mon frère et la famille outre-manche, pour leur soutient tout au long de ces longues années d'études.
Finalement merci à Cristina pour sa patience, sa bonne humeur, ses encouragements incessants et son amour.

Glossary

1, 2, 3… :	Symbols used for the compounds isolated in this work
ACN:	Acetonitrile
API:	Atmospheric Pressure Ionisation (MS)
Apical:	Apex or tip of something (pl. apices)
APCI:	Atmospheric Pressure Chemical Ionisation (MS)
APPI:	Atmospheric Pressure Photo-Ionisation (MS)
Apressed:	Pressed closed to or lying flat against something.
ATP:	Adenosine triphosphate
Buff:	pale yellow-brown colour
COSY:	Correlated spectroscopy (^{1}H NMR)
Cyrrhi:	Jelly made of conidia released by the ostiole of pycnidia.
Conidia:	Generic term referring to a spore produced in vegetative reproduction of a fungus and located on sporulating blotches. Conidia are produced and borne by specialized mycelial hyphae called conidiophores
Da:	Dalton
DAD:	Diode-array detector
DEPT:	Distortion enhancement by polarisation transfer (^{13}C NMR)
EtOAc:	Ethyl acetate
ESI:	Electrospray Ionisation (MS)
EI:	Electron Impact Ionisation (MS)
Guttule:	small drop; spot like small drop
HMBC:	Heteronuclear multiple bond correlation spectroscopy (^{1}H-^{13}C NMR)
HPLC:	High-Performance liquid chromatography
Hyaline:	Transparent, glassy or vitreous
J:	Coupling constant (Hz)
LC-MS:	High-Performance liquid chromatography coupled to mass spectrometry
MeOH:	Methanol
Mycelium:	Microscopic filaments of the vegetative system of fungi which make a thick network.
MW:	molecular weight (in Da) (MS)

m/z:	mass to charge ratio (MS)
NMR:	Nuclear magnetic resonance
Ostiole:	Small opening, pore.
PDA:	Potato dextrose agar
q:	quadruplet (NMR)
Pycnidia:	A rounded, or flask-shaped, asexual fungal fructification that produces conidia (pycnidiospores) characteristic of the imperfect stages of some fungi and of one main group of the Fungi Imperfecti.
s:	singlet (NMR)
sp:	unspecified species
Spore:	A small, usually microscopic, reproductive cell, either sexual or asexual, used for its own preservation and spread.
Teleomorph:	Describes a fungus that reproduces sexually (as opposed to anamorph)
TLC:	Thin-layer chromatography
t :	triplet (NMR)
Umbonate:	An umbo is a softly curved bump in a flat cap of a mushroom. A cap with an umbo is said to be umbonate
UV:	Ultra-violet

Table of contents

Abstract

Grapevine diseases are of great importance as they affect production and harvesting causing serious yield loss. The amount of damage or loss is often dependant on the climate of the region and the cultural practices of the grape growers. Control of these diseases is generally done using fungicide sprays and management techniques such as leaf plucking, pruning, etc. Epidemics do occur from time to time when even the most rigorous management cannot control the disease because of favourable weather conditions.

One usually differentiates trunk and root diseases, e.g. Eutypa dieback and esca, from fruit and foliar diseases such as downy mildew, powdery mildew and grey rot. Grapevine trunk diseases are responsible for significant economic losses to the wine industry worldwide. Symptoms of these diseases include dead spurs, arms and shoots and eventual vine death due to canker formation in the vascular tissue. In Eutypa dieback, deformed leaves and shoots occur as the pathogen invades the ramifications. As cankers develop, yield reductions occur due to the loss of productive wood. The impact of grapevine wood diseases usually becomes more severe as vineyards get older until they weaken and eventually kill vines. Foliage and developing bunches must also be protected from attack by various pests, especially fungal pathogens, for the production of satisfactory yields of good-quality grapes, and especially for adequate vinification.

To maintain economic production it is essential to use specific fungicides and correct application of plant protection products. However, the chemicals used can be non specific or used on a large scale at the wrong time either in the absence of the inoculum of the pathogen or under conditions that are not favourable for the disease development. Thus, the inappropriate use of these products with the increased realisation of environmental issues has lead to the need for growers and managers to adopt responsible and intelligent disease management systems. Understanding of grapevine diseases and their causal agents is vital as it can bring precious information for alternative pathways in management of the pathogens.

Since 1986, grapevine diseases have been one of the main fields of research of the group of Professor R. Tabacchi with works published on esca, eutypa dieback, gray rot and downy mildew. The following project is the continuation of this research with the study of a worldwide spread disease, excoriosis or Phomopsis cane and leaf spot.

This disease is caused by a fungus called *Phomopsis viticola* which can cause serious damage when weather conditions are suitable. The main symptoms are necrotic lesions on canes and shoots, black spots on leaves and, rarely, fruits.
In collaboration with the group of Professor G. Défago of the Swiss Federal Institute of Technology, twelve strains of the fungus were collected from a grapevine field in Ticino, Switzerland. After growing the fungi on an artificial media, chemical metabolites were profiled using high-performance liquid chromatography and biological assays against grapevine leaf disks were performed. We decided to upscale the culture and study further three of the strains. Using the modern current separation and identification techniques, such as HPLC-UV and 1D and 2D NMR, we isolated several secondary metabolites produced by the fungus.
Furthermore, the fungus was grown on grapevine wood pruned after harvest in order to have culture conditions as close to reality as possible. As detection of the metabolites in the wood must allow for low detection limits, LC-(API)-MS was the method of choice for this research.

Keywords

Excoriosis; *Phomopsis viticola*; secondary metabolites; xanthone; phomopsolide B; furanone; cytosporone; sterol.

Résumé

Les maladies de la vigne sont d'une grande importance car elles affectent la production et les récoltes causant de sérieuses pertes. Le dommage causé est souvent dépendant du climat de la région ainsi que des habitudes de culture des vignerons. Le contrôle de ces maladies est généralement fait par l'utilisation de fongicides et par d'autres techniques de gestion qui n'empêchent pas l'apparitions d'endémies de temps à autre, dûs notamment à des conditions climatiques qui favorisent les maladies. On différencie les maladies du bois, comme par exemple, l'eutypiose et l'esca, des maldies foliaires comme le mildiou ou la pourriture grise. Les maladies du bois sont responsables de pertes économiques significatives pour l'industrie vinicole dans le monde entier. Les symptômes de ces maladies sont le brûnissement des rameaux, pétioles et vrilles, le jaunissement des feuilles et éventuellement la mort de la vigne à cause de la formation de chancres dans le système vasculaire de la plante. Pour l'eutypiose et l'esca, au fur et à mesure que les pathogènes envahissent les ramifications, le chancre se développe et le rendement de la vigne baisse à cause de la perte de bois productif.

Pour maintenir une production rentable, il est essentiel d'appliquer correctement les produits de protection. Toutefois, ils ne sont pas spécifiques ou peuvent être mal utilisés c'est-à-dire en l'absence de l'inoculum du pathogène où quand les conditions pour sont développement ne sont pas favorables. Ainsi, l'usage inapproprié des ces produits ainsi que les problèmes environnementaux liés à leurs usages font que le vignerons doivent apprendre à connaître les maladies et leur agent causal afin de trouver des moyens alternatifs pour leur gestion.

Depuis 1986, le groupe du Prof. R. Tabacchi s'est intéressé aux maladies de la vigne avec des travaux de recherche publiés sur l'esca, l'eutypiose, la pourriture gris et le mildiou. Ce projet en est la continuation avec l'étude d'une maladie répandue à travers le monde, l'excoriose. Cette maladie est causée par un champignon, *Phomopsis viticola*, qui peut cause des dommages sérieux lorsque les conditions climatiques sont favorables. Les symptômes sont l'apparition de nécroses sur les rameaux et de point noirs sur les feuilles et parfois sur les fruits.

En collaboration avec la Prof. G. Défago de L'EPFZ, douze souches de l'espèce *Phomopsis* on été collectées d'un vignoble au Tessin, en Suisse. Après avoir cultivé le champignon sur un milieu artificiel, les extraits bruts ont été analysés par chromatographie liquide à haute performance et trois des souches ont été choisies pour un étude plus approfondie. Les extraits

bruts de ces trois souches ont permis l'isolement et l'identification de métabolites secondaires produit par le champignon en utilisant les méthodes modernes de la chimie analytique comme la LC-MS^n et la RMN en une et deux dimensions. La LC-MS a aussi permis l'analyse des extrait de culture du champignon isolés directement du bois de vigne.

Mots-clés

Excoriose; *Phomopsis viticola*; metabolites secondaires; xanthone; phomopsolide B; furanone; cytosporone; stérol.

1. Introduction

Grapevine belongs to the family *Vitaceae,* which includes 14 living genera and more than a thousand species. The plants are herbaceous or woody vines, with tendrils always arising opposite a leaf. Grapevines are perennials that annually produce shoots[1]. Cultivated grapevines exist on the five continents as long as conditions are favourable and in tropical and subtropical areas they can produce more than one crop per year. *Vitis vinifera* is one of the most widespread species from Europe to Asia and has become very diverse with more than 5000 cultivars reported at the end of the 1990's[1].
Grapevine diseases affect production, harvesting and processing by lowering quality, reducing yield and increasing the costs of production and harvesting. Diseases are usually endemic but if the weather is favourable to the development of a specific disease an epidemic may occur with losses ranging from 20 to 80%[1], at a cost of thousands of millions of euros.

Vitis vinifera is very susceptible to various diseases whose causal agents are living organisms such as fungi, bacteria, viruses and nematodes. Fungi are responsible for a number of them among which are powdery mildew, black rot, botrytis rot, anthracnose, eutypa dieback and excoriosis. They are small, usually microscopic, multicellular and filamentous organisms that lack chlorophyll. Their energy derives either from dead plants or animals (saprophytes) or from living ones as pathogens. Infections of plants occur either through direct penetration of tissues or through an injury or a natural opening (stomata, hydathodes, lenticels)[1-3].

One usually differentiates trunk and root diseases, e.g. Eutypa dieback and Esca, from fruit and foliar diseases such as downy mildew, powdery mildew and grey rot. Grapevine trunk diseases are responsible for significant economic losses to the wine industry worldwide. Symptoms of these diseases include dead spurs, arms and shoots and eventual vine death due to canker formation in the vascular tissue. In Eutypa dieback, deformed leaves and shoots occur as the pathogen invades the ramifications. As cankers develop, yield reductions occur due to the loss of productive wood. The impact of grapevine wood diseases usually becomes more severe as vineyards get older until they weaken and eventually kill vines. Foliage and developing bunches must also be protected from attack by various pests, especially fungal

pathogens, for the production of satisfactory yields of good-quality grapes, and especially for adequate vinification.

1.1. *Phomopsis viticola* (Sacc.) Sacc.

Phomopsis viticola (Sacc.) Sacc. is the causal agent of a disease called excoriosis, a term coined by Ravaz and Verge in 1925 and deriving probably from the French word "excorier", or also "Phomopsis cane and leaf spot". It was observed for the first time in Switzerland in 1967. It can be very destructive in regions where the weather stays wet and cool for several days after bud break.
P. viticola belongs to the Phylum Deuteromycotina (the fungi imperfecti, which means it reproduces only asexually by mitosis) and the Class Coelomycetes. As a coelomycete, conidia (asexual non-motile spores) are formed in pycnidia.

The fungus was originally described under the name *Phoma viticola* and isolated from canes of *V. vinifera* collected in 1880 in France by Saccardo. He then transferred the species in 1915 to a new genus called *Phomopsis*. In 1909, in the USA , Reddick described *Fusicoccum viticolum* associated with a disease of *Vitis labrusca*. Later, in 1937, Goidanich, recognizing that the conidia of *F. viticolum* were similar to those described for *P. viticola*, transferred *F. viticolum* to *Phomopsis viticola* and created the name *Phomopsis viticola* (Sacc.) Sacc.[6;7]. Thus, as happens quite often with fungi, the taxonomy of the species has not always been clear, mainly because the description of the species based either on host plant association or on morphological criteria is not reliable due to character plasticity[8]. Moreover, a great number of fungi can be isolated from plant vines which is a complicating factor when trying to associate symptoms with one organism[9]. Indeed, wood diseases are due to a complex of different organisms. For example, Philips isolated 11 different fungi associated with excoriosis symptoms in Portugal[9]. *Phomopsis viticola* was found on 52 canes, *Botriosphaeria dothidea* on 59 and other fungi (*Botriosphaeria obtusa, B. stevensii, Valsaria insitiva, Pleospora* spp., *etc*) between 2 and 9 times. Only the first two showed pathogenicity while the others were probably saprophytes.
In Australia, researchers have distinguished two taxa of *Phomopsis* on grapevine, named *Phomopsis* type 1 and *Phomopsis* type 2, which are responsible for the Phomopsis cane and leaf spot disease[10]. Molecular analysis of these two types found on grapevine allowed clear

distinction between both taxa[4]. The former taxon has been renamed *Diaporthe perjuncta*, the teleomorph of *Phomopsis viticola*, and the latter *Phomopsis viticola*, the anamorph[4;10;11]. The difference is not only genetic but can also be seen by the symptoms caused by the two taxa. *D. perjuncta* is responsible for the bleaching of canes in winter but is not pathogenic to grapevine shoots or buds[4]. The second type is however the real cause for the disease and shows all the typical symptoms[4;5;10;11].

Philips[6] tried to establish if *Diaporthe perjunct*a, found on grapevine canes in Portugal and Australia, could be the teleomorph of *P. viticola* but without success, mainly because the characteristics taken into account (α- and β-conidia, conidiophores, guttulation) did not allow for differentiation.

In a subsequent publication, Philips attempted to clarify the taxonomy of the fungi present on grapevine and their role in excoriosis[7]. Later, Mostert et al.[8] proposed a key to what they refered to as the *Phomopsis* complex, based on cultural, morphological, pathological and molecular data in order to clarify things. They defined the complex as follows:

- *Phomopsis viticola* (Sacc.) Sacc., fusoid-ellipsoid α-conidia, 10 μm long. β-conidia less abundant than α, rarely guttulate, 20-25 x 0.5-1 μm
- *Phomopsis* sp.2, felty colonies, buff with grayish sepia patches. α-conidia with acute apices, 10 x 2 μm , biguttulate. β-conidia curved, 15 x 1 μm
- *P. amygdali*, pathogenic to peaches and grapevine, α-conidia fusoid, acute apices, 5.5 x 1 μm , eguttulate. β-conidia straight, slightly curved, 16 x 1 μm. Both in equal proportions or one dominating.
- *Diaporthe perjuncta*, teleomorph produced in culture, α-conidia biguttulate, fusoid to ellipsoid, 6.5 x 2.5 μm , β-conidia curved, 18 x 0.5 μm
- *Phomopsis* sp. 1, woolly cultures, predominantly white with hazel brown and greyish sepia patches, teleomorph not produced in culture, α-conidia with obtuse apices, 7 x 2 μm , β-conidia (21 x 1 μm) more abundant than α-conidia.

Since then, Crous et al.[12] tried to reassess the species occurring on grapevine plants by combining molecular, morphological, cultural and pathological data. They collected isolates in the Western Cape province of South Africa from plant parts (shoots, pruning wounds and internally in the wood) showing severe *Phomopsis* symptoms and also from asymptomatic

nursery plants. This research resulted in the description of fifteen species of *Phomopsis* on grapevines. The description of selected species is done in the following table (Table 1.1). Other species occurring were *Phomopsis vitimegaspora* and *Diaporthe helianthi*. This is an example of the diversity of fungi that can be found on plants and also the difficulty in the taxonomic classification of fungi and particularly *Phomopsis* spp.. This also has consequences on several pathogenicity tests made by different groups in the sense that they could have been working with morphologically similar but different *Phomopsis* species.

Table 1.1 *Phomopsis spp*. isolated from grapevines according to Crous[12]

Species	Host	Distribution	Cultures
Phomopsis viticola	*Vitis vinifera*	Worldwide	Pale yellow to buff with smoke gray. Fusoid-ellipsoid α-conidia, apex acutely rounded.
Phomopsis sp. 1	*Protea* sp., *Pyrus* sp., *Vitis vinifera*	Australia, Portugal, South Africa	As described by Mostert
Phomopsis sp. 2	*Vitis vinifera*	Italy	As described by Mostert
Phomopsis sp. 3	*Vitis vinifera*	South Africa	Flat, smooth margins, white-straw. α-conidia non-guttulate, ellipsoid
Phomopsis sp. 4	*Vitis vinifera*	South Africa	Umbonate, smooth margins, hazel. Fine fusoid-ellipsoid α-conidia, mulitguttulate
Phomopsis sp. 5	*Vitis vinifera*	South Africa	Appressed, white to olivaceous. Fine α-conidia, wide in the middle. Non guttulate
Phomopsis sp. 6	*Rosa sp., Vaccinium sp., Vitis vinifera*	South Africa, USA	Flat, smooth margins, brown to honey. Large fusoid-ellipsoid guttulate α-conidia
Phomopsis sp. 7	*Vitis vinifera*	South Africa	Appressed, white to buff. Slender fusoid-ellipsoid α-conidia. Non-guttulate
Phomopsis sp. 8	*Vitis vinifera, Prunus sp, Pyrus sp.*	South Africa, USA	White to olivaceous-buff. Slender fusoid-ellipsoid α-conidia. Non-guttulate. Acute round apices
Diaporthe viticola	*Vitis vinifera*	Germany, Portugal	Buff to rosy. Wide in the middle ascopores.
Diaporthe australafricana	*Vitis vinifera*	Australia, South Africa	Ascopores hyaline, smooth, fusoid, wide at septum, 1 to 2 guttules
Diaporthe perjuncta	*Ulmus campestri, U. glabra*	Germany, Austria	Undulating margins, white to straw. Ascopores hyaline, smooth, fusiform, one septate.

Until now research has mainly focused on biological aspects of the fungus. Greenhouse experiments have shown that grapevine cultivars are all susceptible to *Phomopsis* to a certain degree[5;10]. Inoculation of shoots of red and white grape varieties with mycelial plugs of a

Phomopsis colony taken from 8-day old cultures produced extensive dark brown, longitudinal lesions on all cultivars tested (Figure 1.1). The average length of the lesion was 1.3 cm on white cultivars while the red ones showed a greater variability, from lengths of ca. 0.4 to 2 cm, with the Grenache cultivar showing greater susceptibility. No lesions developed on shoots inoculated with agar only (control) as they remained green and healthy throughout the experiment. The fungus was re-isolated on PDA from the margin of the lesions [5;10]. The lesions observed are probably due to the fact that hyphal growth causes cell disruption by physically forcing the cells apart rather by intracellular growth[5;13].

Figure 1.1 Lesions caused by *Phomopsis* on (from left) white cultivars: Semillon, Sauvignon Blanc, Chardonnay and red cultivars: Shiraz, Grenache, Cabernet Sauvignon and Merlot (reprinted from Rawnsley[10]).

Pezet and Pont have shown that elemental sulfur is accumulated in the cirrhus of the fungus and acts as a self-inhibitor of α-spore germination[14;15]. This sulfur comes from the desulfuration of β-mercaptopyruvate by an enzyme, β-mercaptopyruvate desulfurase, and starts accumulating just before the end of the growth stage and before the differentiation of the pycnidia[14;15].

1.1.1. Disease symptoms

Spots or lesions on shoots and leaves are common symptoms of the disease. Small, black spots on the internodes at the base of developing shoots are quite frequent (Figure 1.2)[16]. The spots may develop into elliptical lesions that may grow together to form irregular, black,

crusty areas. Under severe conditions, shoots may split and form longitudinal cracks[5;8;17;18]. Although cane lesions often appear to result in little damage to the vines, these lesions are the primary source of overwintering inoculum for the next growing season.

Other symptoms are dark brown to black necrotic lesions on the canes which makes them so brittle they easily break. Shoots may fail to develop from infected buds[11;16;17]. Infected young shoots, rachises and petioles show chlorotic spots which enlarge and turn black. If the infections on a shoot are numerous, they often merge to form dark patches which will crack and become open fissures[16].

(a)

(b)

Figure 1.2. (a) Infected shoot (b) Infected leaves (Reprinted by kind permission from B. Rawnsley [10])

Infected leaves, bunch stalks and petioles initially show chlorotic spots with dark centres[16]. These can be irregular or circular in shape. They enlarge and turn brown to black, appearing as streaks or blotches[11]. The fungus will also cause fruits to rot, the infecton usually coming from lesions on the rachis or pedicel. The fruits eventually turn brown and shrivel (Figure 1.3)[17]. All parts of the grape cluster (berries and rachises) are susceptible to infection throughout the growing season[16;19], however, most infections appear to occur early in the growing season. Lesions developing on the first one or two rachises on a shoot may result in premature withering of the cluster stem. Infected clusters that survive until harvest often produce infected or poor-quality fruit.

If not controlled early in the growing season, berry infection can result in serious yield loss under the proper environmental conditions[19]. Berry infections first appear close to harvest as

infected berries develop a light-brown color. Black, spore-producing structures of the fungus (pycnidia) then break through the berry skin, and the berry soon shrivels[1;16]. Fruit rot symptoms caused by *Phomopsis* generally do not appear until close to harvest on mature fruit. Research has shown that berry infection can occur throughout the growing season even though most infections probably occur early in the season (pre-bloom to two to four weeks after bloom)[19]. Once inside green tissues of the berry, the fungus becomes latent and the disease does not continue to develop. Infected berries remain without symptoms until late in the season when the fruit matures. If wood is infected, pycnidia can form on lesions when the wood is pruned. Spores can be washed by rain onto grapes which will be in turn infected.

(a) (b)

Figure 1.3 (a) Shrivelled fruits infected by *P.viticola* (b) Pycnidia on the grape berry.

In winter, pycnidia and irregular dark blotches occur on the surface of infected shoots. Pycnidia may be so numerous that they lift the epidermis, giving the surface a white to silvery sheen[1;17]. This bleaching is often associated with the disease, indicating that *Phomopsis* causes a physiological change in grapevine tissue as it colonises the epidermal cells and developing pycnidia force the layer of epidermal cells away from the cortex[10]. However, it is not typical of *Phomopsis* and can be due to other fungi[7]. The fungus has been reported to be found in dormant buds and buds and nodes [8].

1.1.2. Disease cycle

P. viticola overwinters as mycelium or pycnidia in the bark or in dormant buds (Figure 1.4). The pycnidia are 0.2 to 0.4 mm in diameter. In spring, pycnidia will erupt through the

epidermis of canes and other dead or injured tissues of the vine. An ostiole opens at the peak of a short neck which is usually round and smooth. Pycnidiospores arise through this opening in the shape of long curled yellowish cirri or in a gelatinous mass[17] and propagated by rain onto other neighbouring vines or other tissues[7;10;17]. These cirrhi contain several thousand spores. Mycelium will grow and spread from these spores thus allowing infection of healthy parts of the plant. Infection takes place when relative humidity is at 100% and affects only young tissues. The optimal temperature for infection is 23°C but α-spores germinate between 1 and 37°C[20].

The first symptoms appear from 21 to 30 days after inoculation. The fungus will stay active throughout the growing season as long as temperatures are cool. In dry, warm climates the fungus becomes inactive. The disease will quickly spread and become severe if it rains continuously for several days during early spring, otherwise it stays endemic.

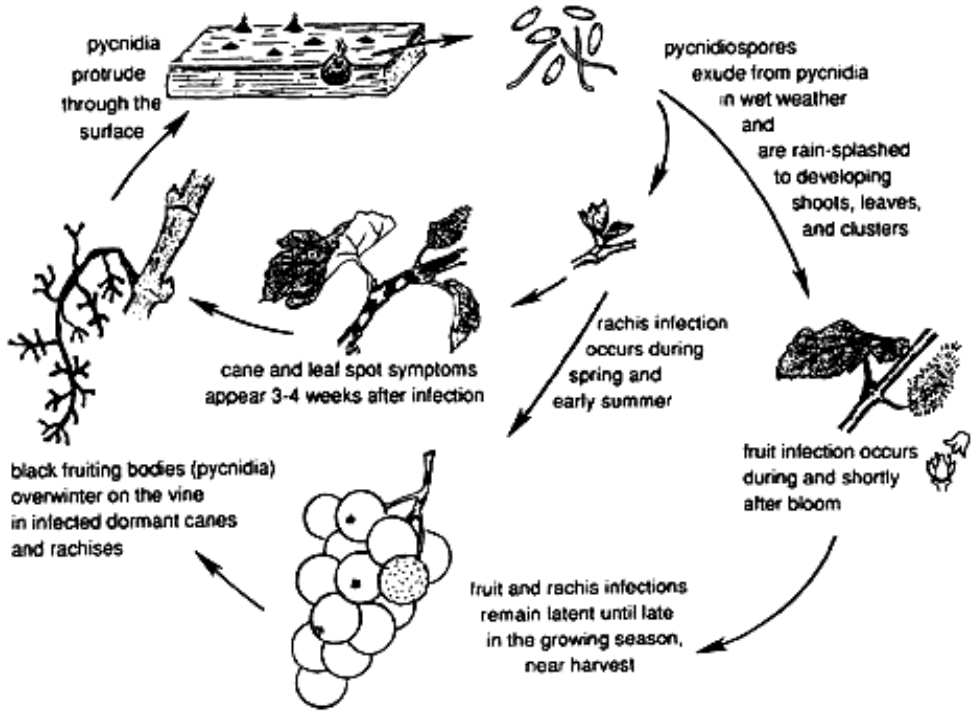

Figure 1.4. The disease cycle

Prolonged periods of rain and cold weather are vital factors for the development of an epidemic[7;10;17]. However, spread within the vineyard is localized because the fungus spreads mostly within the vine rather than from vine to vine. Because of this, the disease usually does not spread quickly but rather builds up progressively over a number of years.

Inside the Pycnidium, there can be two types of pycnidiophores. The first type has a pointed apex and produces single, hyaline elliptical spores, the alpha spores, which measure 7-10 x 2-4 μm, are elliptical with a pointed apex and a guttule at each end (Figure 1.5)[17]. The second type of pycnidiophores is shorter and produces the beta spores which are long, curved threadlike and measure 18-30 x 0.5-1 μm [8;10;17;21]. The function of these second type of spores which are known to not germinate is not yet determined[17;21]; however it has been shown that production of these spores can be induced, notably by changing the carbon to nitrogen ratio of the culture medium[21].

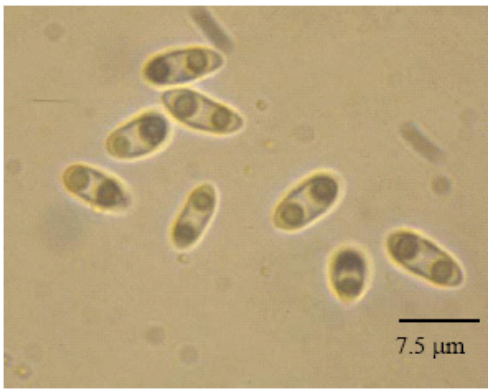

Figure 1.5. Bi-guttulate α-spores of *P. viticola* (Reprinted by kind permission from Dr. B. Rawnsley[10])

In culture, mycelium of *P. viticola* is hyaline or light brown, septate and forms a dense colony growing in concentric rings (Figure 1.6). Some portions of the mycelium turn black as the culture ages. Pycnidia can be formed in the dark portions of the mycelium.

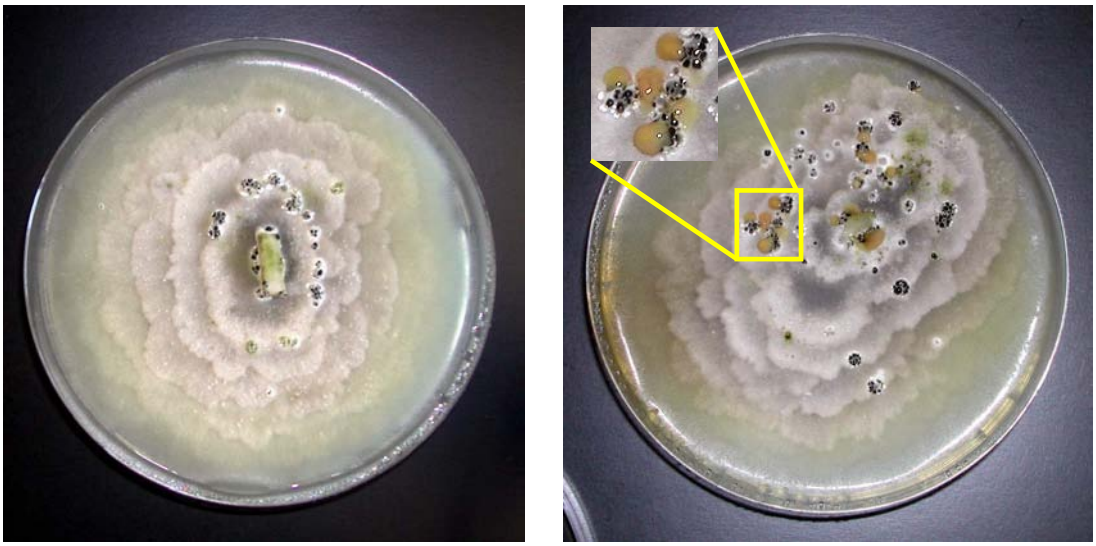

Figure 1.6. Culture of *P. viticola* on potato dextrose agar with (right) pycnidia and cirrhi

1.1.3. Disease management

Vine cultivars differ widely in their susceptibility which also seems to vary with location[5;10;22]. When planting new material, it should be pathogen free and diseased wood should be pruned and destroyed [17]. Protective chemicals such as captan, folpet or maneb can be applied to prevent infection[18;22]. It has also been shown in field experiments that the mixture fosetyl-Al and folpet is successful in reducing sporulation of the fungus by approximately 95%[18]. Spray shouls begin at bud burst and should be repeated after 8-10 days.

Eradicant chemical sprays (dinoseb, sodium arsenite) can also be used to kill pycnidia and spores on the surface of vine parts[22] 2 to 3 weeks before the buds swell, but as they are highly toxic for humans and environment, they have been banned in most European countries. The European and Mediterranean Plant Protection Organisation (EPPO) recommends the use of either chemicals (azoxystrobin, dichlofluanid, folpet, fosetyl-aluminium, kresoxim-methyl, mancozeb, maneb, metiram, propineb, sulphur) with two to three treatments when temperatures are low and shoot growth slow[22]. Later in the season, sterol biosynthesis inhibitors can also be effective[22].

1.2. Aim of the work

Until now, no study of the secondary metabolites produced in cultures of the fungus *Phomposis viticola* has been made. The aim of the present project is to isolate and identify metabolites produced by strains of the fungus and test their biological activity. Another goal is to see if different strains of the *Phomopsis* species produce the same compounds or if there are differences in the types of chemical structures the compounds have. Finally an assay will be made to check if growing the strain on an artificial media results in the same metabolite production than on grapevine wood.

The knowledge of the type of metabolites produced would help to understand the biological pathways of the fungus and determine their role in the development of the disease symptoms.
In order to achieve this, strains of the *Phomopsis* sp. were collected from a grapevine field in Ticino. Metabolites obtained from crude extracts of culture on artifical media were profiled using high-performance liquid chromatography and biological assays with grapevine leaf-

disks were performed. In order to obtain sufficient amounts of the metabolites so that their structures can be determined by 1D and 2D NMR techniques, culture will have to be up-scaled. Other modern current separation and identification techniques, such as HPLC-UV and LC-API-MS, will be used for the purification of the compounds and their identification in crude extracts .

1.3. Secondary metabolites from *Phomopsis* sp.

Despite the fact that until now, no study has been made regarding the production of secondary metabolites by *P. viticola*, a rich variety of metabolites produced by the genus *Phomopsis* have been isolated. A few selected ones are shown in Figure 1.7.

Phomopsis oblonga, which has been reported to produce boring/feeding deterrents for elm bark beetle produces, amongst others, two lactones, phomopsolide A and phomopsolide B [24].

Phomopsis convolvulus is a host-specific pathogen of field bindweed (*Convolvulus arvensis*)[25]. From cultures of this fungus, an ergosterol peroxide, convolvulopyrone, convolvulanic acid A and B, convolvulol and other metabilites were isolated. The two acids were shown to have phytotoxic effects on leaves and thus could be used as herbicides against the weed.

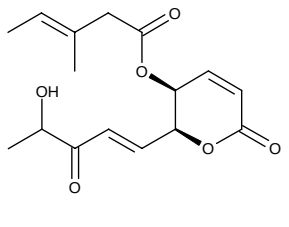

Phomopsolide A and B (*P. oblonga)*

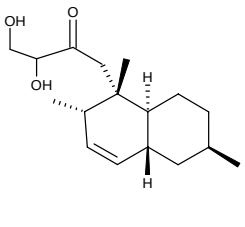

Phomodiol (*P. oblonga)*

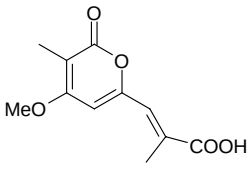

Convolvulopyrone *(P. convolvulus)*

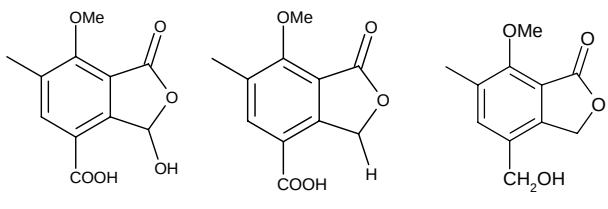

Convolvulanic acids A (left) and B (middle) and Convolvulol (right) (*P. convolvulus)*

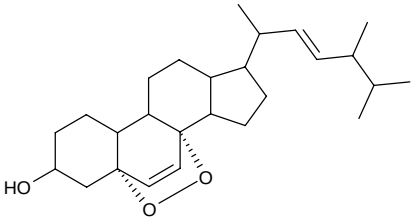

Ergosterol peroxide *(P. convolvulus)*

Figure 1.7. : Chemical structures of some isolated compounds from *P. oblonga* and *P.convolvulus* species

Phomopsis longicolla an endophytic fungus of endangered mint produces three dicerandrols (A, B and C) [26] that display antibacterial activity against *Staphylococcus aureus* and *Bacillus subtilis*. Three (±)-phomozines (A, B and C) were isolated from *Phomopsis helianthi* and phomopsichalasin[27], phomopsidin[28], phomoxanthones A and B[29] or esters of phomalactone[29;30] from unspecified *Phomopsis spp*.

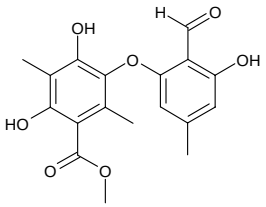

(±) Phomozin (*P. helianthi)*

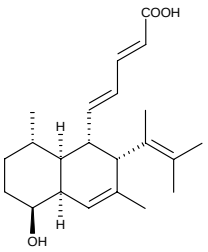

Phomopsidin (*Phomopsis* sp.*)*

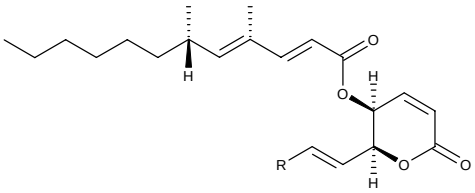

Ester of Phomalactone (*Phomopsis* sp.*)*

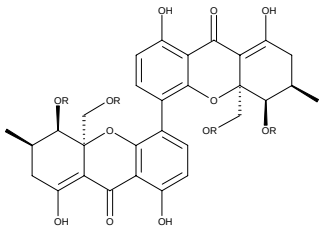

R = Ac
Phomoxanthone A, (*Phomopsis* sp.*)*

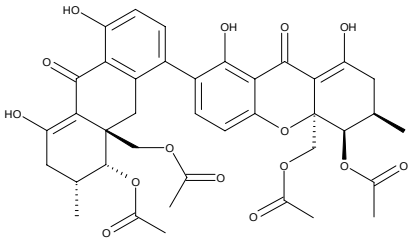

Phomoxanthone B (*Phomopsis* sp.*)*

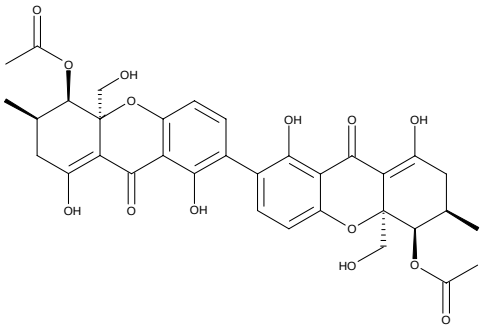

Dicerandrol C (*P. longicolla)*

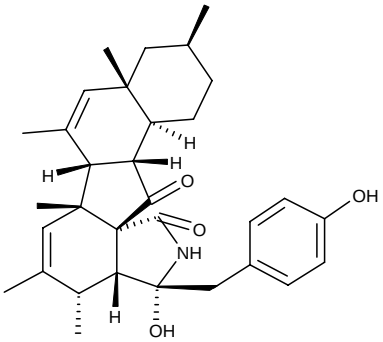

Phomopsichalasin (*Phomopsis* sp.)

Figure 1.8 Chemical structures of some isolated compounds from *Phomopsis helianthi, longicolla* and unspecified species

These different metabolites show diverse biological activities. For example, phomopsichalasin showed antibacterial activity, phomopsidin showed inhibitory activity against assembly of microtubule proteins and the phomoxanthones were found to exhibit in vitro antimalarial and antitubercular activities.

1.4. Analytical techniques

Fungal secondary metabolites are an important source of new structures for drug compounds. The discovery of penicillin in 1928 by Fleming led later to the discovery of potent antibiotics isolated from microbial broths[31]. Since then, there has been a continuous search for new bioactive compounds. They were first searched in soil fungi but now, as the amount of new molecules isolated is decreasing, research has turned to endophytic fungi[31].

The inherent diversity and complexity of natural products extracts makes the analysis and isolation of compounds very difficult. The use of high performance liquid chromatography (HPLC) coupled to diode-array UV-Vis detection, has undoubtedly made things much easier, allowing for quick and efficient characterisation of crude extracts [23;24;27;32-36]. It is now a widespread technique and has been used for many practical applications, for example to determine the profile of mycotoxins produced by moulds in foods[33], to screen trichotecenes in fungal cultures [37] or to identifiy marine mycotoxins produced by *Trichoderma koningii*[38].

The development of electrospray ionisation mass spectrometry (ESI-MS) in the 1980's has also dramatically helped the chemists. Whereas earlier techniques of ionisation such as electron impact (EI) could only be used to analyse thermally stable, low molecular weight, volatile compounds, ESI allows the analysis of a much wider range of molecules, from proteins to small organic molecules or inorganic salts. Another advantage is that analytes can be analyzed directly from the liquid phase, and thus can be coupled to separation techniques such as HPLC or capillary electrophoresis (CE) [39;40]. Despite the apparent problems of maintaining a high vacuum for the mass spectrometer with the flow rates used in HPLC, the ESI interface is perfectly suited to resolve these problems since ionisation happens at atmospheric pressure[40-43].

However, before ESI was used, several paths had been explored in the 1960's in order to resolve this coupling problem between HPLC and the mass spectrometer. Among these, the moving belt interface was used in the 1970's. With this technique, the eluent coming from the HPLC column were transported into the ionisation chamber by a belt. During this transport, solvent was evaporated and completely eliminated before entering the source, which could be EI, chemical ionisation (CI) or fast-atom bombardment (FAB). Two differentially pumped vacuum locks would ensure the transition between atmospheric pressure and the vacuum of the source.

The Particle Beam Interface was first described in 1984. In this case, the mobile phase of the HPLC was evaporated before ionisation in order to increase the analytes concentration. It was then sprayed through a small hole into a spray of uniform droplets. This happened in the ionisation chamber which was at atmospheric pressure and room temperature. Analytes were then transferred to the source, either EI or CI, with a pumping system eliminating small molecules.

Another technique used was the continuous flow- FAB (fast atom bombardment). With this system, the mobile phase was enriched with 10% of glycerol and then passed through a porous frit in steel. This frit was the target of the FAB. Ionisation consisted in a beam of either Xenon or Argon which was bombarded on the target: the compound dissolved in the glycerol matrix. With this beam, ions were ejected out of the matrix without the need of heat. In the continuous flow mode, the surface of the target was continuously renewed by the eluent coming from the HPLC.

Reversed-phase chromatography is the separation method widely used with LC-MS analyses as aqueous mobile phases with polar organic solvents (such as methanol or acetonitrile) are highly compatible with ESI.

Atmospheric pressure chemical ionisation (APCI) and atmospheric pressure photoionisation (APPI) are also widely used, broadening the range of ionisable molecules. LC-API-MS techniques have now become the most powerful methods for natural products screening and analyses. The description of the three techniques (ESI, APCI, APPI) that were used in this research project and the mechanisms involved are given in the following points (1.4.1; 1.4.2; 1.4.3) while the difference in application is given in Figure 1.9. The application of ESI is for relatively polar compounds with low to very high molecular weight (~100'000) since compounds can be multi-charged with this technique. APPI and APCI are used for compounds of low to medium polarity and with molecular weights ranging from 50 to a few thousand Daltons.

The most common analysers used in LC-MS are the quadrupole, time-of-flight (TOF), ion-trap (IT) and Fourier transform-ion cyclotron resonance (FT-ICR or FT-MS), each of them having advantages and disadvantages. The quadrupole consists of four metallic parallel rods arranged in a square. Voltages are applied to the rods to create electromagnetic fields that allow to direct ions down the centre of the square. This analyser can operate in full scan mode or single-ion monitoring (SIM).

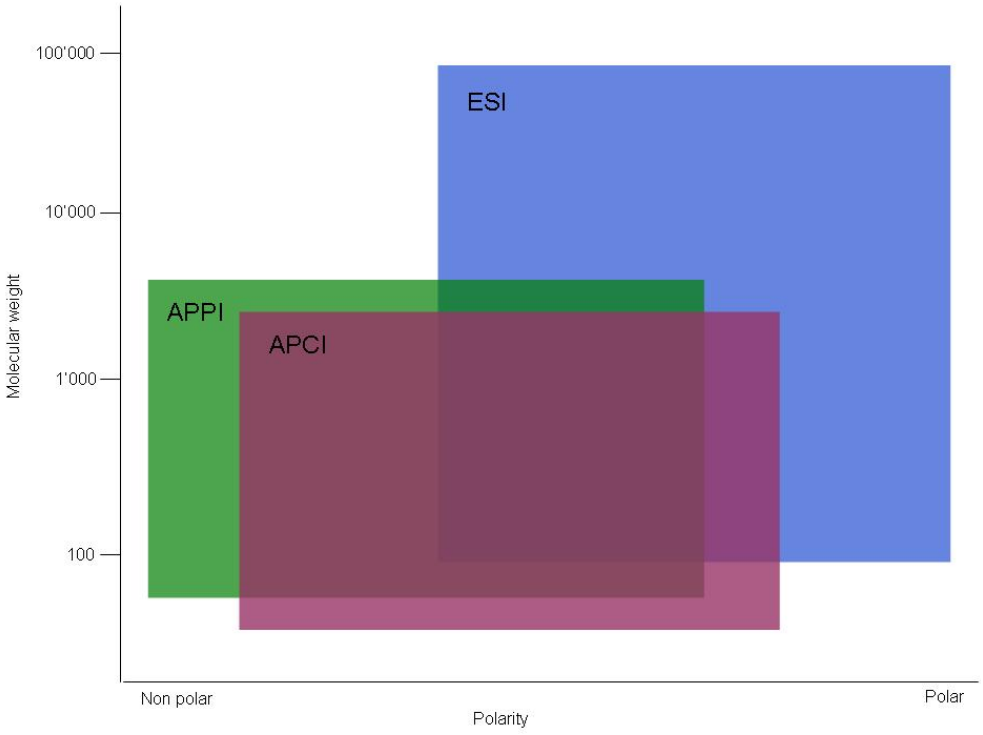

Figure 1.9 The different ranges application of ESI, APCI and APPI

For the TOF mass analyser, a uniform electromagnetic force is applied to the ions causing them to accelerate down a flight tube. As lighter ions travel faster, they arrive first to the detector: mass-to charge-ratio of the ions is determined by their arrival time[44;45].

In FT-MS, ions are trapped in a chamber with high electrical and magnetic fields which makes them have circular orbits[46]. A high radio-frequency electrical field is applied so that the ions generate a time-dependent current. This current is converted by Fourier transform into orbital frequencies of the ions which correspond to their mass-to-charge ratios. They can perform multiple stage mass spectrometry, have a wide mass range and excellent resolution but are the most expensive analysers.

Ion traps consist of a circular ring electrode plus two end caps that together form a chamber. Ions entering the chamber are “trapped” there by electromagnetic fields while another field can be applied to selectively eject ions from the trap. Ion traps have the advantage of being able to perform multiple stages of mass spectrometry (MS^n) without additional mass analyzers. We used this analyser during the current study.

1.4.1. Electrospray ionisation

When working in ESI-MS, a dilute solution of an analyte is injected through a capillary which is held at a high potential, from 2 to 5 kV (Figure 1.10)[47].

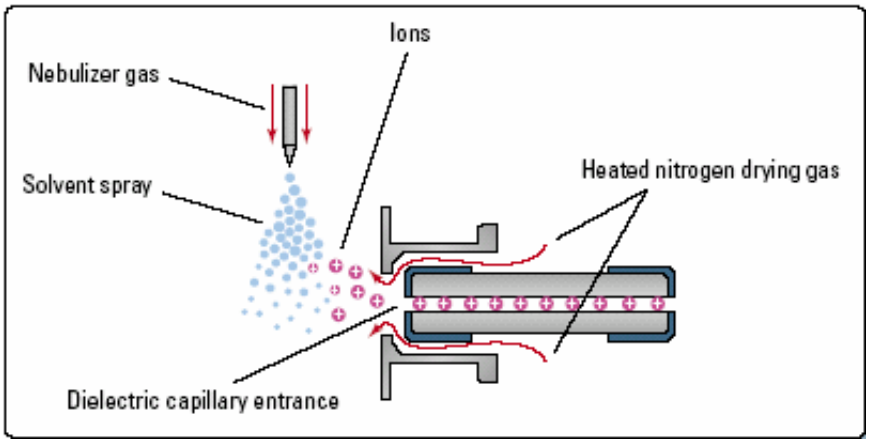

Figure 1.10 ESI source configuration (© 2001 Agilent technologies, Inc)

Depending on the analytes studied, this voltage can be either negative or positive. The voltage produces an electric field gradient that will generate a spray of highly charged droplets that will go through a heated capillary to the analyser of the mass spectrometer due to the pressure and potential gradient. During this stage, the droplets reduce in size by a mechanism known as Coulomb fission or solvent evaporation[48]. Nebulisation of the solution is also facilitated by a sheath gas, usually nitrogen. At the interface the liquid protrudes from the capillary tip in what is known as a ‘‘Taylor cone’’ (Figure 1.11)[48-51].

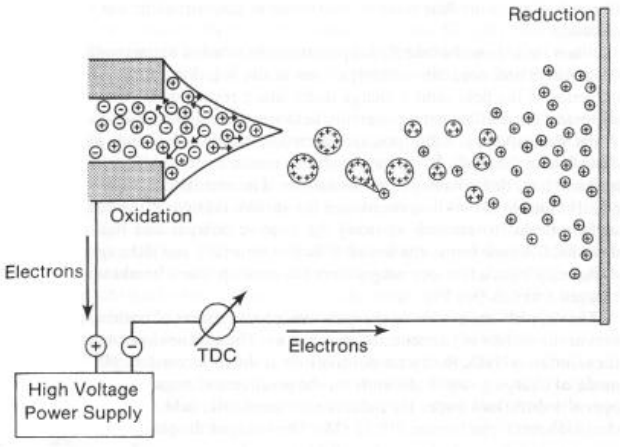

Figure 1.11. Formation of the Taylor cone at the tip of the capillary [53]

This is the result of the electrophoretic movement the ions undergo caused by the electric field. In the positive ion mode, anions migrate in the direction of the metal capillary whereas cations migrate away, in the direction of the counter-electrode. When the field is high enough, the cone will produce charged droplets via a budding process (when surface tension is exceed by the applied electrostatic force). At the counter-electrode, where there is a continuous arrival of charged species of one polarity, there is a reduction, a kind of electrical circuit being completed. The source is akin to an electrolytic cell where electrolysis maintains the charge balance in order to have a continuous production of charged droplets, according to Kebarle et al..[47;51;52]. The size and diameter of the droplets is influenced by numerous parameters including the flow rate of the solution, the solvent properties and the applied potential. When the solution reaches the Rayleigh limit (the point at which coulombic repulsion of the surface charge is equal to the surface tension of the solution), droplets that contain an excess of positive or negative charges break from its tip (Figure 1.12). These droplets move through the atmosphere towards the entrance of the heated capillary, and generate charged analytes.

There are mainly two theories to explain the production of the ions, one attributed to Dole which has been coined the charged residue model, CRM, and another one by Iribarne and Thomson, the ion evaporation model, IEM[41;48-50;53;54].

The CRM assumes that the increased charge density due to solvent evaporation causes large droplets to divide into smaller and smaller droplets (a phenomenon also called sometimes the coulomb fission mechanism), and will finally end up as single ions.

The second theory, IEM, suggests that the increased charge density that results from solvent evaporation eventually causes coulombic repulsion to overcome the liquid's surface tension, resulting in a release of ions from droplet surfaces. Sampling of the desolvated ions is made using a heated capillary or a skimmer device.

The charge states of the ions in the gaseous state reflects the charge state in the condensed phase but it can be modified because of ion-molecule collisions which means that multiple charged species can be observed. This is of high importance as it allows the analysis, for example, of proteins which can be seen as $[M+nH]^{n+/n}$ ions in the m/z range below 2000 [50].

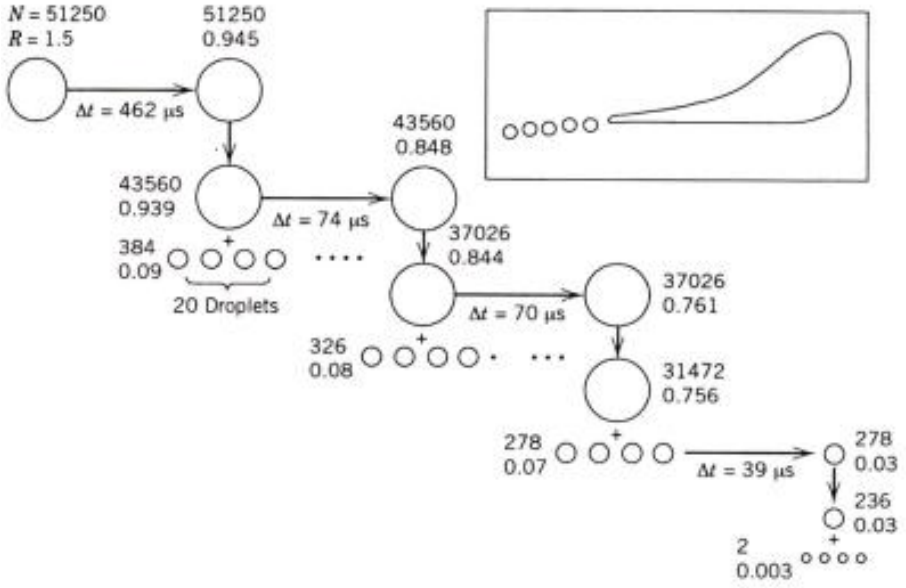

Figure 1.12. Coulombic fission of the droplets. The first parent droplet produces 20 "offsprings" droplets, released by a process termed "droplet jet fission" which carry 2% of the mass and 15% of the charge. N = number of elementary charges and R the radius (μm) . ΔT (μs) is the time until next fission[48;53].

This accounts for the extensive use of ESI for biological studies. Different cationised species, deriving from the same neutral analyte and charge number, may also be observed; such as sodium adducts that can replace protons in the formation of positive ions. This will yield cations of the form $[M+Na+(n-1)H]^{n+}$ which will be separated from the $[M+nH]^{n+}$ analogue by 22 m/z[48].

1.4.2. Atmospheric pressure chemical ionisation

Atmospheric pressure chemical ionisation (APCI) is a technique applicable to a wide range of polar or non-polar molecules. However as multiple charging rarely happens it is used usually for molecules with a weight under 1500 Da. Due to this and the high temperature used, its not the most adequate method for large biomolecules.

In the case of APCI the eluent is vaporised through a graphite tube heated at 450-550°C (Figure 1.13). A vapour of solvent and analytes is produced in the source and ionisation is induced by a discharge from the corona needle. The solvent ions transfer charge to the analytes by chemical reactions. Solvent is eliminated by the gas. Ions are transferred by a heated capillary then through a skimmer and then to the mass analyser.

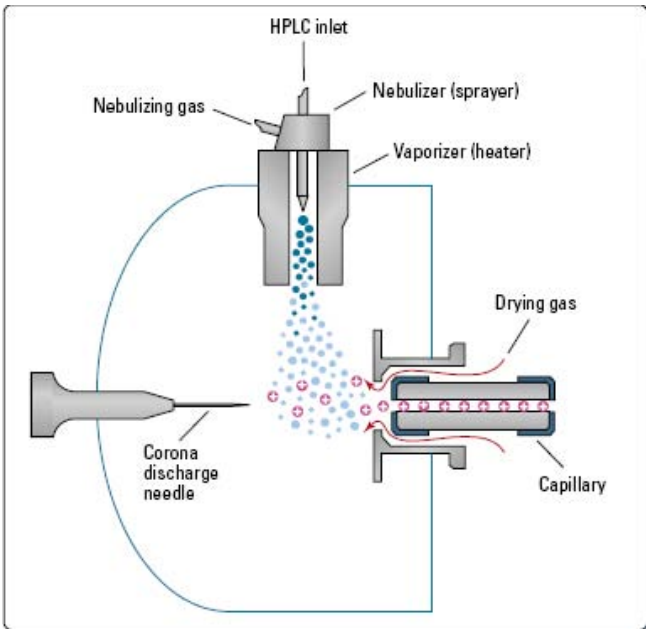

Figure 1.13 APCI source configuration (© 2001 Agilent technologies, Inc)

In the positive-ion mode, a series of ion formation reaction occur, first of all:

$$e^- + N_2 \rightarrow N_2^{+\cdot} + 2e^-$$

Then there is secondary ion formation:

$$N_2^{+\cdot} + H_2O \rightarrow H_2O^{+\cdot} + N_2$$

$$H_2O^{+\cdot} + H_2O \rightarrow H_3O^+ + HO^\cdot$$

And finally a proton transfer to form the charged species:

$$H_3O^+ + M \rightarrow (M+H)^+ + H_20$$

In the negative ion mode, $(M-H)^-$ is formed by the abstraction of a proton by OH^-.

APCI is a very robust gas phase ionisation technique, not as soft as ESI, but has the advantage of not being affected by changes in buffer strength.

1.4.3. Atmospheric pressure photoionisation

Atmospheric pressure photoionisation (APPI) is a new technique and a rapidly growing ionisation method. It relies on the ionisation of analytes by photons produced by a vacuum-ultraviolet light (Figure 1.14).

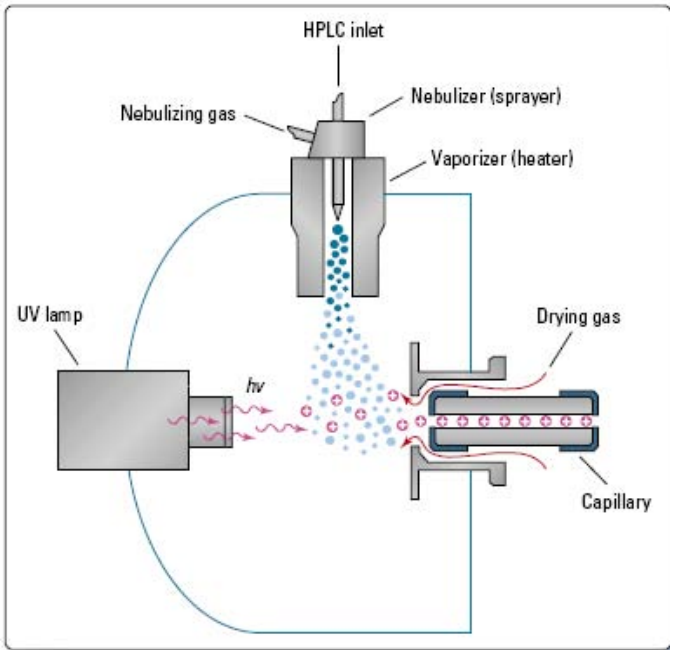

Figure 1.14 APPI source configuration (© 2001 Agilent technologies, Inc)

Once the photon is absorbed by the molecule an electron is ejected to form a molecular radical ion ($M^{+\cdot}$). This happens when the energy of the irradiating photon is higher than the ionisation potential (IP) of the molecule. Small molecules, such as major constituents of air, and most solvents (e.g. water, methanol, acetonitrile, etc) have higher IP than that of the photons of standard lamps used and thus do not interfere[55].

Because the ion $M^{+\cdot}$ has an unpaired electron it can react via collisions, especially as the environment is at atmospheric pressure. One of the reaction that can occur is the abstraction of a hydrogen atom to form a $[M-H]^-$ species. Other parasitic reactions can occur like proton transfers or collisional quenching, i.e. recombination either with the gas or a mobile phase molecule[56].

It is however observed that an important decrease of sensitivity is observed when there is an abundance of solvent vapour (water or methanol) in the sample. Thus formation of this solvent vapour decreases the ion formation.

Usually a hydrogen discharge lamp with a photon energy of 10.2 eV is used to create the ions but its ionisation potential is lower than the IP's of the common HPLC solvents (water: IP = 12.6 eV, methanol: IP = 10.8 eV, acetonitrile: IP = 12.2 eV) thus reducing the number of ions created [56;57]. One way to improve this is by ionising a bigger fraction of the molecules of the total from the LC eluent. This can be achieved by adding an ionisable dopant in high

quantities in the eluent[56;57]. The dopant (D) functions as an intermediate between the photons and the analytes (AB) by either transferring protons or by charge exchange:

$$D + h\nu \rightarrow D^{+\cdot}$$
$$D^{+\cdot} + AB \rightarrow D + AB^{+\cdot}$$

Two dopants are mainly used, i.e. acetone (IP = 9.70 eV) and toluene (IP = 8.83 eV). The presence of protonated ions can be explained by the fact that the mobile phase (MP) can also intervene and act as intermediates[56;58]:

$$D^{+\cdot} + MP \rightarrow [D\text{-}H]^{\cdot} + [MP+H]^{+}$$
$$[MP+H]^{+} + AB \rightarrow MP + [AB+H]^{+}$$

Thus, methanol, or acetonitrile, can form clusters with toluene which can rearrange and fragment, either by losing an H or a benzyl radical ($C_7H_7^{\cdot}$)[56]. In general, the proton transfer between toluene molecular ion and a solvent molecule takes place when the proton affinity (PA) of the solvent is higher than that of the benzyl radical (PA = 831.4 kJ/mol)[56](Figure 1.15).

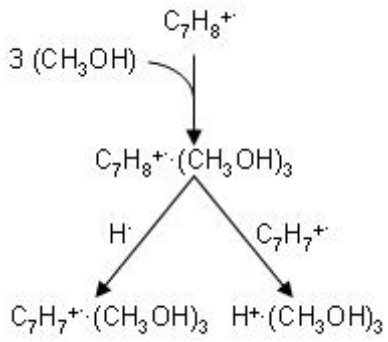

Figure 1.15 Cluster formation in APPI

This is why it works with methanol (PA = 754.3 kJ/mol) and acetonitrile (PA = 779.2 kJ/mol), which form solvent and solvent/water clusters that have higher Pas than that of the monomers and $C_7H_7^{\cdot}$. However, this is not the case for water, hexane or chloroform and thus no transfer is observed. Other mechanisms occur but they are not completely understood. It has been shown that acetonitrile for example can isomerise to form precursor ionic species[56].

1.4.4. The ion trap

The quadrupole ion trap consists of three electrodes, two of them being virtually identical and having a hyperboloidal geometry (Figure 1.16). These are called the end-cap electrodes, each of them having a single small aperture. The first one lets the ions in the trap and the second one send them to the detector. The third electrode, called the ring electrode, is also of hyperboloidal geometry and resembles a napkin holder. The geometries of the three electrodes are defined so that they produce an ideal quadrupole field which, in turn, will produce a parabolic potential well for the confinement of the ions.

Ions are ejected from the trap by increasing linearly the amplitude of the radiofrequency (r.f.) potential applied to one of the ion trap electrodes. As the ionic species are ejected from the potential well at specific r.f. amplitudes and as the rate of increase and initial amplitude are known, the mass to charge ration can be determined for each ion. One of the conditions of this method is that the ions must be contained in the centre of the trap which is achieved by momentum dissipating collisions with helium atoms.

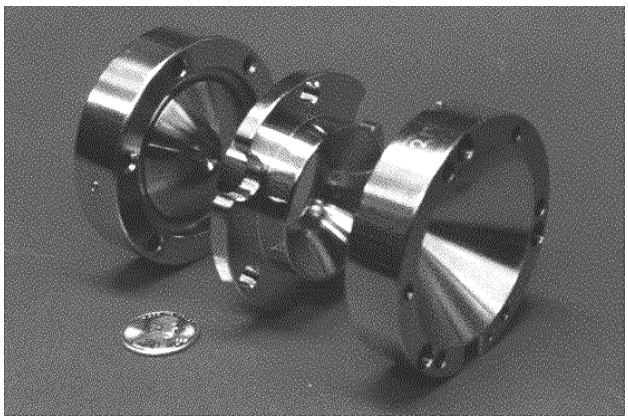

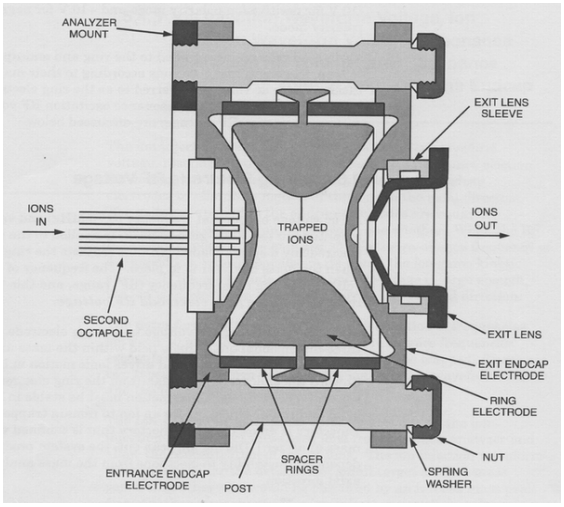

Figure 1.16 The three electrodes of the ion trap opened (left) and a cross section view (right) (© Agilent technologies, Inc.)

It has been found that the motion of the ions in the trap can be described mathematically by the solutions to the equation of Mathieu. The applied electric potential, Φ, on the ring electrode is:

$$\Phi = U + V\cos(2\pi ft)$$

With:

f: the frequency [Hz]

t: time [s]

U: a direct current potential

V: the amplitude of the radiofrequence

The motion of the ions is characterized by two secular frequencies, one axial and one radial. The trapping parameters can be described by these two dimension parameters according to the z axis:

$$a_z = \frac{-16eU}{m\left(r_0^2 + 2z_0^2\right)\Omega^2} \qquad q_z = \frac{8eV}{m\left(r_0^2 + 2z_0^2\right)\Omega^2}$$

With:

r_0: internal radius of the ring electrode

z: axial direction

e: electronic charge

m: mass of an ion

z_0: axial distance from the centre of the trap to the closest end-cap electrode

For the LCQ instrument, r_0 = 0.707 cm and z_0 = 0.785 cm.

The solutions for the Mathieu equation can be of two sorts, either periodic and unstable or periodic and stable. The second type determines the motions of ions in an ion trap. In Figure 1.17, the shaded region A in graph (2) represents the z and r directions in which the trajectories of the ions are stable simultaneously. The $\beta_z = 1$ boundary intersects with the q_z axis at 0.908 which corresponds to the ion of lowest mass-to-charge ration that can be stored in the ion trap.

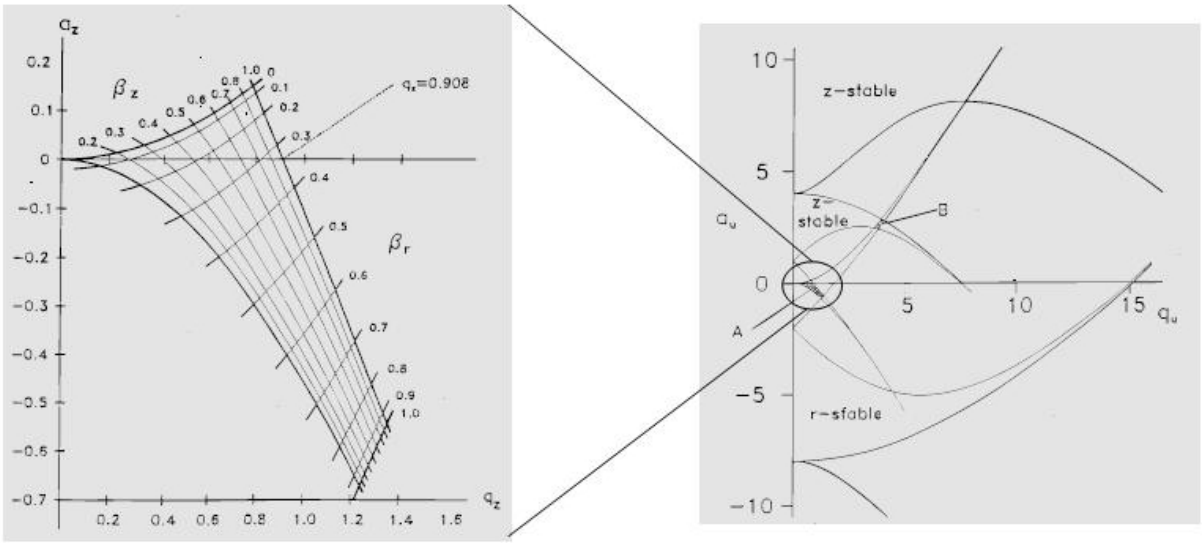

Figure 1.17 Mathieu stability diagram (right) in az and qz space and the stability region A (left)

When V increases, the ions on axis q_z will move to a higher q_z. When qz = 0.900 the ions pass in an excited state and when q_z = 0.908 they are at the limit of the resonance ejection and are ejected through the hole in the end-cap electrode to the detector. Thus by applying small supplementary oscillating potentials (of a few hundred millivolts) on the end-cap electrodes, ion motion can be excited upon resonant irradiation. This will allow to remove unwanted ions so as to isolate specific mass-to-charge ions (i.e. single-ion monitoring modes, SIM), to increase ion kinetics so as to create collisions with helium atoms (collision induced dissociation (CID) and thus MS^n experiments, to increase ion kinetics so as to move them towards one of the end-cap electrodes and thus be ejected to the detector.

1.4.5. NMR techniques

Nuclear magnetic resonance was first observed in 1946 and, until the 1970's, one dimensional NMR was the only technique used with the ^1H the most commonly observed nucleus. Apart from ^1H and ^{13}C spectra, other techniques exist, often employing complex pulse sequences to obtain specific information, which are very useful in determining structures from spectra. The following ones were used for this work:

- DEPT-135 (Distortionless Enhancement by Polarisation Transfer) is a one-dimension technique which allows to determine the carbon multiplicities, the number indicating

the flip angle of the editing proton pulse in the sequence, which can be of 45, 90 or 135°. In this case, with an angle of 135°, CH and CH_3 carbons give positive signals whereas CH_2 give negative ones. Carbons that do not bear protons are not seen because the technique relies on polarisation transfer,i.e. the transfer of proton magnetisation onto the directly bound carbon

- The COSY experiment (COrrelation SpectroscopY) is used to identify mutually coupled protons and is the most widely used 2D experiment. It can establish connectivities when a large number of coupling networks need to be identified, as it maps all correlations with a single experiment. The pulse sequence consists of a variable delay time, t_1 and an acquisition time t_2. The experiment is repeated many times with different values of t_1 and the data acquired during t_2 is stored. The value of t_1 is steadily increased throughout the experiment. During a typical experiment, something on the order of a thousand individual FID patterns, each incremented in t_1, are recorded. The cross-peaks show the correlation of pairs of nuclei by means of their spin-spin coupling. In the COSY spectrum of a complete molecule, the result is a complete description of the coupling partners in the molecule.

- The Heteronuclear multiple quantum correlation (HMQC) experiment identifies protons with their directly bound carbons. The techniques uses magnetisation transfer from the proton to its directly attached carbon atom, and back onto the proton for higher sensitivity. Thus, non-protonated carbons or protons bound on heteroatoms will not give a response. The conversion of transverse magnetisation is mediated by a delay $1/^1J_{CH}$ and a carbon 90° pulse. The size of $^1J_{CH}$ depends on the hybridisation of the carbon: 120 Hz for a sp^3, 160 Hz for a sp^2 and 250 Hz for a sp carbons. When aromatic compounds are present, or alkene fragments, $^1J_{CH}$ 140 Hz is a good compromise. The results are displayed in a similar manner to those from COSY, with one dimension of the 2D map representing ^{13}C chemical shifts and the other representing ^1H chemical shifts. Crosspeaks in the contour plot define to which carbon a particular proton (or group of protons) is attached, and it is therefore possible to map ^{13}C assignments from known ^1H assignments. One peak is observed at the frequency of each protonated-carbon resonance, although two can be seen with

diastereotopic CH_2 groups. HMQC is more sensitive than the equivalent experiment HETCOR because it is proton detected.

- The Heteronuclear multiple bond correlation (HMBC) experiment allows to identify proton nuclei with carbon nuclei that are separated by more than one bond. The pulse sequence uses zero and double quantum coherence between J-coupled protons and carbons to label each proton with the frequency of a remote carbon. It is closely related to HMQC as it uses the same principles to convert transverse magnetisation into zero and double quantum coherence. However, the sequence timings are optimised for much smaller coupling constants and therefore seeks the correlations across more than one bond that arise from long-range couplings. A filter is used to suppress crosspeaks arising from one-bond proton-carbon interactions. These ^{1}H-^{13}C couplings typically occur with significant intensity over only 2 and 3 bonds ($^{n}J_{CH}$ usually <10 Hz), but may be apparent over 4 bonds in conjugated systems. Correlations across heteroatoms other than carbon can also be seen with this techniques.

2. Material and methods

2.1. Fungal strains

Ten fungal strains were collected from the wood of grapevine plants in a vineyard in Ticino at Riva San Vitale (Switzerland) by Danilo Christen (ETH Zürich) in 2002. The following list gives the code of the *Phomopsis* strains and in brackets the *V. vinifera* cultivars they were collected from: 00 (unknown), 110 (Merlot), 180 (Cabernet Sauvignon), 239 (Cabernet Sauvignon), 275 (Merlot), 279 (Cabernet Franc), 281 (Cabernet Franc), 282 (Cabernet Franc), 283 (Merlot), and 301 (Cabernet Sauvignon).

In order to decide which strains would be selected for a further upscale study, each strain was grown on ten Petri dishes containing potato-dextrose agar (PDA) for 21 days in the dark at 23 ± 1°C, as proposed by Mostert et al.[8] and then extracted with ethyl acetate according to the procedure described in section 2.1.1. The results of this selection are given in section 3.1.

The three strains selected strains for in-depth study were strains 180, 239 and 283. Strains 180, 239, 275 and 281 were identified by the Belgian Coordinated Collections of Microorganisms (BCCM), of the University of Louvain-la-Neuve, Belgium, according to Mostert et al..[8]. Strain 180 belongs to *P. viticola* (Sacc.) Sacc., strain 239 and 281 belong to the *Phomopsis viticola* complex and strain 275 is an unidentified species belonging to the *Phomopsis* genus.

2.1.1. Fungal cultures and extraction

The fungal strains were grown on PDA in Petri dishes for 21 days in the dark at 23± 1°C.

The fungus was grown on Potato Dextrose Agar (PDA) purchased from Fluka (Cat. N° 70139). Thirty nine grams of agar were dissolved in 1L of deionised water and autoclaved for 25 minutes at 120°C. The solution was then poured in 9 cm diameter Petri dishes under a laminar flow. Inoculation was done by cutting small squares (~ 5 mm) from mother strains and placing them in the center of the dishes that were then sealed with parafilm.

The strains were regularly subcultured from the mother strains. Extraction was performed by cutting up the agar plates with the fungus on it, putting the pieces in 2.5 L Erlenmeyers

flasks, adding ethyl acetate and then extracting using a mechanical agitator. The extraction lasted 48 hours during which the solvent was changed three times. The extract was then evaporated on a rotary evaporator under vacuum et 30°C.

The crude extract obtained was fractionated by open column silica chromatography (mesh 63-200 µm) using solvents of increasing polarity (hexane, chloroform, ethyl acetate, acetone and methanol) to yield 15 to 20 fractions. Each fraction was analysed by TLC and then further purified by the most appropriate method. Since several crude extracts were necessary to obtain sufficient amounts of the compounds for analysis and since these extracts were different between each other, the fractions in which the compounds were found and the methods used for their purification were always different and adapted to the situation: a silica gel open column, a neutral aluminium oxide column, a gel-exclusion column (LH-20) or by preparative TLC silica gel chromatography were the most common methods used.

The first fractions usually contained a certain amount of lipids (up to 50%) and were thus re-chromatographed with an open 32-63 µm mesh silica gel column. Sample purification was monitored by TLC or by routine ^{1}H 200 MHz NMR analysis. Compounds were further purified by semi-preparative HPLC before being analysed by the standard 1D and 2D NMR techniques and mass spectrometry in order to determine the structure of the metabolites.

2.2. Fungal cultures on grapevine wood

The grapevine wood of the chasselas cultivar was pruned after harvest in a field at the Agroscope of Changins, Switzerland. The wood was left to dry at room temperature for several months and was then ground into a coarse powder which was left to macerate in water. After 48 hours it was strained and 800 grams were put in a plastic bag equipped with a filter to allow gas exchanges. The bags with the wood were then sealed and sterilized at 120 °C in an autoclave for 50 min. After cooling down, each bag was inoculated with 4 to 6 pieces (app. 0.5 x 0.5 cm) of PDA on which the fungus had grown for 7 days and then sealed again (Figure 3.49). A control was made by inoculating the bags with PDA only.

After 21 days, the content of the bags was extracted. For this the powdered wood was left to macerate in deionised water for 24 hours, the water being changed once after 8 hours. The two water extracts (after 8 h and 24 h of maceration) were combined and then centrifuged at

3000 rpm for 10 min in order to precipitate the small wood particles. The supernatant was filtered on a Büchner funnel with a round filter paper and then extracted with ethyl acetate in a 5 L separatory funnel. The solvent was evaporated to obtain the first crude extract, the "water extract".

After this treatment, the wood was left to macerate with ethyl acetate for 24 hours, the solvent being changed once after 8 h. As for the previous treatments the extract was centrifuged, filtered and evaporated to obtain the second crude extract, the "AcOEt extract".

2.3. Bioassays

The toxicity of the isolated compounds and of the different fungal strains was tested on grapevine leaves of *V. vinifera cv. Chasselas*. The compounds were dissolved in 1 mL of a 2% ethanolic solution in water in order to obtain 100, 200 and 500 µg of compounds in each well. The leaf-disks were excised carefully in deionised water with a cork borer to avoid major veins from the sampled leaves. Three to fours disks (∅ 5 mm) were placed in the wells containing the compounds. Water was then added in order to obtain a total volume of 1 mL and no more than 2% ethanol. The concentrations tested were 100, 200 and 500 µg .

A control was made by placing the three disks in the 2% aqueous ethanol solution. A positive control solution was made using eutypine, because it is a well-known phytotoxic compound produced by another fungus pathogen of grapevine, *Eutypa lata*. Activity of the compounds was based on visual assessment of the extent of the necrotic lesions after 24 h at room temperature. The necrosis rating was given as a percentage compared to the total leaf-disk surface which is of 19.63 mm^2 (leaf radius 2.5 mm).

2.4. Solvents

Solvents used for extraction, solubilisation, column chromatography were of technical quality and were distilled twice before being used.

Methanol, acetonitrile and tetrahydrofuran used for HPLC were all HPLC-grade and were purchased from SDS (cat. n° 093337G21; Peypin, Fr) for MeOH and from Acros Organics (Geel, Be) for ACN (cat n° 325730025) and for THF (cat n° 268290025).

2.5. TLC

Thin-layer chromatography (TLC) was used for routine analyses and chemical screening of crude extracts, fractions and isolated pure compounds.
TLC analyses were performed on different types of plates:

- Pre-coated Merck silicagel 60 F_{254} aluminium sheets (Merck, Darmstadt) for normal phase TLC
- Merck RP-18 plates for reversed-phase chromatography
- Neutral aluminium oxide plates were purchased from Macherey-Nagel

Typical solvent mixtures used for elution on normal phase plates were $CHCl_3$/MeOH 9/1 (v/v), AcOEt/MeOH 4/1 (v/v) and $CHCl_2$/toluene/cyclohexane/acetone 9/2/2/1 (v/v/v/v). Conditions were obviously adapted to the specificity of each sample analysed. The revelators used were either UV (254 and 366 nm) or a chemical spray reagent. The latter consisted of a spray of either 1% sulphuric acid in MeOH or 1% sulphuric acid in MeOH with vanillin (10mg/L). The plate is sprayed with this mixture then heated at over 400°C for a few seconds.
For Rp-18 plates, a MeOH/H_2O mixture was used.

Preparative TLC was also performed using 20x20 cm preparative silica plates (Uniplates) with a layer thickness of 0.5 mm. This technique was used for the purification of small quantities (< 10 mg) which could not be performed on open columns. The solvent mixtures used was first determined by analysis on normal phase TLC late.

2.6. Open columns

The size of the column and the granulometry of the silica gel were determined according to the amount of the sample and the degree of separation desired.
For the fractionation of the crude extract silica gel with particle size ranges 63-200 µm was employed whereas particle size ranges 32-63 µm was preferred for purification of the different fractions (Chemie Brunschwig AG, Basel, CH).
Isocratic systems or stepwise gradient eluents were employed, depending on the nature of the components and of their separation. When the sample was soluble in the starting eluent, the sample was deposited as a solution. As in our case the samples were insoluble (for example

the crude extracts), a solid deposit was made by mixing the sample with a quantity of silica gel corresponding to 2-3 times its weight and dried by rotary evaporation before application to the top of the column.

Some separations were performed using gel exclusion chromatography with Sephadex LH-20 (Amersham biosciences). The eluent was either methanol or a 1:1 mixture of chloroform:methanol. The columns used were usually long and thin (70 x 1.2 cm or 70 x 1 cm).

2.7. HPLC

2.7.1. Analytical HPLC

Analytical high pressure liquid chromatography was used to:

- analyse crude extracts and fractions
- guide the separation and isolation processes
- optimise the conditions for semi-preparative HPLC
- check the purity of the isolated products

Two HPLC systems were employed: the Hewlett Packard HP-1050 and the HP-1090 series II, both equipped with a diode-array detector (DAD) for UV-Vis detection. Data recording and analysis was done with the HP ChemStation software. These equipments allowed analyses in isocratic mode or gradient mode.
The analytical column used was a Nucleosil 100-7 C-18 (250 x 4.6 mm i.d., granulometry 7μm, cat. n° 721609.46, Macherey-Nagel, Düren, Germany) with a guard column of the same material (CC 8/4 Nucleosil 100-5 C18, cat n° 721602.40, Macherey-Nagel, Düren, Germany).
Solvents were filtered on a Millipore nylon membrane 66 (0.45 μm x 47 mm, Supelco, Bellafonte, USA). Degassing was done continuously with Helium (Carbagas, CH).

The standard run used for crude extract analysis, compound screening, purification check, and the different LC-MS analyses was as follow:

Time [min]	Solvent percentage	
	MeOH	H_2O
0	40	60
5	40	60
30	90	10
40	100	0
45	100	0

The flow rate was set at 1 mL/min, temperature was room temperature (20-24°C) and detection was made at 220, 254, , 280, 320, 360 and 450 nm.

The following retention times were obtained in these conditions for the isolated metabolites: compound **1**: 22.8 min, compound **2**: 19.7 min, compound **3**: 7.3 min, compound **4**: 10.3 min, compound **5**: 28.7 min, compound **6**: 38.1 min, compound **7**: 13.3 min, compound **8**: 12.6 min, compound **9**: 5.7 min.

2.7.2. Semi-preparative HPLC

Semi-preparative HPLC was used in order to purify the compounds isolated. The semi-preparative column were used was a Nucleosil 100-7 C-18, (250 x 8 mm i.d., Macherey-Nagel) connected to either a HP-1090 series II, HP-1050 or Waters 600 system equipped with a UV-vis detector. The flow rate was set to 3.5 ml/min and the UV detection to 254 nm. Separations were done at a temperature of 40°C on the HP-1090 and at room temperature (20-25°C) for the HP 1050. Optimal separation conditions were first determined using analytical systems and then conditions were adapted to the semi-preparative scale.

2.8. Mass spectrometry

The mass spectroscopy analyses were performed on two instruments: the LCQ (Thermofinnigan, San José, California) equipped with either an ESI or an APCI source and a quadrupole ion trap; and the LC/MSD (Agilent technologies) equipped with either an ESI or

an APPI source and a quadrupole ion trap. The ionisation conditions were adapted for each analysis but were generally used as described below:

- For the LCQ :
  - ESI : spray voltage 3-6 kV, sheath gas flow rate (N_2) 80 arb, capillary voltage 10 to 50V, heated capillary temperature 200°C.
  - APCI: discharge current 4-5 μA, vaporizer temperature 450°C, sheath gas flow rate (N_2) 80 arb, capillary temperature 150 to 200 °C ; in the negative ion mode : source current 3-4 μA, vaporization temperature 450 °C, sheath gas flow (N_2) 80 arb, capillary temperature 150 °C.

- For the LC/MSD :
  - ESI: source voltage 3-6 kV, nebuliser 20-40 psi, dry gas 12 L/min, dry temp. 300°C, capillary voltage 10 to 30 V, heated capillary temperature 200°C.
  - APPI: nebuliser 60 psi, dry gas 12 L/min, dry temp. 300°C, heated capillary temperature 200°C, addition of the dopant (acetone) was done postcolumn before sample nebulisation via a low volume tee at a flow rate of 20 L/mn.

2.9. LC-MS

High performance liquid chromatography (HPLC) coupled with mass spectrometry (MS) and DAD-UV detection, was performed for the analysis of the crude extracts of the strains as it allows for a high selectivity and efficacy of separation for the HPLC and structural information with low detection limits for the MS detection.
Mass spectrometry detection was done by the same equipment as described in point 2.8 and was connected to either HPLC machines as described below:

- The LCQ was connected to an Agilent-1100 system (degasser, pump and UV detector). Injections were done manually via a Rheodyne injector and controlled by the HP 110 controle module G1323A.

- The LC/MSD was connected to an Agilent-1100 system (degasser, pump, injector and DAD-UV detector) equipped with an automatic sampler and controlled by the HP-ChemStation® software.

For both instruments, the ion trap allowed for multiple stage tandem mass spectrometry, MS^n analysis, single ion monitoring (SIM) and multiple reaction monitoring (MRM).

2.10. NMR

NMR spectra were not only used to elucidate the structure of compounds but also for routine analyses of the fractions of the crude extracts.

^1H, ^{13}C NMR, DEPT 135, COSY, HMQC and HMBC spectra were recorded on a Bruker AMX-400 instrument at 400 (^1H) and 100 MHz (^{13}C). The HMBC spectra were recorded with a reverse-head for extra sensitivity.

Compounds **6** and **9** were analysed at the University of Fribourg by Mr. F. Fehr using a Bruker Avance DRX500 instrument at 500 and 125 MHz for the ^1H and ^{13}C spectra respectively.
Routine ^1H NMR spectra were recorded on a Gemini XL-200 Varian instrument at 200 MHz. Deuterated solvents ($CDCl_3$ (δ_H = 7.26 ppm), CD_3OD (δ_H = 3.34 ppm) and aceton-d6 (δ_H = 2.09 ppm) Cambridge Isotopes Laboratories, CIL, Andover, USA) were used to measure NMR spectra. The shifts are indicated in ppm, with tetramethylsilane (TMS) used as external standard.

3. Results

3.1. Strain selection

Ten strains of *Phomopsis* were studied in the project. The strains were collected from a grapevine field in Ticino, Switzerland (see Material and Methods, 2.1).
Even though it is quite impossible to isolate, purify and identify all compounds produced by the fungus, due mostly to the small amount of compounds that are produced, HPLC provides a very powerful method for the separation and detection of metabolites. One of the advantages is the detection of groups of compounds belonging to the same families, as biosynthetically related metabolites usually have the same chromophore groups. Hence, this technique was used for the screening of the ten strains and to decide which strains would be selected for further up-scale study. The crude extracts obtained were thus analysed by HPLC (see section 2.7 for more details) coupled to a DAD. This detector has the advantage of being able to measure absorbance at different wavelengths. Since it is not known what kind of chemical structures to expect, absorbance was measured at several wavelengths: 220, 254, 280, 360 and 450 nm. Only the chromatograms at 254 nm are shown here but all of them were taken into account.
For one hundred Petri dishes extracted (per strain), the crude extract weighed approximately 1.0 g with approximatively 40 to 50% of this being lipids, depending on the extract.

Strains 00, 110 and 301 seem to have produced very little UV absorbing compounds (Figure 3.1 and Figure 3.2), the chromatograms bearing nearly no UV absorbing peaks. Strains 239, 279, 281, 282 and 283 are more productive with peaks well distributed over a wide range of polarities which could be the result of a big chemical diversity although some compounds, such as stilbenes, do not have a great chemical diversity but are spred over a wide range of polarities (Figure 3.1 and Figure 3.2).
The chromatograms of strains 00 and 301 display several peaks but all with very small intensities. For strain 110, there is one major peak at a retention time of 25 minutes but the rest of the chromatogram bears barely any peak. With strain 180, there are several peaks but all rather in small quantities. For strain 239, the chromatogram shows a vast amount of different compounds, especially in the 15-35 minute time range, and also with high intensities. For strain 275, there are two major compounds that stand out at 24 and 31 min

and a few other peaks but with smaller intensities. Strains 279, 281 and 282 show interesting chromatograms with a good amount of compounds produced. The two former strains have several polar compounds coming out before 35 min. The chromatogram of strain 283 has five peaks standing out, with quite a lot of other compounds distributed all over the range of polarities.

Another point taken into account for the selection was bioassays with leaf disks to test the toxicity of the strains using the procedure described in section 2.3. Activity was assessed visually and was rated in the following manner: - : no activity, + : weak, ++ : strong, +++ : very strong (weak activity would correspond to a leaf disk surface less than 20% necrosed and strong more than 50%). In accordance with the chromatograms, the tests showed that strains 00 and 110 have weak activity. Strains 279, 281, 282, 283 and 301 all exhibit strong activities.

Based on results of the two tests, strains 180, 239 and 283 were chosen for upscale study. Strains 239 and 283 because they produced a reasonably elevated amount of compounds and showed high toxicity. Strain 180 because, despite the fact that its chromatogram bore few UV absorbing compounds, they showed toxicity and also because this strain was identified as belonging to the *Phomopsis viticola (Sacc.)* Sacc. species whereas the other strains were only identified as belonging to the genus *Phomopsis* (see Material and methods, 2.1, for further details). Time constraints did not allow us to study the remaining strains despite the interesting activites they showed.

Table 3.1 Results of the leaf-disk assays

Concentration	Strain								
	00	110	180	239	279	281	282	283	301
250 mg/L	+	-	-	-	+++	+++	+++	++	++
500 mg/L	++	++	++	+	+++	+++	+++	++	++

(- : no necrosis observed, + : weak , ++ : strong, +++ : very strong activity)

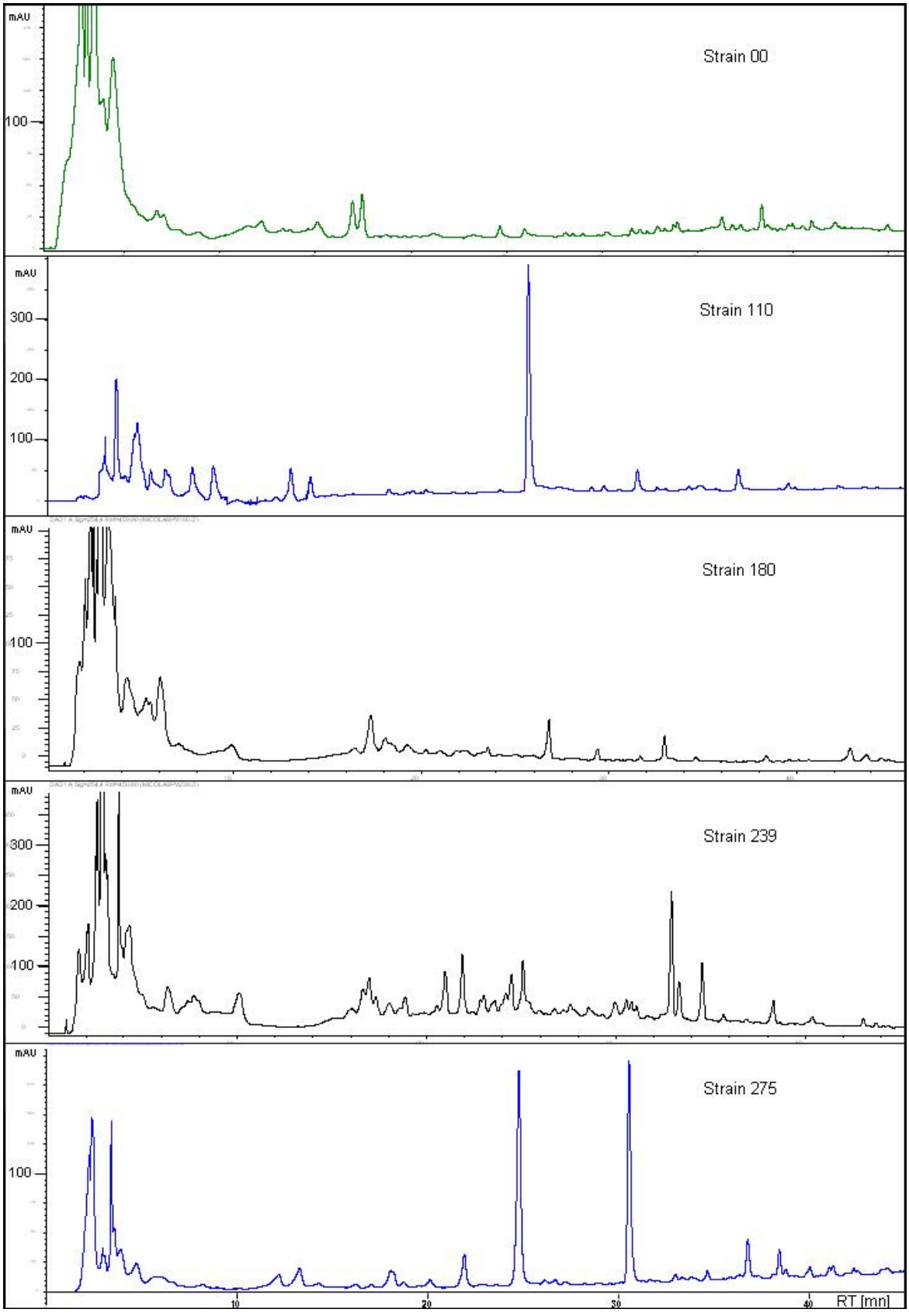

Figure 3.1 UV chromatograms of strains 00, 110, 180, 239 and 275 at 254 nm at 21 days (standard HPLC run)

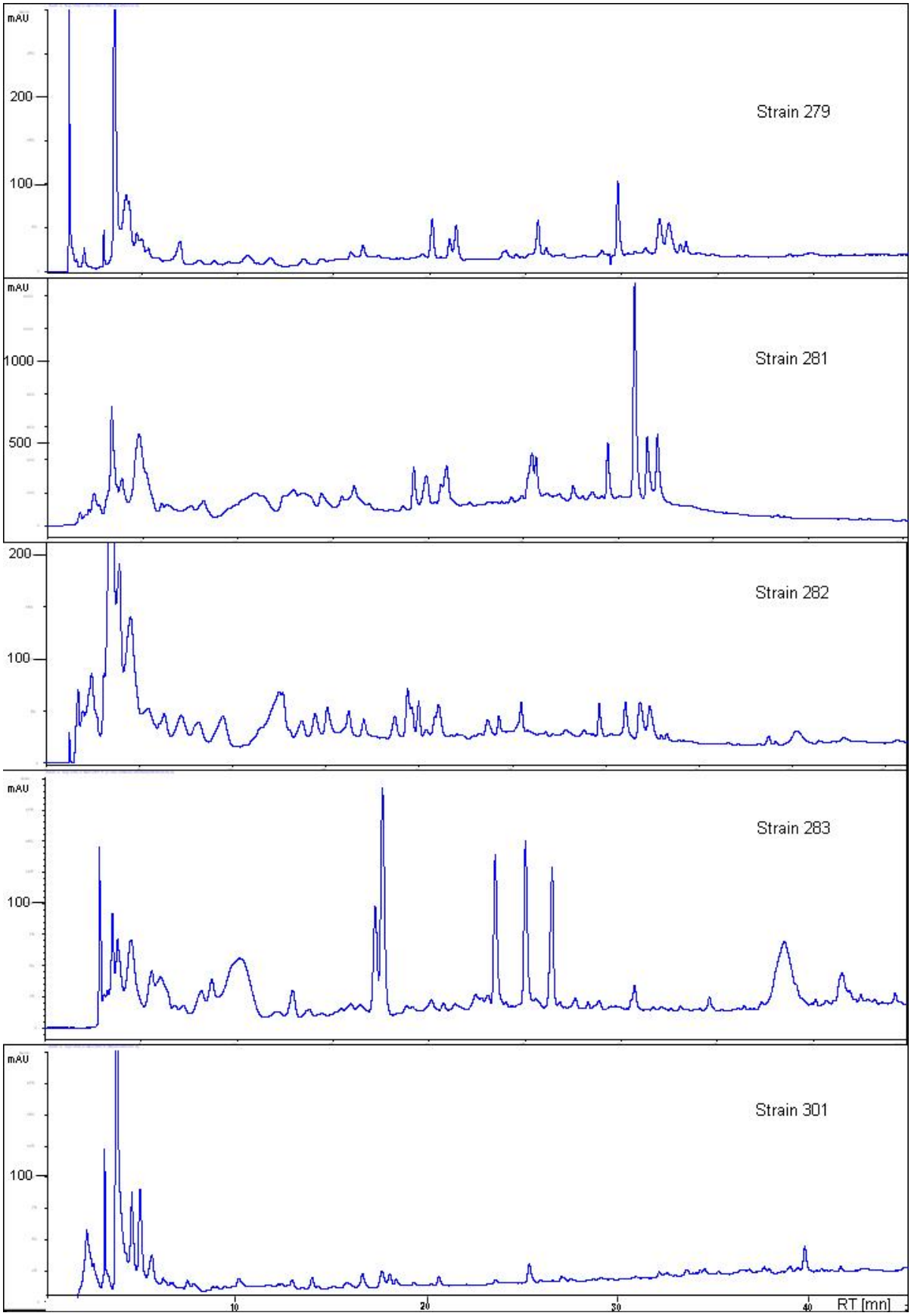

Figure 3.2 UV chromatograms of strains 279, 281, 282, 283 and 301 at 254 nm (standard run)

3.2. Strain growth time

In order to determine the optimal growth time for the isolates, strains 180 and 239 were selected and grown for 14, 21, 28 and 35 days. One hundred Petri dishes were inoculated per strain. After 14 days of growth, 25 Petri dishes were taken and extracted with ethyl acetate. This operation was repeated after 21, 28 and 35 days. Once the solvent was evaporated, the crude extract was weighed and then analysed by HPLC (see Experimental, 2.7.1). Once again, absorbance was measured at several wavelengths: 220, 254, 280, 320, 360 and 450 nm.

There was a important weight increase of the crude extract from the two strains over time until 28 days. Later, a decrease occurred (Graph 3.1). This might be due to the fact that, after 28 days, the Petri dishes were completely filled by the fungus and there was no more substrate available for its development. Degradation of the metabolites could also be possible by enzymatic activity by the fungus. Furthermore, there was differences on the amount of crude extract obtained from the two strains (Figure 3.3).

This difference in metabolite production is also reflected in the chromatograms of the different strains (Figure 3.4 and Figure 3.5) which show very different profiles. After 14 days, only a few peaks can be observed for both strains whereas several peaks can be observed at 21 and 28 days. For strain 180, nearly no UV absorbing compounds can be seen at 28 and 35 days in the 10-35 min time range, contrasting sharply with the chromatogram at 21 days. The difference between strains is also flagrant as strain 239 produced many more UV absorbing compounds than strain 180. As for strain 239, there are less peaks present after 21 days but, strangely enough, the chromatogram at 35 days has more peaks than at 28 days.

Based on these considerations, the two strains were grown for 21 days for the current study, which seems to be the optimal growth time for metabolite production in our conditions.

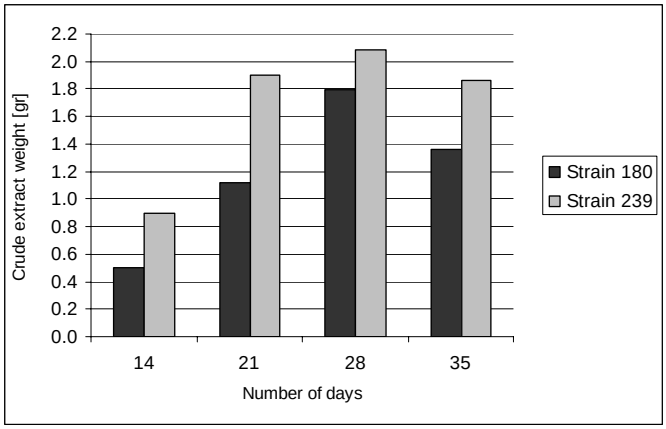

Figure 3.3 Weight of the crude extracts for strains 180 and 239 at different growth times.

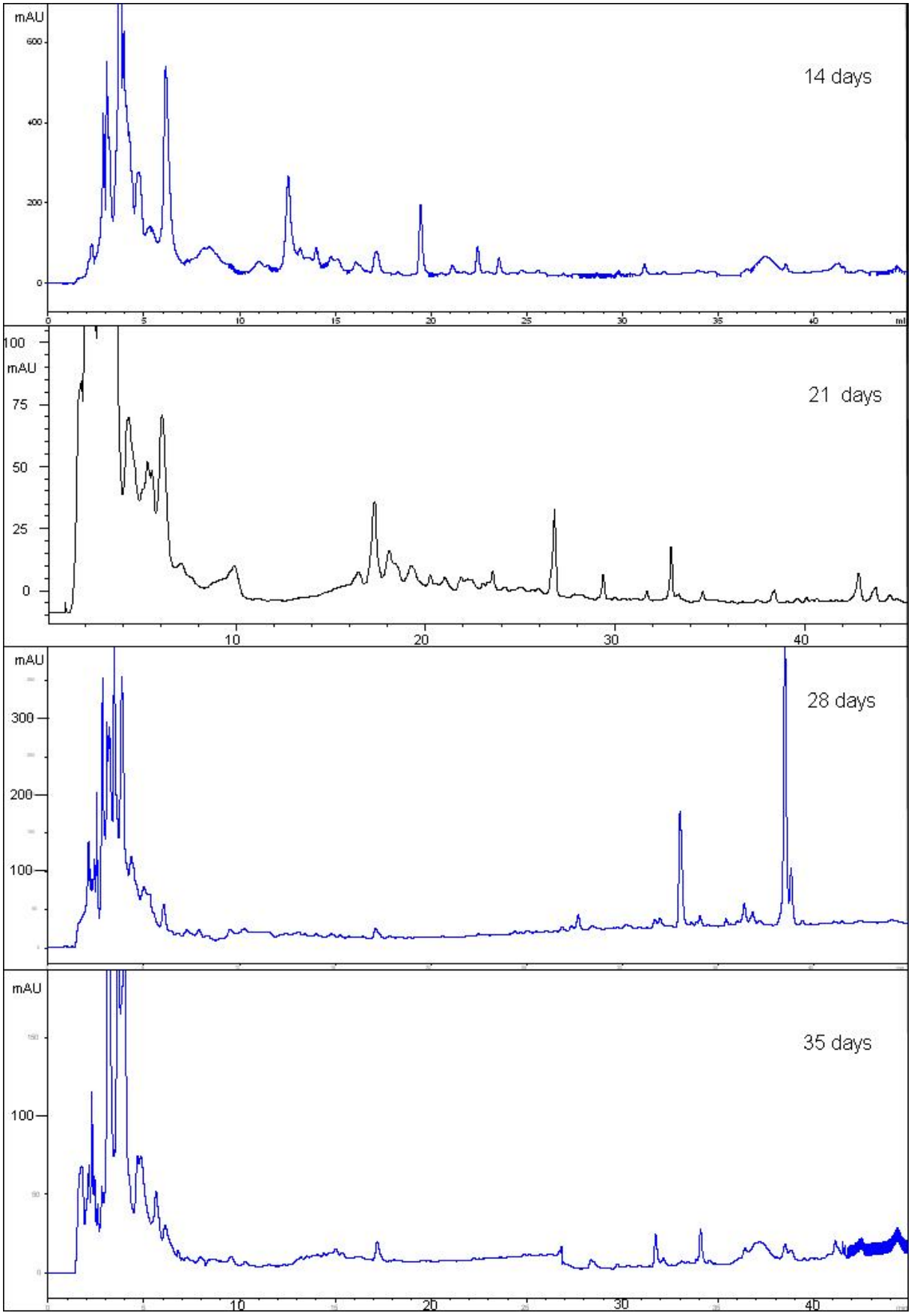

Figure 3.4 Chromatogram at 254 nm of the extract of strain 180 at 14, 21, 28 and 35 days

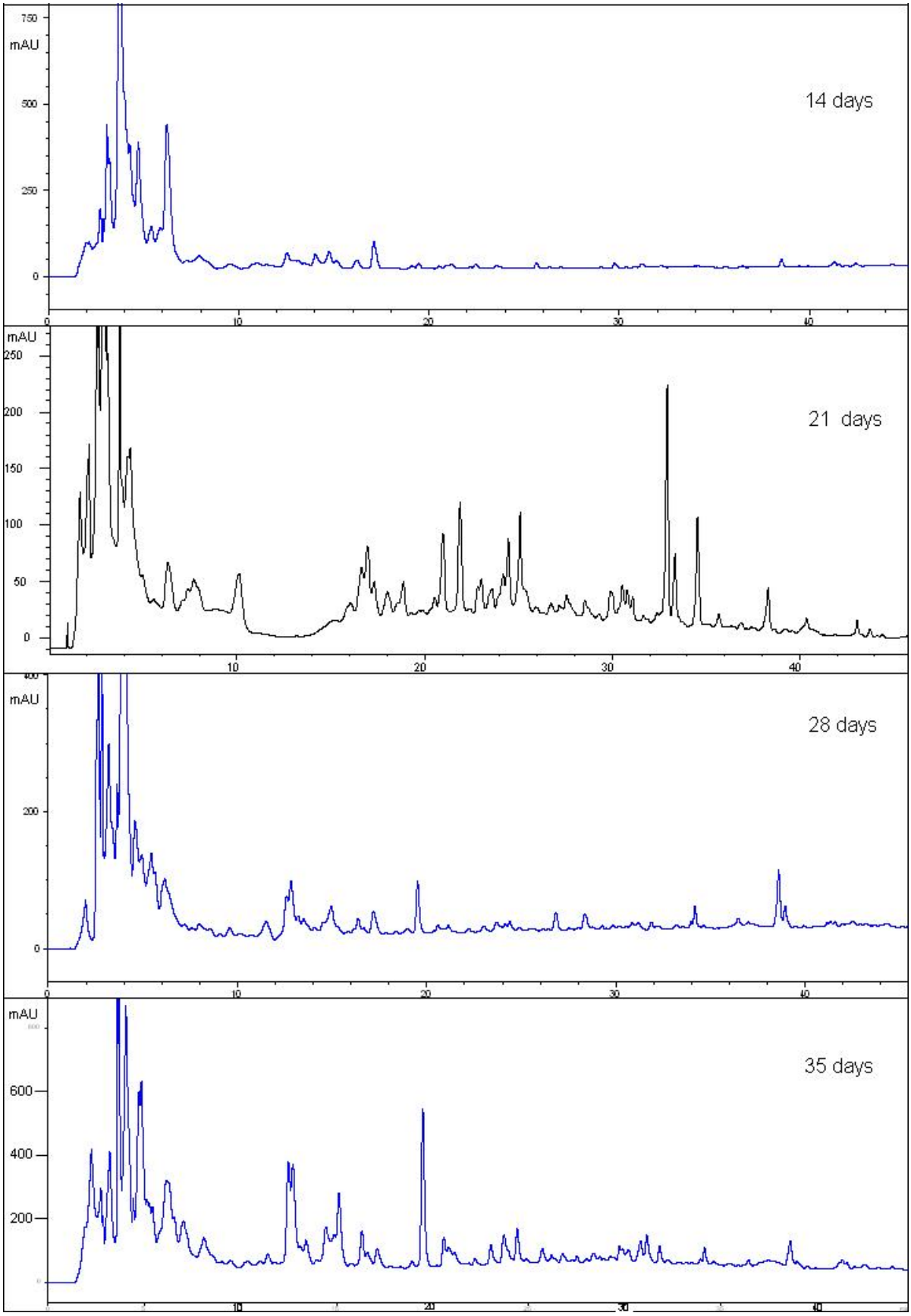

Figure 3.5 Chromatogram at 254nm of the extract of strain 239 at 14, 21, 28 and 35 days

3.3. Isolated compounds

Nine compounds were isolated from the crude extracts of *Phomopsis* sp. (Figure 3.6). In order to isolate and identify these compounds, several crude extracts had to be obtained by repeatedly sub-culturing the fungi and the compounds isolated from each crude extract in order to have sufficient amounts for analysis, typically 1 to 2 mg of each compound. Each of these extracts were different from each other and thus the isolation procedure were never twice the same and had to be adapted to each situation. Hence, the compounds were never purified twice in the same manner.

Among these, compounds **2**, **4**, **5**, **6** and **8** are to our knowledge new natural products. Compounds **1**, **3**, **7** and **9** had already been isolated from fungi[61-63].

Compounds **1** to **6** and **9** were isolated in strain 239, compound **4** in strain 180 and **5** in both strains 180 and 239 and compounds **7** and **8** from strain 283. All compounds were isolated in quantities ranging from 1 to 2 mg by accumulation from several crude extracts. They were all purified by semi-preparative HPLC except for the two xanthones, **1** and **2**, that were purified by semi-preparative TLC.

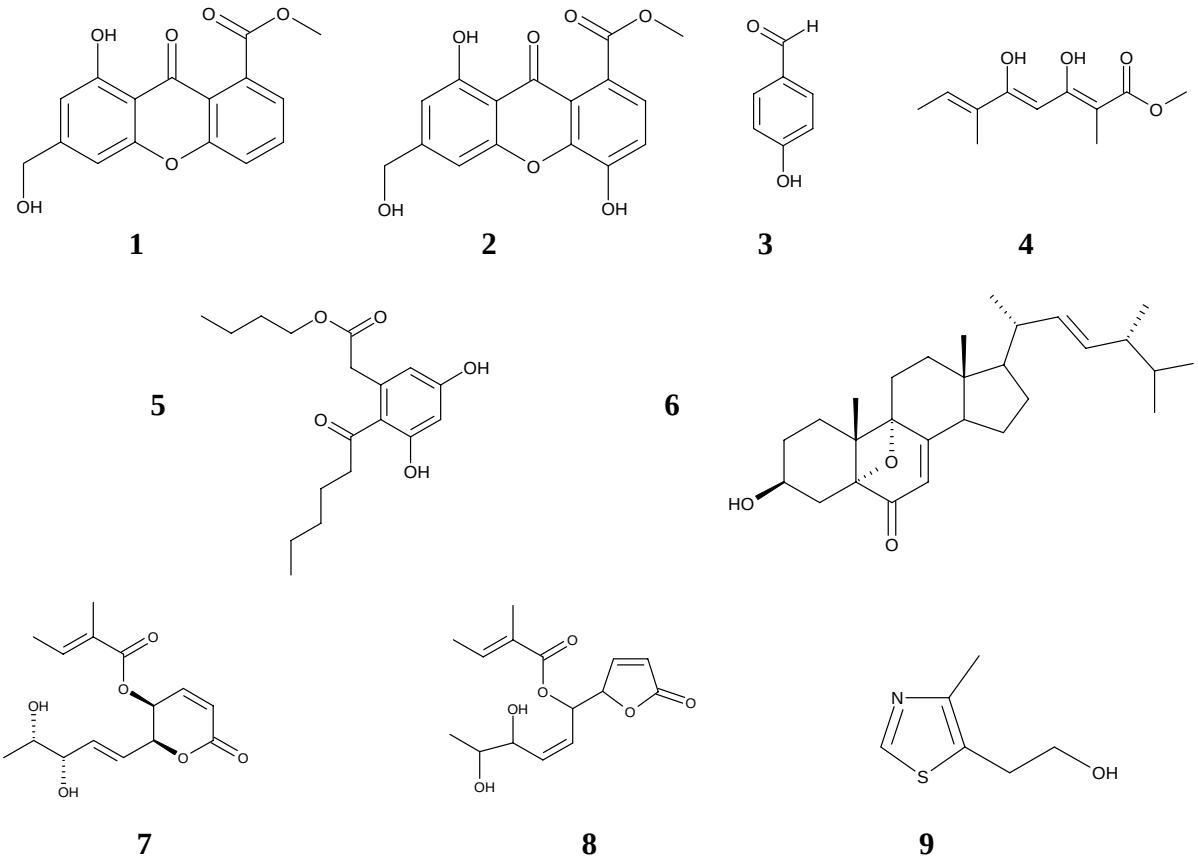

Figure 3.6 The structures of the isolated metabolites

3.3.1. Compound 1: 1-carboxymethyl-6-(hydroxymethyl)-8-hydroxy-xanthone (Sydowinin A)

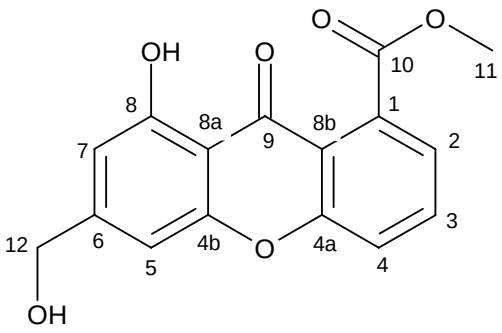

The first isolated compound is 1-carboxymethyl-6-(hydroxymethyl)-8-hydroxy-xanthone which was purified by preparative TLC (Rf 0.49 with Pre-coated Merck silicagel 60 F_{254} aluminium sheets, CH_2Cl_2/toluene/cyclohexane/MeOH 9/1.8/2/1.2 v/v/v/v, yellow spot with

1% H_2SO_4/MeOH, see section 2.5) . It has a retention time of 22.8 min with the standard HPLC run (Figure 3.10).

This compound, Sydowinin A, was first isolated and described in 1975 by Hamasaki et al.[63;64] who had isolated it from a mold (*Aspergillus sydowi)*. However, the identification of this compound was only done by its ^{1}H NMR spectrum and chemical reactions. Here we report for the first time the complete characterisation by ^{13}C and 2D NMR.

Hamasaki and our ^{1}H spectra show the same signals with five aromatic protons, three protons for a methyl group and two protons of a CH_2 (Figure 3.8). The coupling constants and the COSY spectrum show that three of the aromatic protons, at 7.78, 7.56 and 7.33 ppm, are on the same ring and the other two, at 6.95 and 6.70 ppm, on another one.

For one of the rings, the ^{1}H- ^{13}C HMBC spectrum (Figure 3.9) shows the correlation between the protons H-2 and H-4 (at 7.33 and 7.56 ppm respectively) with the carbon C-8b at 117.8 ppm and the correlation of protons H-3 and H-4 (at 7.78 and 7.56 ppm) with carbon C-4a (156.3 ppm). The proton H-2 and those of a methyl group at 4.0 ppm are correlated with the carbon C-10 at 170.0 ppm thus suggesting the presence of a free methylic ester attached to the aromatic ring by carbon C-1. On the second ring, the coupling constant (J = 1.3 Hz) between the two protons H-5 and H-7 indicates a *meta*-coupling. The ^{1}H-^{13}C HMBC spectrum shows the correlation between the two aromatic protons H-5 and H-7 with the carbon of a CH_2OH moiety. The presence of a hydroxyl group on the carbon C-8 (162.0 ppm) is confirmed by the signal of the proton at 12.17 ppm due to the hydrogen bond with the oxygen of the carbonyl group.

Thus, it appears that the two rings must be linked by an ethylenic moiety which is confirmed by the chemical shifts of the two carbons atoms C-4a and C-4b (156.4 and 156.3 ppm) linked to the same oxygen and the presence of the carbonyl C-9 at 180.9 ppm which is correlated to the proton H-5.

The ESI-(+) mass spectrum of the compound gave a peak at m/z 323.1 Da which corresponds to the $[M+Na]^+$ ion and the APCI-(+) spectrum gives one peak at m/z 300.9 Da $[M+H]^+$ and one at m/z 269.2 corresponding to the loss of the CH_3O moiety $[M+H-31]^+$. The molecular formula of the compound is $C_{16}O_6H_{12}$ with a mass of 300.27 Da.

Comparison of the carbon chemical shifts with those of various closely related compounds found in the literature confirmed our findings[61;65-70]. Ayer et al.[65] isolated from a fungus (*Leptographium wageneri*) two xanthones, one of which was also substituted in position 1 by a carboxymethyl and in position 8 by a hydroxyl group (Figure 3.7). Comparison of the carbon chemical shifts with our values is given in

Table 3.2.

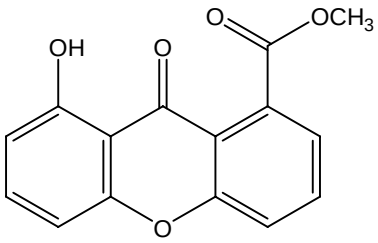

Figure 3.7 Structure of the xanthone isolated by Ayer et al. [65]

Table 3.2 Chemical shifts for compound **1** (in $CDCl_3$) and comparison with literature (^{13}C: 100 MHz, $CDCl_3$; ^{1}H: 60 MHz DMSO-d6)

	Compound **1**		Literature[63;65]	
Position	^{13}C NMR	^{1}H NMR	^{13}C NMR[65]	^{1}H NMR[63]
1	133.8 (C)	-	133.7	-
2	122.9 (CH)	7.33 (dd)	122.7	7.46
3	135.4 (CH)	7.78 (dd)	135.1	7.85
4	119.9 (CH)	7.56 (dd)	119.5	7.60
4a	156.4 (C)	-	156.1	-
4b	156.3 (C)	-	155.8	-
5	104.5 (CH)	6.95 (d, J =1.3Hz)	111.0	6.93
6	152.5 (C)	-	137.2	-
7	108.5 (CH)	6.70 (d, J=1.3Hz)	106.9	6.72
8	162.0 (C)	-	155.8	-
8a	108.2 (C)	-	109.0	-
8b	117.8 (C)	-	117.6	-
9	180.9 (C)	-	181.1	-
10	170.0 (C)	-	169.6	-
11	53.6 (CH_3)	4.0 (s)	53.2	3.88
12	64.7 (CH_2)	4.75 (s)	-	4.56

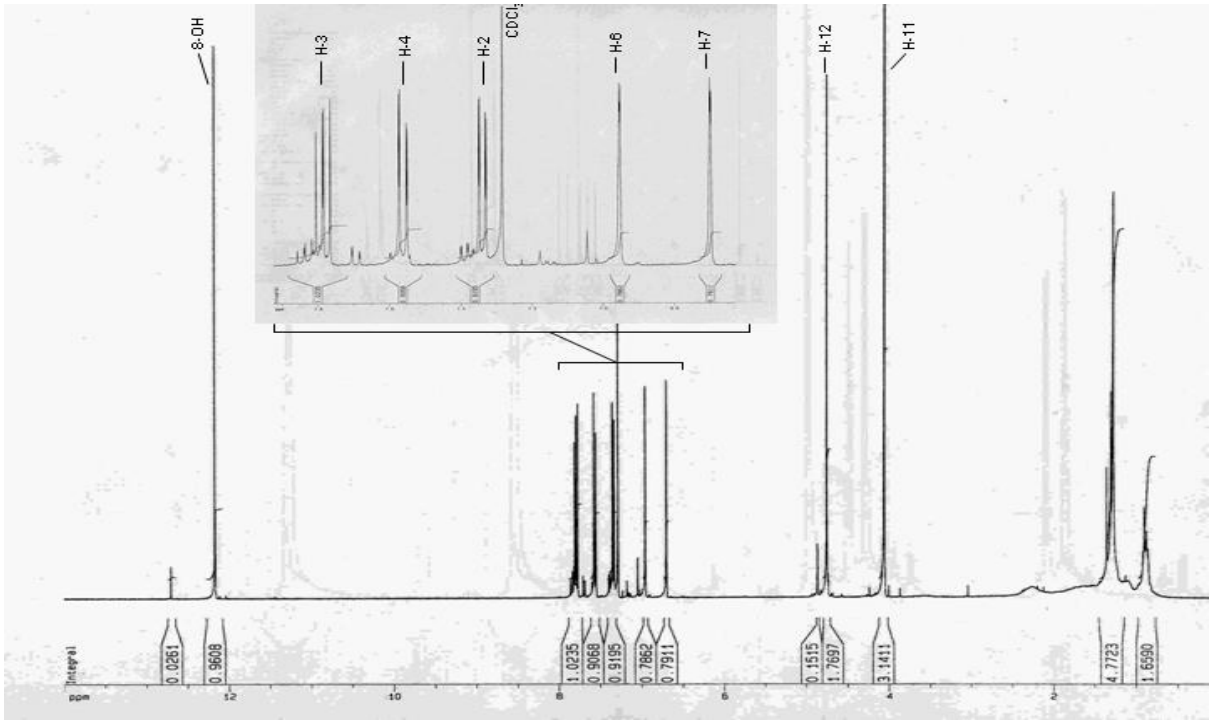

Figure 3.8 ^{1}H NMR spectrum of compound **1**

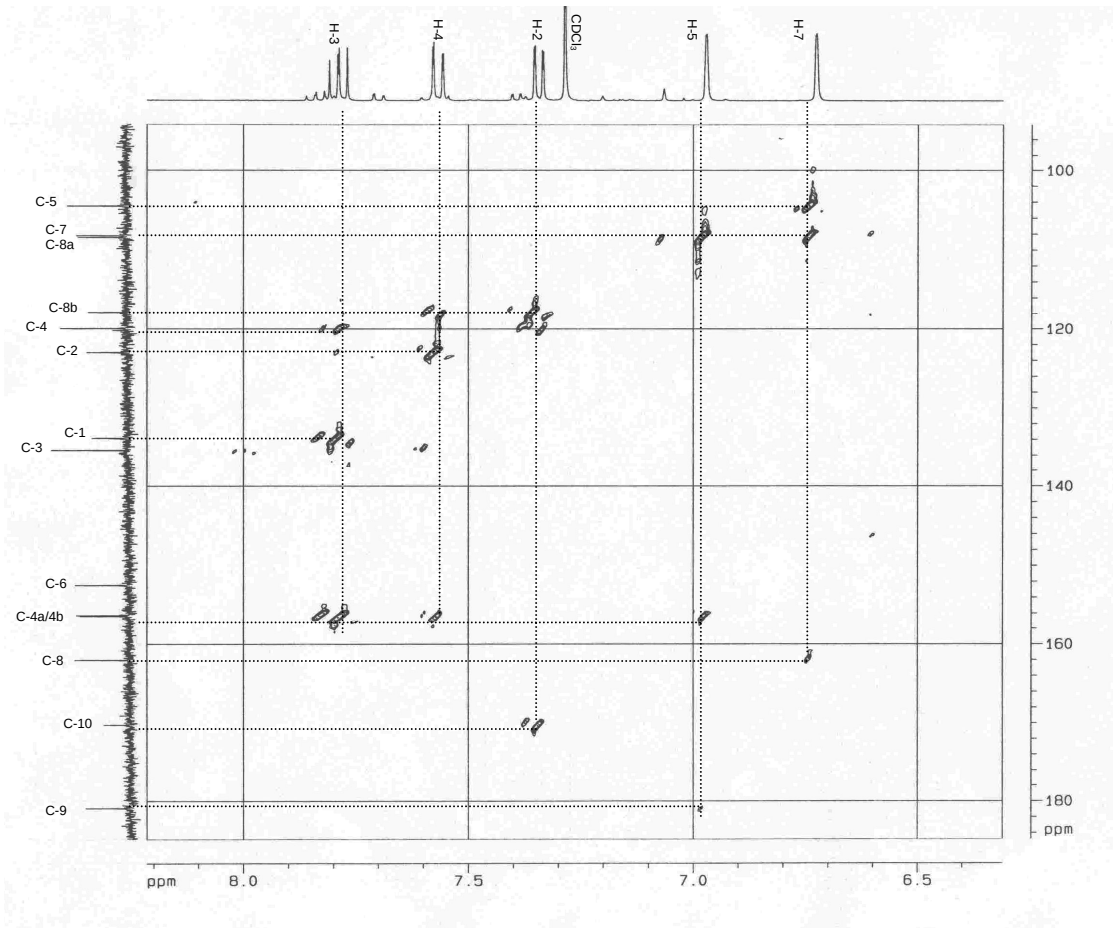

Figure 3.9 HMBC spectrum of compound **1**

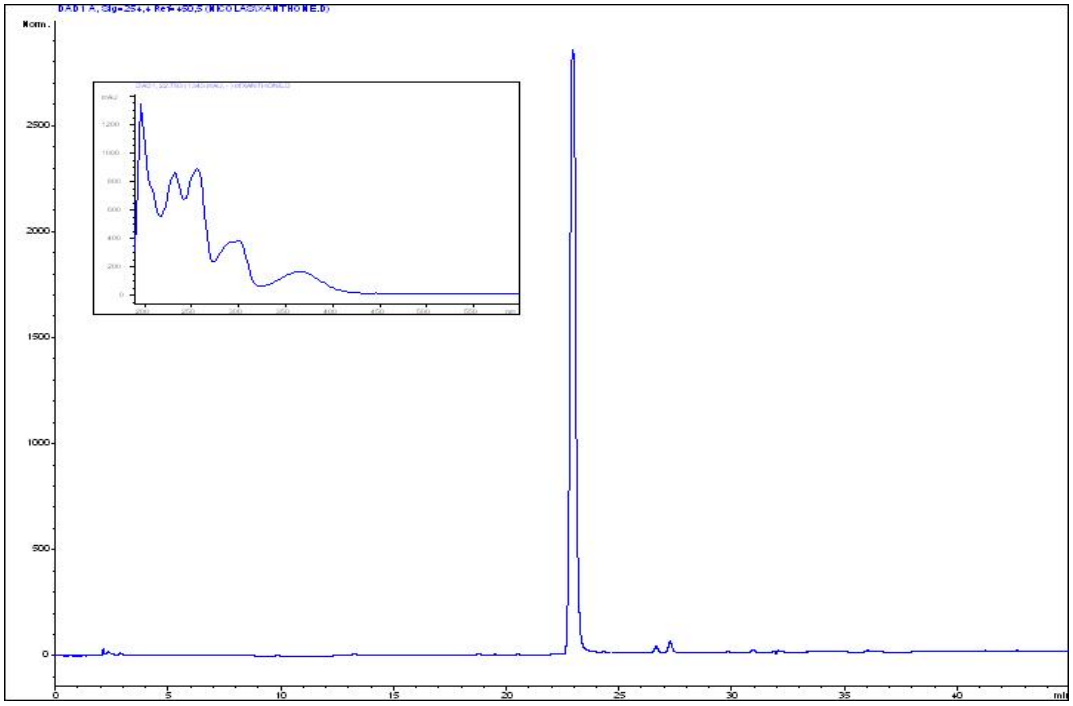

Figure 3.10 HPLC chromatogram of compound **1** (254 nm; standard run)

3.3.2. Compound 2: 1-carboxymethyl-4-hydroxy-6-(hydroxymethyl)-8-hydroxy-xanthone

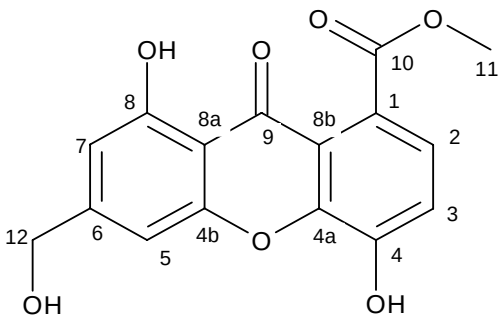

Compound **2** was isolated as a mixture with compound **1** in a 1:1 ratio. It has a retention time of 19.7 min with the standard HPLC run. By TLC, the Rf is 0.35 with pre-coated Merck silicagel 60 F_{254} aluminium sheets, CH_2Cl_2/toluene/cyclohexane/MeOH 9/1.8/2/1.2 v/v/v/v, yellow spot with 1% H_2SO_4/MeOH, see section 2.5.

Due to the small quantities (less than 1 mg), it was not possible to separate both compounds but the NMR spectra were still exploitable. Once the peaks for compound **1** were eliminated in the ^1H NMR spectrum (Figure 3.11), it appeared that the main difference between both was

the fact that **2** had only four aromatic protons (Figure 3.11). H-5 and H-7 are the same but there is one proton less on the first ring. These two protons appear as doublets with a coupling constant of J = 9.1 Hz, thus suggesting an *ortho* positioning.

In the long-range ^{1}H- ^{13}C HMBC spectrum (Figure 3.12), the proton signal at 7.37 ppm correlates with the same carbons than for compound **1**, i.e. C-8b and C-10, which suggests that it must have the same position, H-2. Consequently, the proton at 7.51 ppm will be in position 3. Whereas H-2 of compound **1** correlated with the carbon C-4 at 119.9 ppm, H-2 of **2** correlates with a carbon at 150.02 ppm thus indicating that it must be linked to a hydroxyl group.

These finding are confirmed by LC-ESI-MS/MS where the molecular ion peak $[M]^{+}$ of compound **2** is found at m/z 315.7 Da in the positive ion mode, and the MS^2 gives a peak at m/z 285, which would correspond to the loss of the OCH_3 moiety ($[M-31]^{+}$) confirming the molecular formula as $C_{16}O_7H_{12}$.

Chromatogram comparison between **1** and **2** is given in Figure 3.13 with their respective UV spectra.

Table 3.3 Chemical shifts for compound **2** in CD_3OD

Position	Compound **2**	
	^{13}C NMR	^{1}H NMR
1	130.39 (C)	-
2	120.30 (C)	7.51 (d, J = 9.1 Hz)
3	125.05 (CH)	7.37 (d, J = 9.1 Hz)
4	150.02 (C)	-
4a	151.37 (C)	-
4b	156.5 (C)	
5	104.25 (CH)	6.97 (d, J = 1.1 Hz)
6	153.3 (C)	-
7	107.5 (CH)	6.73 (d, J = 1.1 Hz)
8	161.65 (C)	-
8a	107.49 (C)	-
8b	118.06 (C)	-
9	181.12 (C)	-
10	169.2 (C)	-
11	52.23 (CH_3)	3.96 (s)
12	63.36 (CH_2)	4.67 (s)

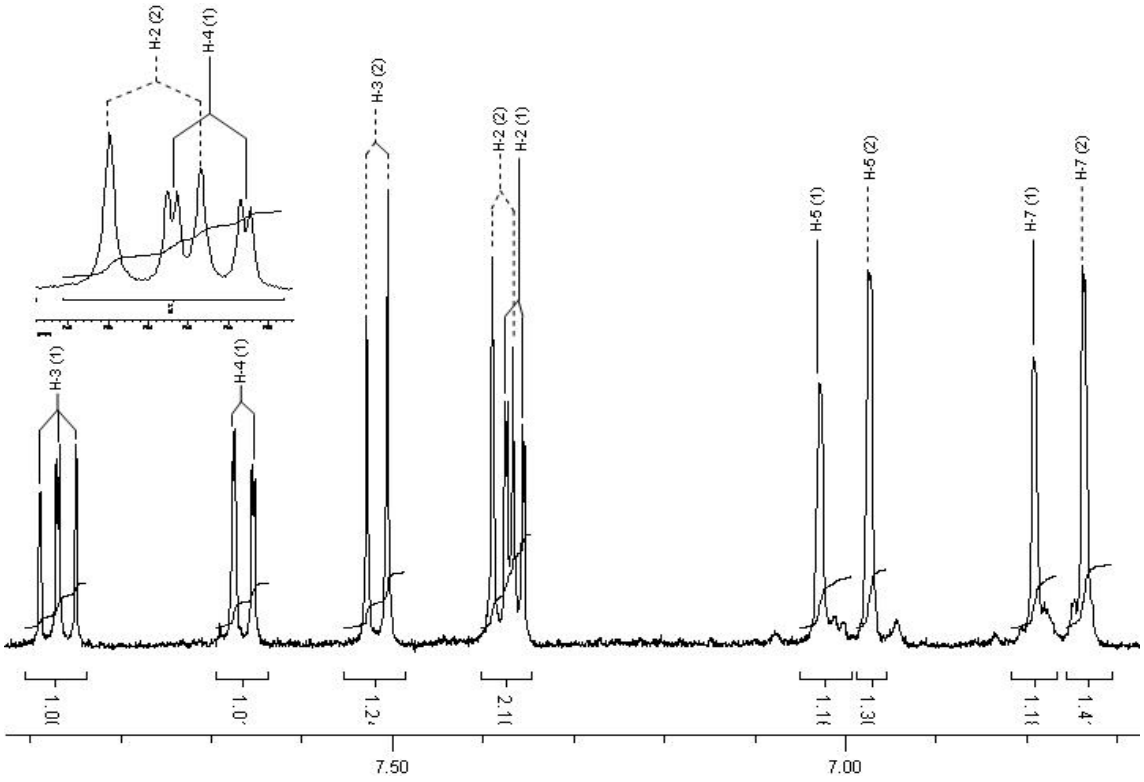

Figure 3.11. ^{1}H NMR spectrum of the mixture of compound **1** and compound **2** in the high-field region

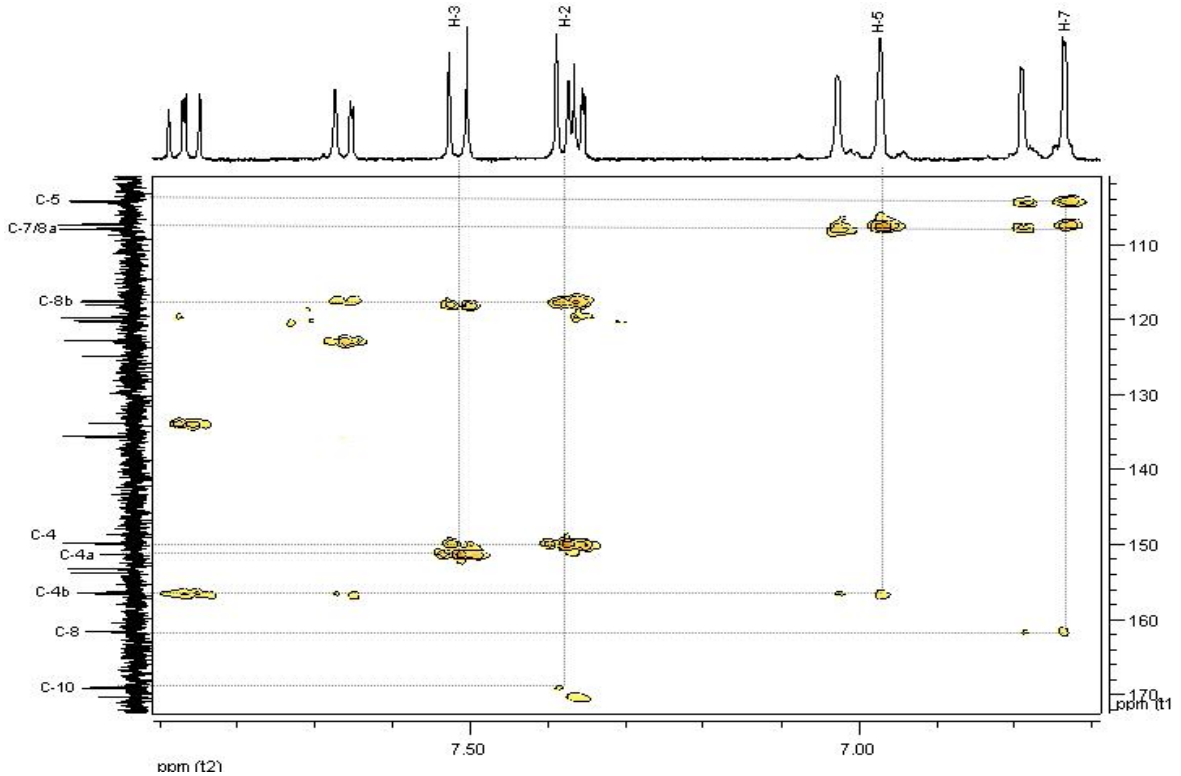

Figure 3.12. Long-range HMBC spectrum of the mixture of compounds **1** and **2**

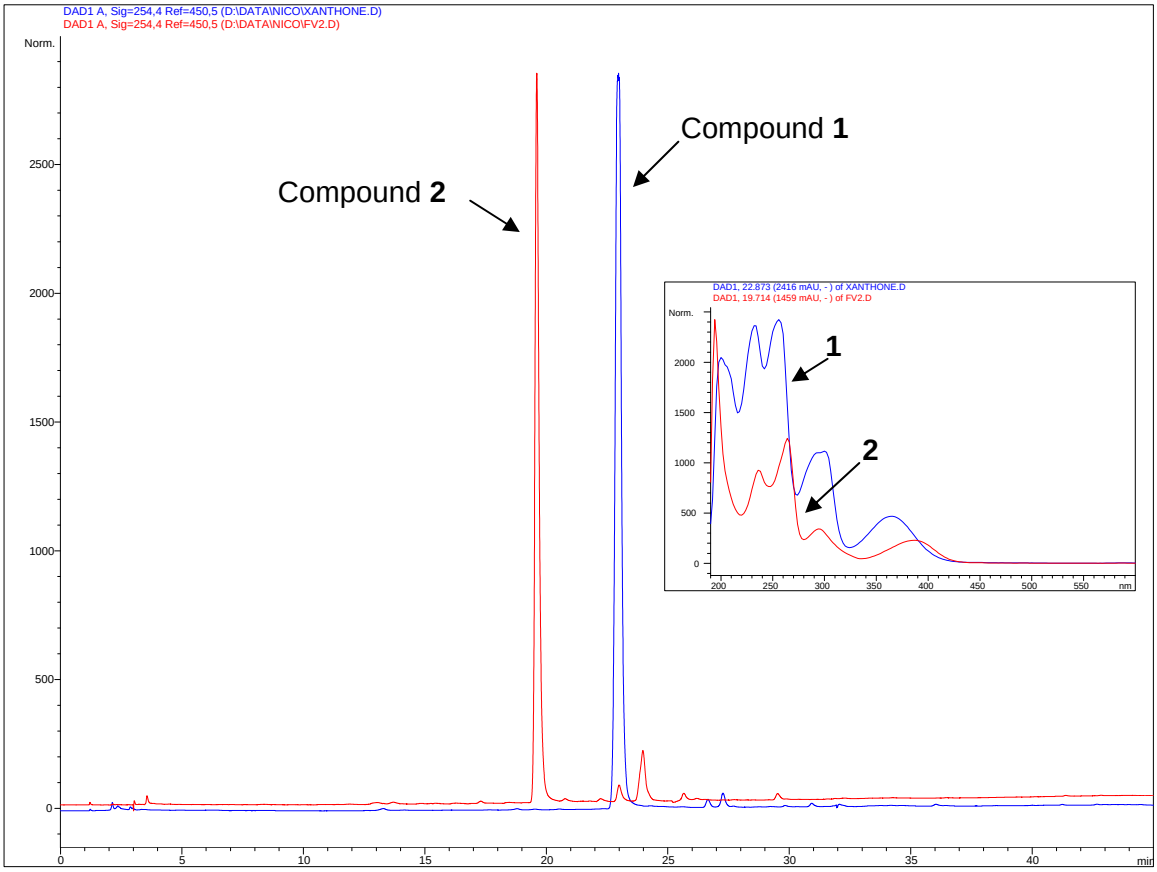

Figure 3.13 HPLC chromatogram comparison of compounds **1** and **2** with their respective UV spectra

3.3.3. Compound 3: *p*-hydroxybenzaldehyde

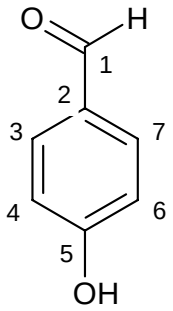

Compound **3** was found to be *p*-hydroxybenzaldehyde. It has a retention time of 7.3 min with the standard HPLC run (Figure 3.14)

The ^{1}H NMR spectrum showed only three signals at 9.89 (s), 7.83 (dt, J= 2.58 & 8.6Hz) and 6.98 ppm (dt, J = 2.58 & 8.6Hz), with the two latter signals integrating for two protons. It can

be deduced that the molecule is symmetric but also that two carbons of the aromatic ring are substituted.

The carbon spectrum gave five signals at 191.33, 161.83, 132.81, 130.37 and 116.35 ppm, the first chemical shift suggesting the presence of an aldehyde and the second one a hydroxyl group attached to an aromatic ring.

The ESI-(-) confirmed these findings with the molecular peak at m/z 121.1 $[M-H]^-$.

Table 3.4 Chemical shifts for compound **3** in $CDCl_3$

Position	^{13}C NMR	^{1}H NMR
1	191.33 (CH)	9.89 (s, 1H)
2	130.37 (C)	-
3/7	116.35 (2xCH)	7.83 (dt, 2H, J=2.58 & 8.6Hz)
4/6	132.81 (2xCH)	6.98 (dt, 2H J= 2.58 & 8.6Hz)
5	161.83 (C)	-

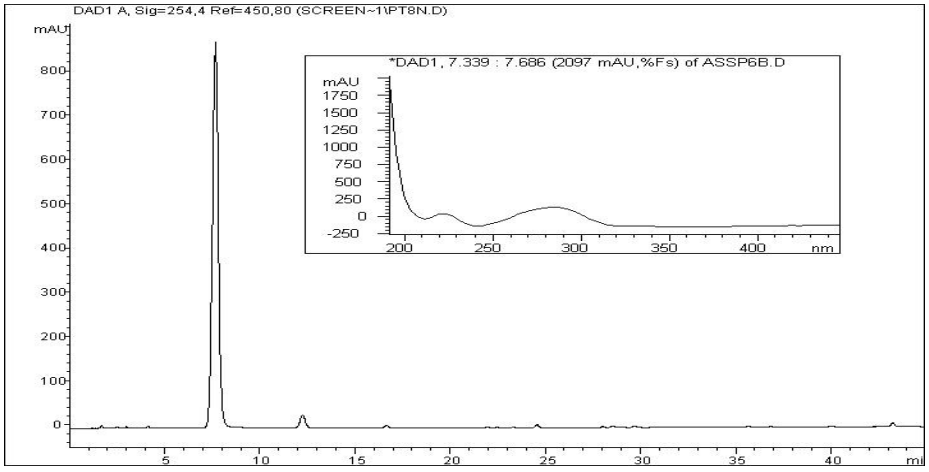

Figure 3.14 HPLC UV chromatogram of compound **3** (254 nm; standard run)

3.3.4. Compound 4: methyl 3,5-dihydroxy-2,6-dimethyl – octa-2,4,6-trienoate

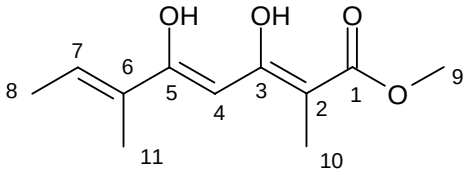

Compound **4** has a retention time of 10.3 min with the standard HPLC run (Figure 3.18) and a Rf of 0.26 with pre-coated Merck silicagel 60 F_{254} aluminium sheets, CH_2Cl_2/toluene/cyclohexane/Acetone 9/2/2/1 (v/v/v/v), black spot when sprayed with 1% H2SO_4/MeOH, see section 2.5.

The ^{1}H spectrum shows two singlet signals at 6.7 and 6.1 ppm and four singlets integrating for methyl groups at 3.9, 1.96, 1.91 and 1.86 ppm. The ^{13}C spectrum shows signals for five quaternary, two tertiary and four methyl carbons. Three of the quaternary carbons are oxygenated, with signals at 166.3, 165.5 and 160.6 ppm. ^{1}H-^{13}C correlations in the HMBC spectrum (Figure 3.17) can be seen between the proton H-7 at 6.7 ppm with the carbon at 160.0 and the methyl at 12.5 ppm. The protons of the methyl group (H-11) at 1.91 ppm are correlated to the carbons C-7, C-6 and C-5. The proton H-4 at 6.1 ppm is correlated with the carbons at 166.3, 160.0, 127.0, 102.0 ppm thus establishing its central position. The protons of the methyl C-10 at 9.0 ppm are correlated to three carbons, at 166.3, 165.0 and 102.0 ppm. Thus, four structures are proposed for this compound, **4**, **4'**, **4''**, and **4'''** (Figure 3.15). Proposition **4'''** was discarded since the two carbons bearing the same oxygen would probably have chemical shifts around 140 ppm and not 165.5 and 160.6 ppm as found. Compounds 4' and 4" would be very likely however only a NOe NMR experiment would allow to assign the structure with certainty.

The APCI-(-) mass spectrum shows a peak at 194.4 which would correspond to the $[M\text{-}OH\text{-}H]^-$ ion. The molecular formula is $C_{11}H_{16}O_4$ with a MW of m/z 212. Da. The UV spectrum shows two maxima at 254 and 294 nm in MeOH (ε = 690500 and 688369 respectively).

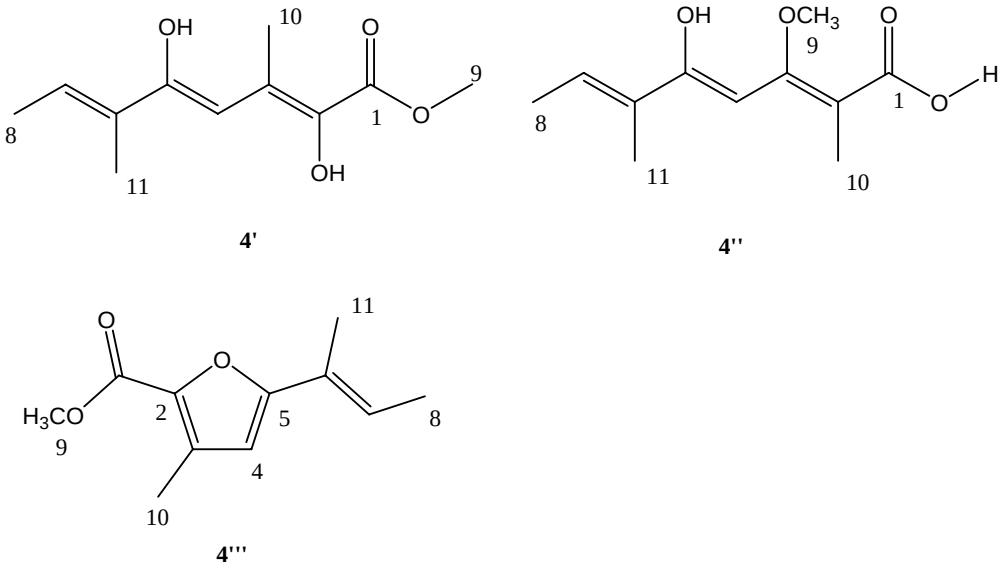

Figure 3.15 The three other possible structures proposed for **4**

Table 3.5 Chemical shifts for compound **4** in $CDCl_3$

Position	^{13}C NMR	^{1}H NMR
1	166.3 (C)	-
2	102.3 (C)	-
3	165.4 (C)	-
4	91.8 (CH)	6.10 (s, 1H)
5	160.6 (C)	-
6	127.3 (C)	-
7	130.1 (CH)	6.70 (s, 1H)
8	14.6 (CH_3)	1.86 (d, 3H)
9	56.5 (CH_3)	3.90 (s, 3H)
10	9.0 (CH_3)	1.96 (s, 3H)
11	12.5 (CH_3)	1.91 (s, 3H)

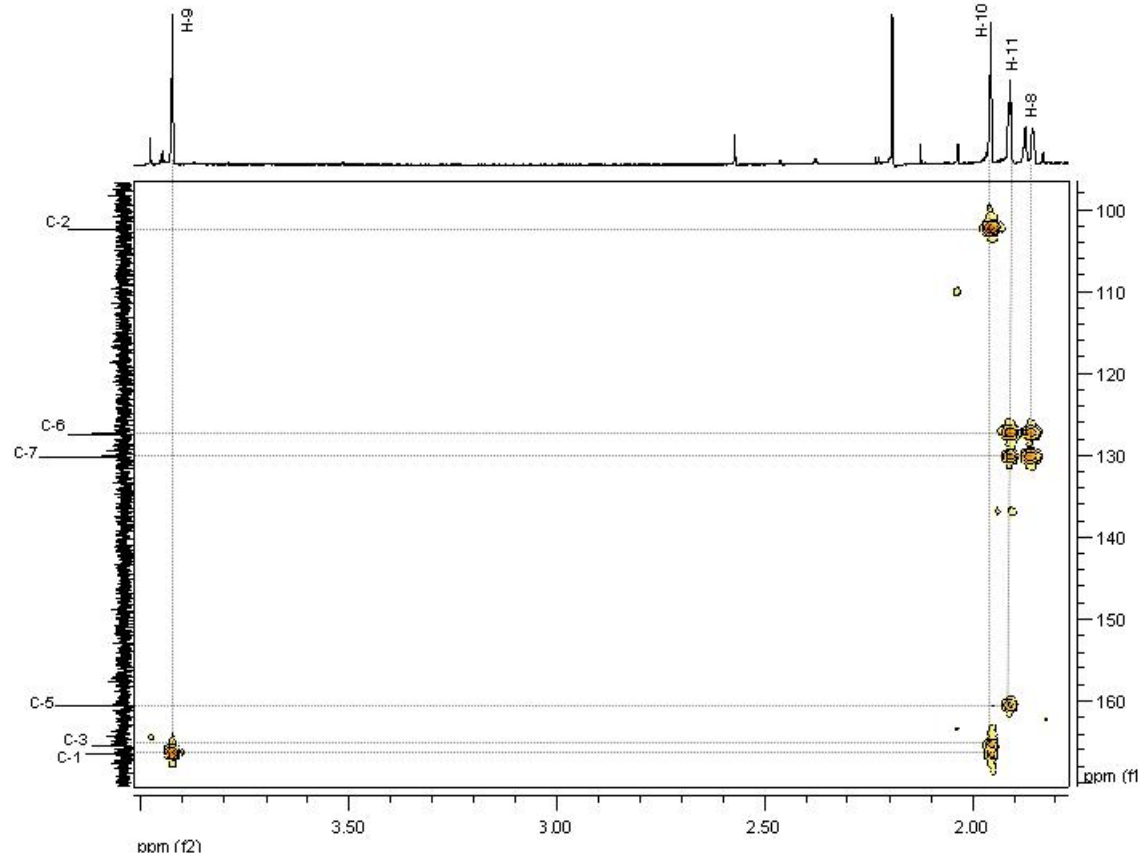

Figure 3.16 HMBC spectrum for compound **4** in the high field region

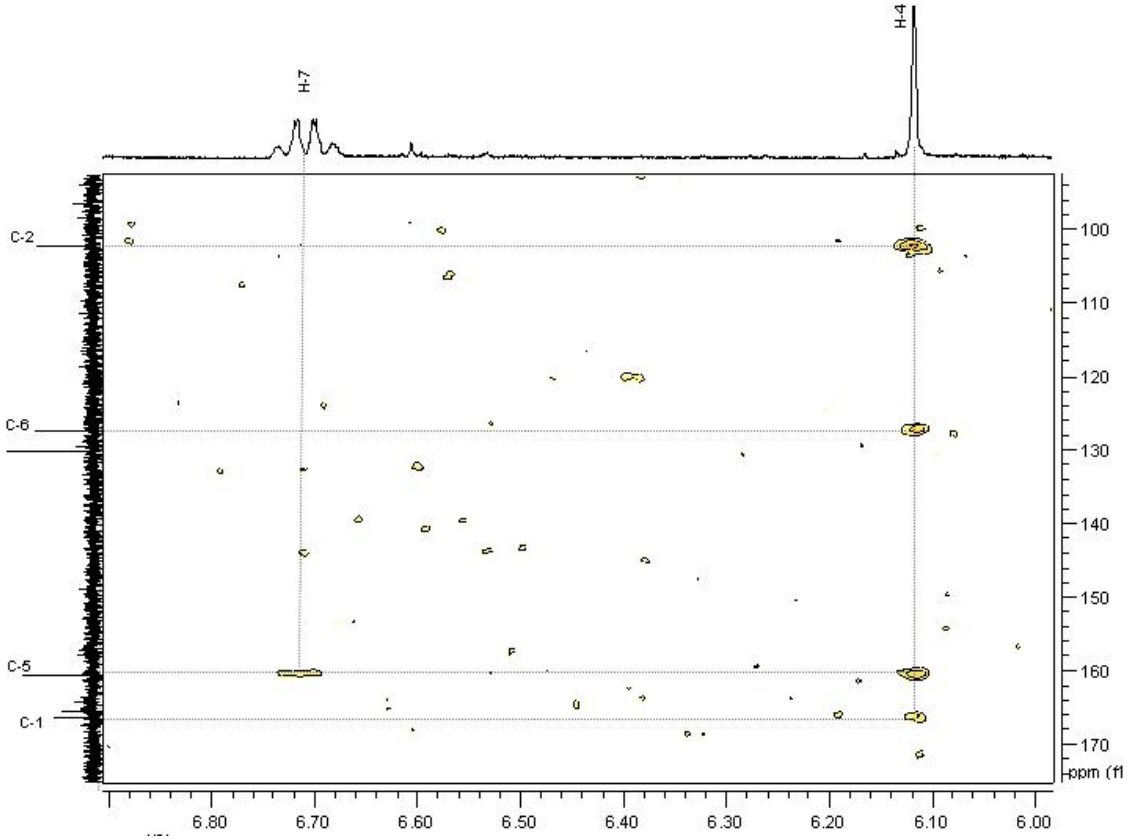

Figure 3.17 ^{1}H-^{13}C HMBC spectrum for compound **4** in the low field region

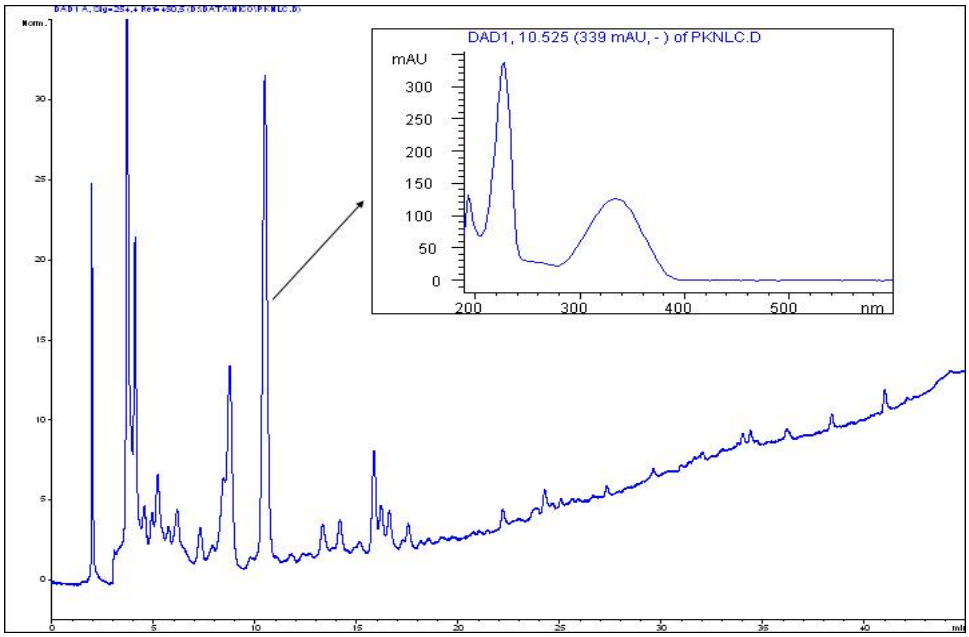

Figure 3.18 HPLC chromatogram of compound **4** (254 nm; standard run) and its UV spectrum

3.3.5. Compound 5: Cytosporone F

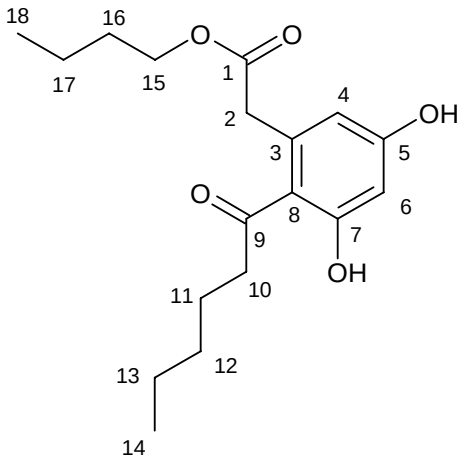

Compound **5** has a retention time of 28.7 min with the standard HPLC run (Figure 3.23) and a Rf of 0.35 by TLC ($CHCl_2$/toluene/cyclohexane/MeOH 9/2/2/1 (v/v/v/v), violet spot at 366nm, turns black when sprayed with 1% H_2SO_4/MeOH and heated). It was purified by

preparative HPLC using a gradient of MeOH/H_2O (0 min: 70% MeOH, 15 min: 80% MeOH, flow: 3.5 ml/min, RT: 11 min).

A similar compound, cytosporone B, was reported to be isolated from cultures of two fungi, one belonging to the *Cytospora* sp. and the other to the *Diaporthe* sp. (Figure 3.19)[61]. The difference between cytosporone F and cytosporone B resides in the length of the two side chains. The numbering system used here refers to the one used by Brady et al.. [61] The name of "Cytosporone F" is porposed for this compound.

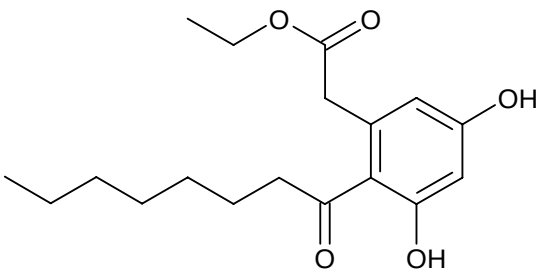

Figure 3.19 Structure of cytosporone B, isolated by Brady et al.. [61]

The ^{1}H-NMR spectrum shows that the two protons H-4 and H-6 are *meta*-coupled (J = 2.4 Hz). There are also two signals with chemical shifts at 4.22 and 3.85 ppm indicating the presence of two CH_2O moieties (Figure 3.20).

The ^{13}C-NMR spectrum shows the presence of two carbonyls at 207.1 and 171.9 ppm, two methyls, eight secondary carbons and an aromatic ring with two oxygenated carbons at 164.7 and 160.7 ppm, two quaternary carbons at 137.07 and 116.9 ppm and two tertiary carbons at 112.7 and 103.6.

The ^{1}H -^{13}C HMBC spectrum shows that the aromatic proton at 6.30 ppm is correlated to the tertiary carbon at 113.07 and the oxygenated carbons at 164.72 and 160.77 ppm (Figure 3.21). The second aromatic proton, at 6.28 ppm, is correlated to the carbons at 160.77, 103.67, and 42.19 ppm.

The CH_2 at 42.19 ppm is linked to the ring with the carbon at 117.0 and its protons at 3.85 ppm are correlated to the carbons at 171.9, 160.4 and 112.7 ppm (Figure 3.21).

Comparison of the carbon chemical shifts with the literature[61] (Table 3.6) confirms our results. The ESI mass spectrum in negative ion mode gave a peak at 321.9 Da corresponding to the $[M-H]^-$ ion.

Table 3.6. Chemical shifts for compound **5** (in $CDCl_3$) and of cytosporone B (^{13}C:100 MHz, Acetone-d_6)

Position	Compound **5**		Literature[61]
	^{13}C NMR	^{1}H NMR	^{13}C NMR
1	171.91 (C)	-	171.6
2	42.19 (CH_2)	3.85 (s, 2H)	40.1
3	137.00 (C)	-	137.0
4	103.67 (CH)	6.30 (d, 1H, J=2.4Hz)	102.5
5	164.72 (C)	-	160.7
6	113.07 (CH)	6 .28 (d, 1H, J=2.4Hz)	111.8
7	160.77 (C)	-	159.7
8	117.00 (C)	-	120.8
9	207.12 (C)	-	206.3
10	43.83 (CH_2)	2.84 (t, J =7.4Hz)	44.4
11	25.40 (CH_2)	1.71 (m)	25.0
12	29.64 (CH_2)	1.27 (m)	30.0
13	29.51 (CH_2)	1.32 (m)	29.9
14	14.50 (CH_3)	1.30 (m)	32.5
15	62.06 (CH_2)	4.22 (q, J=7.2Hz)	23.3
16	32.11 (CH_2)	1.29 (m)	14.3
17	23.03 (CH_2)	1.28 (m)	61.0
18	14.56 (CH_3)	0.89 (m, 3H)	14. 5

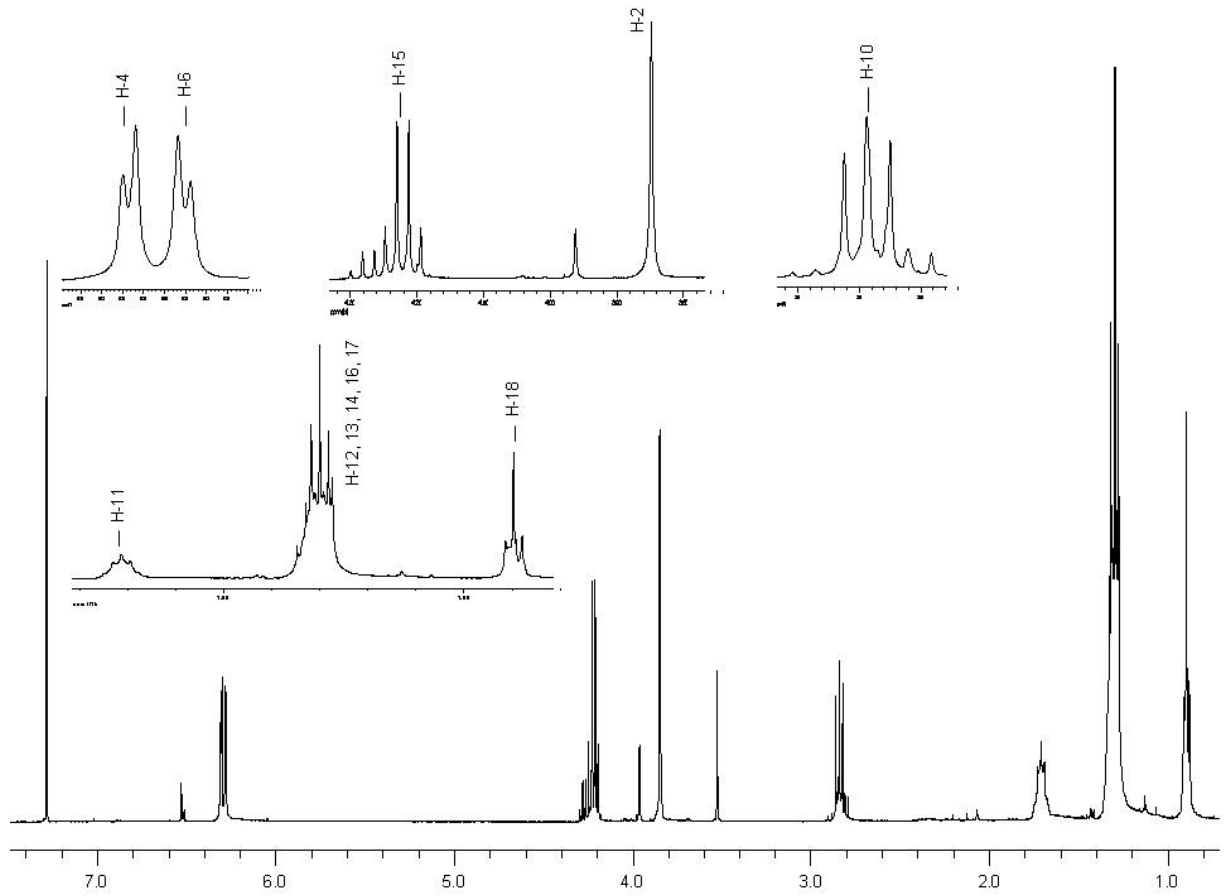

Figure 3.20. ^{1}H NMR spectrum of compound **5**

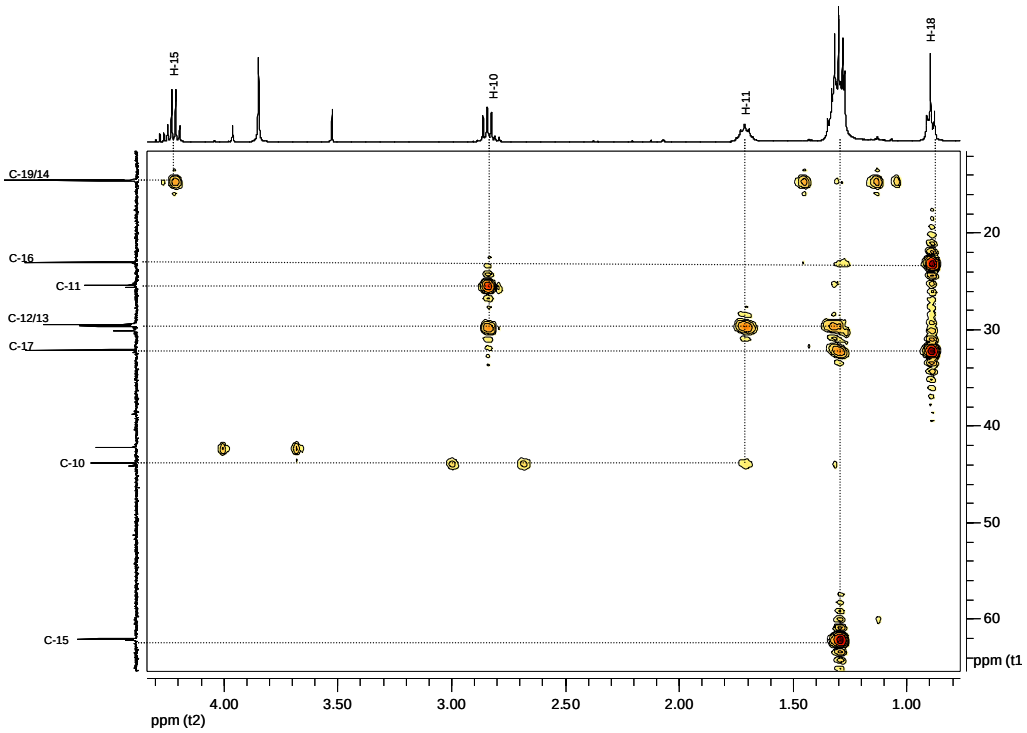

Figure 3.21. Long-range HMBC correlation spectrum in the high-field region of compound **5**

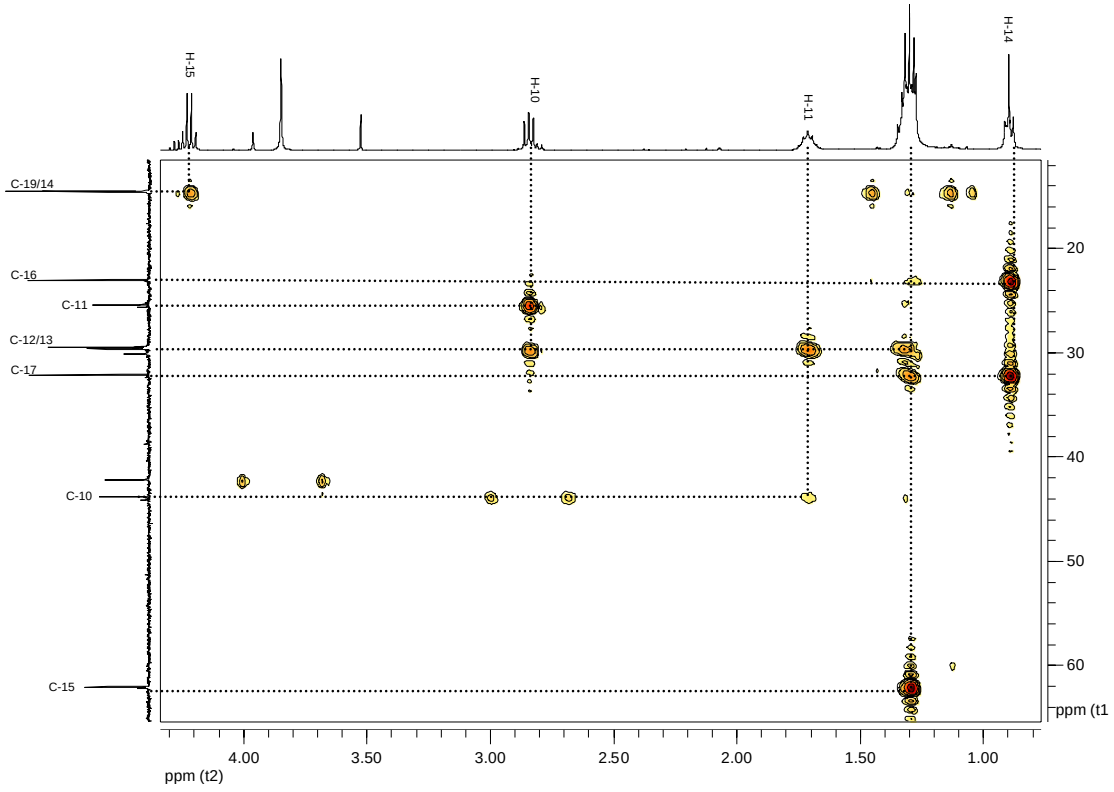

Figure 3.22. Long-range correlation spectrum in the low-field region of compound **5**

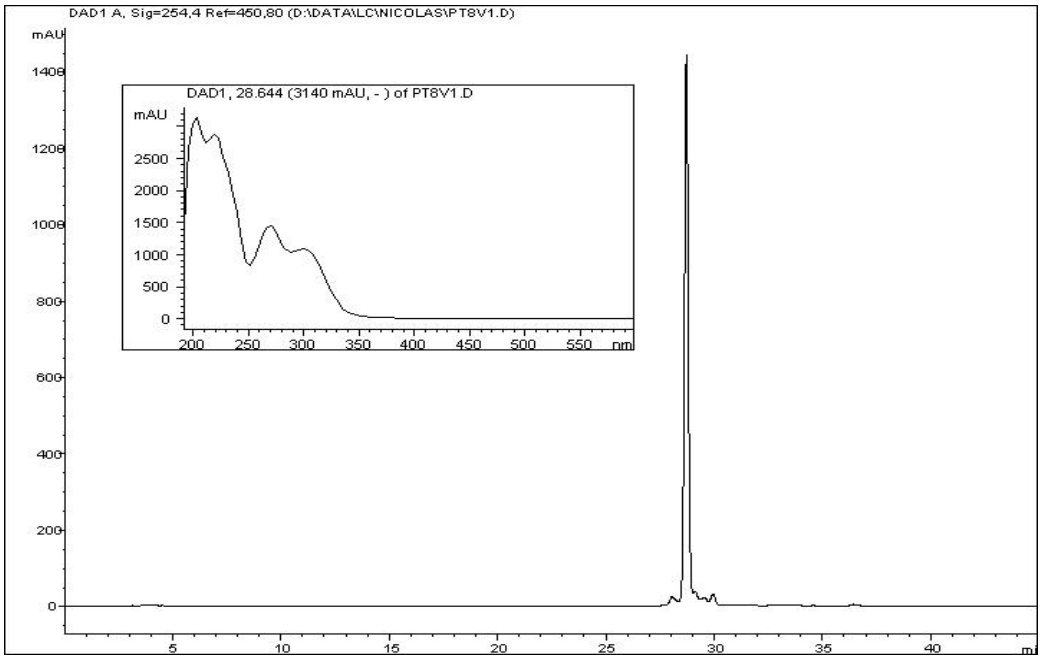

Figure 3.23 HPLC chromatogram of compound **5** (254 nm; standard run)

3.3.6. Compound 6: 22*E*, 24R-3β-hydroxy-5α, 9α-oxacyclobutane-ergosta-7, 22-dien-6-one

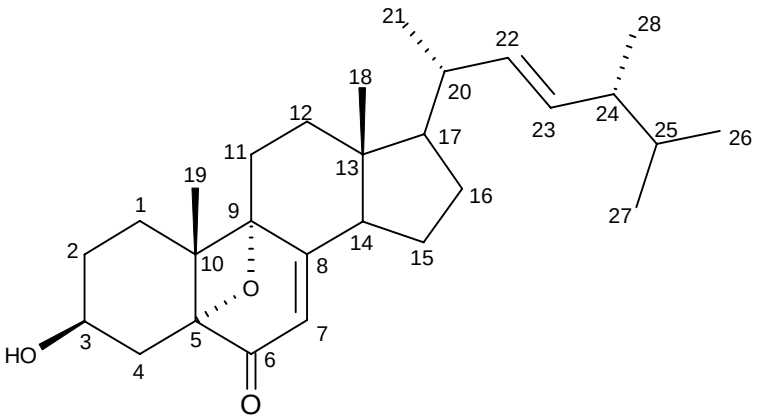

Compound **6** is a sterol with a retention time of 38.1 min with the standard run (Figure 3.28). It was purified by semi-preparative HPLC using a 30% MeOH/H_20 mixture at a flow rate of 3.5 ml/min at 40°C.

The ^{13}C NMR spectrum shows the presence of 28 carbons with, amongst others, one ketone signal at 197 ppm, two double bonds with signals at 164.2, 135.0, 132.2 and 119.9 ppm and 6 methyls at 21.09, 20.5, 19.9, 19.6, 17.6 and 12 ppm thus suggesting a steroidal structure.

The structure of the side chain of the sterol was determined with the COSY and HMBC spectra (Figure 3.25 and Figure 3.27). The olefinic protons H-22 and H-23 appear as doublet of doublets with a large coupling constant (J = 15.6 Hz) between both indicating a *trans* configuration[71]. The COSY shows the correlation between protons H-22 with H-20 and H-23 with H-24. The end of the chain is terminated by two methyls which appear as two doublets (J = 6.8 Hz) and correlate with carbons C-24 and C-25 in the ^{1}H -^{13}C HMBC spectrum. The chain is linked to the sterol skeleton by carbon C-17. This evidence is supported by the ^{1}H -^{13}C HMBC between the methyl protons of C-21 and C-17. The high field shifted methyl proton signal at 0.6 ppm (H-18) suggests the presence of the double bond in position Δ^{7} as was reported by Aiello et al.[72]. This is further supported by the ^{1}H-^{13}C correlation between the proton H-14, at 2.7 ppm, with carbons C-7 and C-8 at 119.9 and by the ^{1}H-^{1}H spectrum showing the correlation between the two protons H-7 and H-14.

In general, fungi only produce sterols with 24-β configuration[71;73] and, as the coupling constants are consistent with those reported for the closely related 22E, 24R-3β, 5α-dihydroxyergosta-7,22-diene-6-one (Figure 3.24)[71-74] , configuration of the side chain can be deduced to be the same.

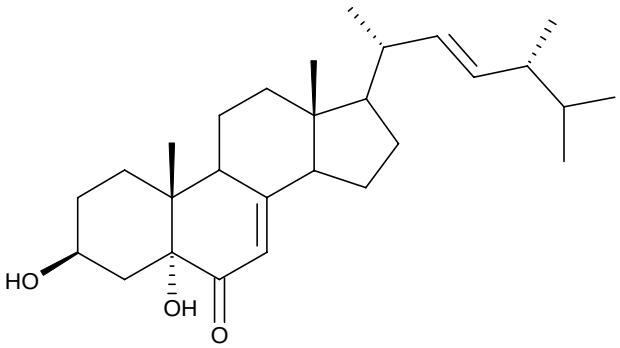

Figure 3.24 Structure of the 22E, 24R-3β, 5α-dihydroxyergosta-7,22-diene-6-one

In the ^{1}H NMR spectrum (Figure 3.26), a signal at 4.04 ppm appears as a seven-line multiplet which is characteristic of H-3 of 3-β sterols[72]. It seems that the relatively low chemical shift of this proton is caused by the presence of an oxygen on carbon C-5. This evidence is further

supported by the lack of correlation in the COSY spectrum between the 4-α (δ 2.06) and 4-β (δ 1.76) protons with protons other than H-4 and H-3[72].

The chemical shift of proton H-7 (δ 5.64) and those of the carbons of the double bond (δ 199.9 and 164.2) indicated the presence of the -C(O)-CH=C- system which is located as in Δ^7-6-keto-sterols. This is in agreement with other spectral data and literature[72]. H-7 and H-14 are coupled together, as indicated by the coupling constant (J = 2.1 Hz) and the COSY spectrum. An alternative location would be as a $\Delta^{9(11)}$-12-keto-sterol but this must be discarded in regard of the HMBC spectra which clearly shows correlations between the methyl H-18 and C-12.

Comparison of these results with those reported for the ergostane in Figure 3.24 show very close chemical shifts in the ^{13}C NMR spectrum (See Table 3.7)[71;72;74]. However, one difference arises with normal 5-OH- Δ^7-6-keto-sterols as the H-7 correlates in the HMBC spectrum not only with the oxygenated carbon C-5 (δ 79.8) but also with another oxygenated carbon at 74.7 ppm. This is also the case with the protons H-1, H-19 and H-12 which all show correlations with carbon C-5.

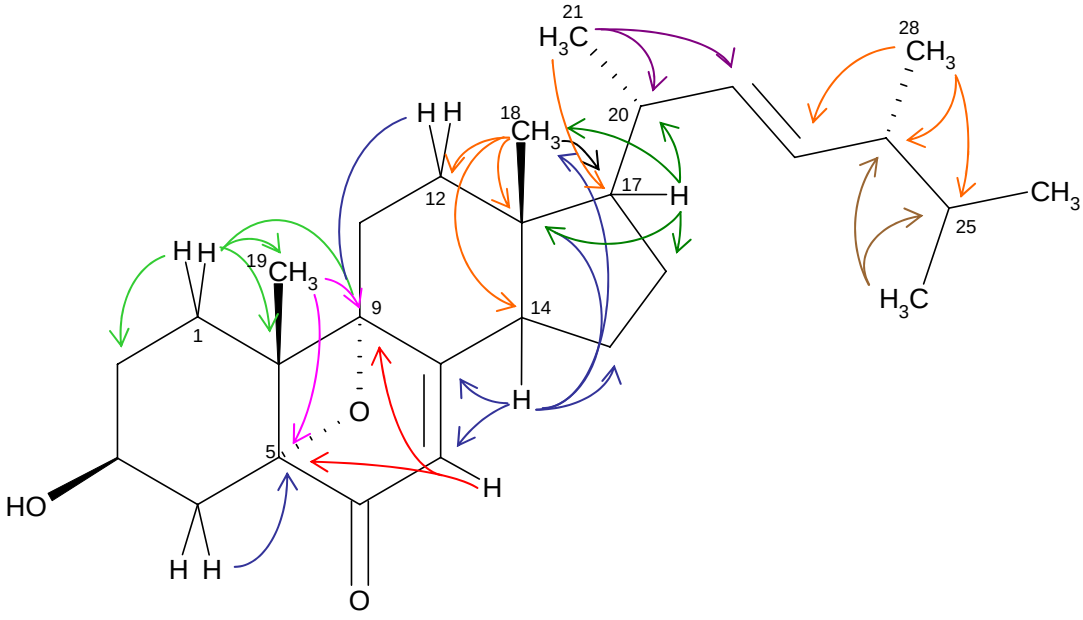

Figure 3.25 Selected long-range correlations for compound **6**

It seems then that C-9 must also be hydroxylated. However, this is in contradiction with the mass spectrum. The APPI, APCI and EI mass spectra of the compound all give the same molecular formula $C_{28}H_{42}O_3$ for the compound (APPI: m/z 427.4 $[M+H]^+$, APCI: m/z 427.4 $[M+H]^+$, EI: m/z 426.06 $[M]^+$ (21%)). The APPI spectrum also display two ions at m/z 409.4 and 391.5 corresponding to the loss of one and two molecules of water, $[M-H_2O+H]^+$ and $[M-2H_2O+H]^+$ respectively. Consequently, there cannot be a supplementary hydroxyl group and the most likely possibility is that the C-5 and C-9 carbons form an oxacyclobutane type ring. The configuration of this bridge is most likely to be α, first because the chemical shift of the neighbouring C-4 is comparable to that of similar 5α-OH sterols (δ 37.3 ppm for **6** and 39.1 for the ergostane (Figure 3.24)) whereas it is of 30 ppm for 5β-OH ones. Moreover, those with a hydroxyl in position C-5 are very common, but *cis*-fused A/B rings are unusual[71].

Table 3.7 Chemical shifts for compound **6** and comparison with literature [71]

Position	Compound **6**		Literature[71]
	^{13}C NMR	^{1}H NMR	^{13}C NMR
	125 MHz, $CDCl_3$	500 MHz, $CDCl_3$	100 MHz, pyridine-d_5
1	25.4 (CH_2)	2.3	31.6
2	30.1 (CH_2)	1.94	31.2
3	67.2 (C)	4.04 (sept.,)	67.0
4	37.3 (CH_2)	2.06	39.1
5	79.8 (C)	-	77.3
6	197.4 (C)	-	200.0
7	119.9 (CH)	5.64 (d, J = 2.1 Hz)	120.6
8	164.2 (C)	-	163.9
9	74.7 (C)	-	44.2
10	41.9 (C)	-	41.2
11	28.8 (CH_2)	1.88	22.1
12	34.9 (CH_2)	1.71	37.7
13	45.3 (C)	-	44.6
14	51.8 (CH)	2.7	55.8
15	22.4 (CH_2)	?	22.7
16	27.9 (CH_2)	?	28.2
17	56.0 (CH)	1.43	56.0
18	12.3 (CH_3)	0.60 (s)	12.7
19	20.5 (CH_3)	1.00	16.4
20	40.3 (CH)	2.01	40.6
21	21.1 (CH_3)	1.01 (J = 6.5 Hz)	21.3
22	135.0 (CH)	5.2 (J=15.3 Hz and 7.6 Hz)	135.8
23	132.5 (CH)	5.17 (J=15.3 Hz)	132.3
24	42.8 (CH)	1.84	43.1
25	33.1 (CH)	1.46	33.3
26	20.0 (CH_3)	0.80 (d, J=6.8Hz)	20.1
27	19.6 (CH_3)	0.82 (d, J=6.8Hz)	19.8
28	17.6 (CH_3)	0.9 (d, J=6.8Hz)	17.8

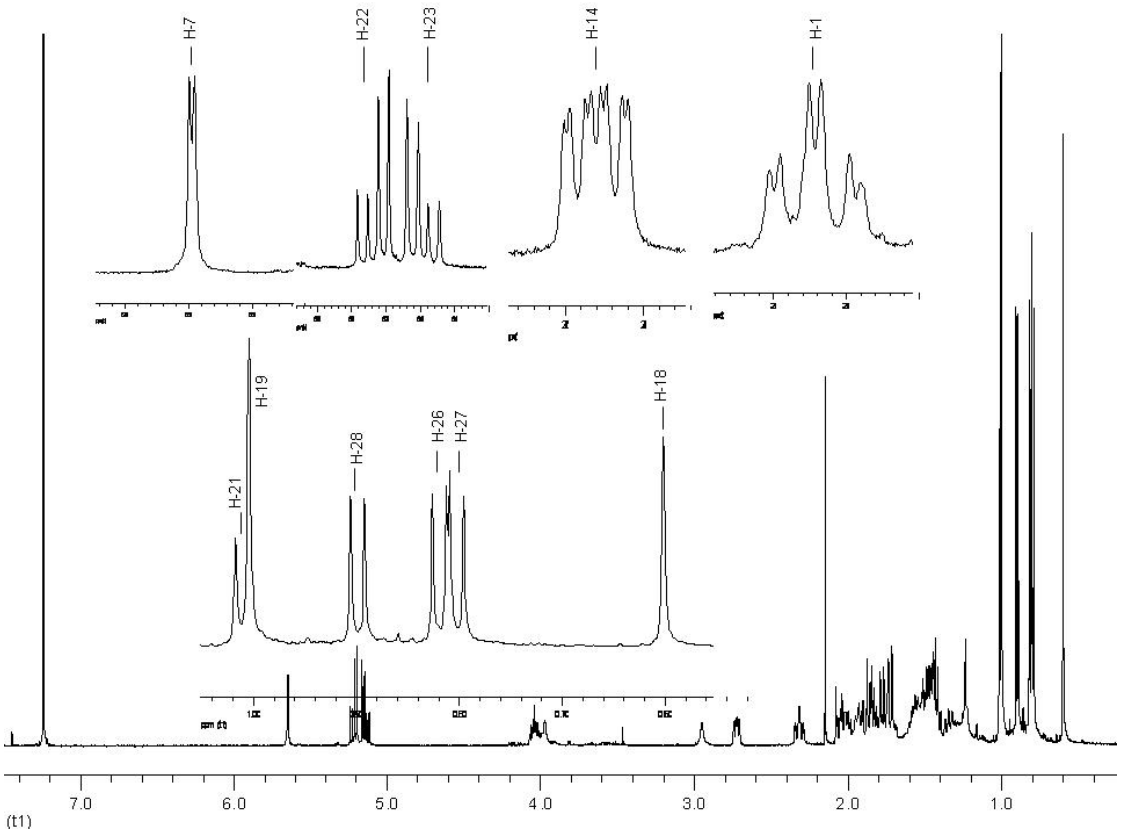

Figure 3.26 1H NMR spectrum of compound **6**

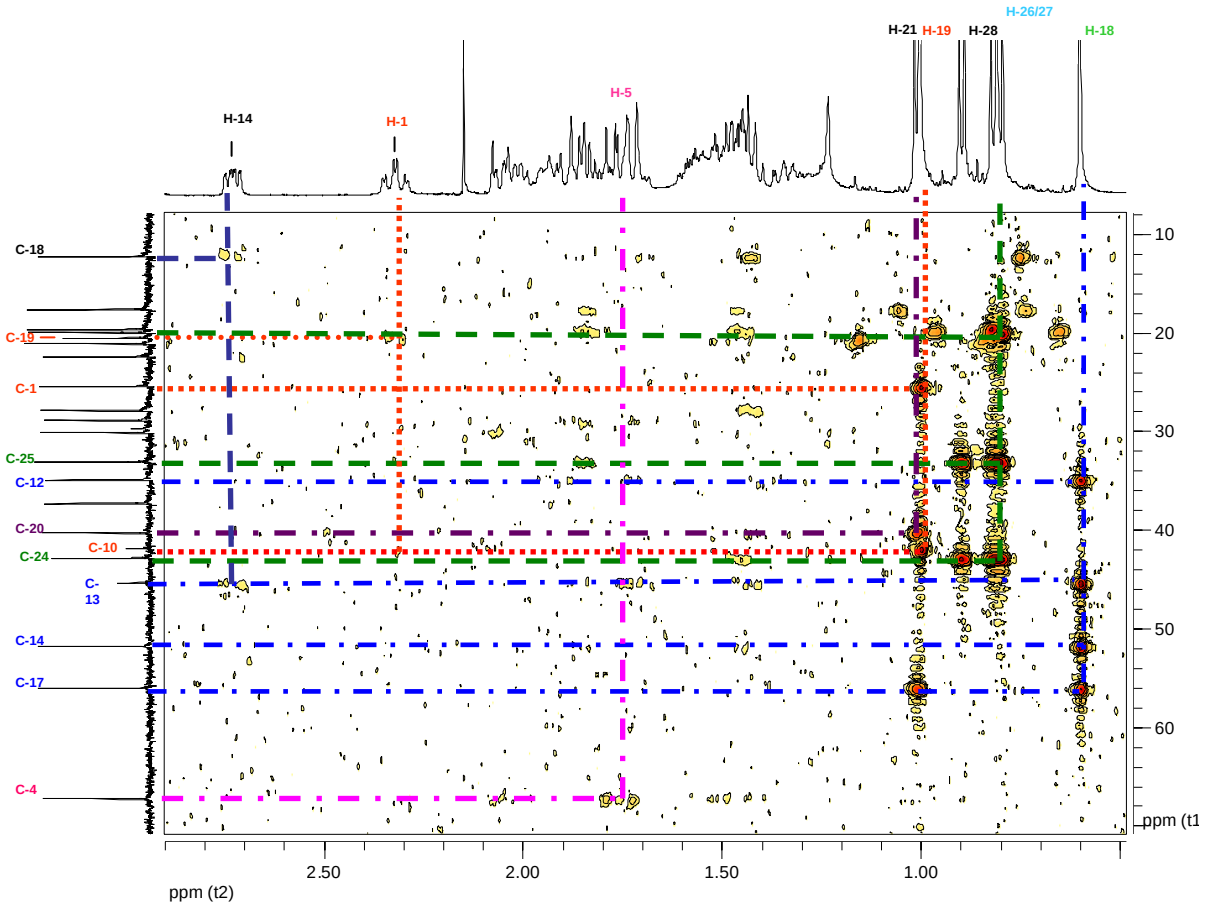

Figure 3.27 Long-range HMBC correlation spectrum for compound **6**

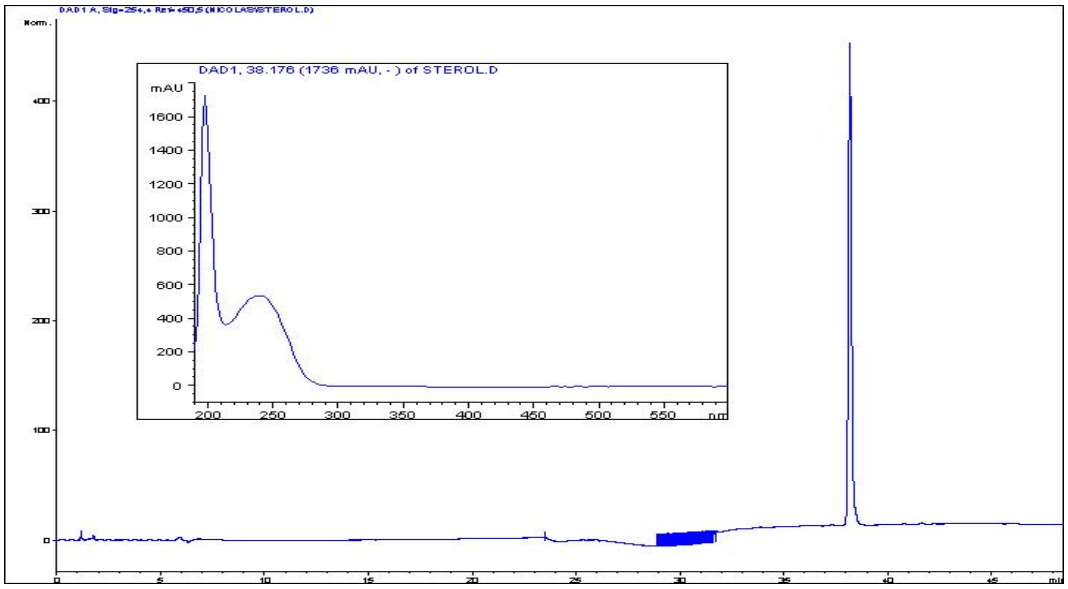

Figure 3.28 HPLC chromatogram of compound **6** (254 nm, standard run)

3.3.7. Compound 7: Phomopsolide B: 5*S*-(2''-methylbut-2*E*-enoate) -6*S*-(3'*S*, 4'*S*-dihydroxypent-1'-*E*-ene)-2*H*-pyran-2-one

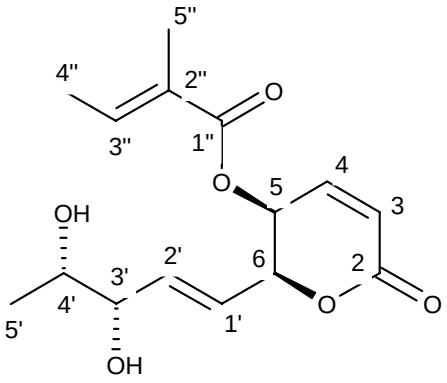

Compound **7** was isolated from an extract of strain 283. It has a retention time of 13.3 min using the standard HPLC run (Figure 3.32). It was purified by semi-preparative HPLC using the following run (0 min: 10% MeOH, 20 min: 10%, 30 min: 40 % and 45 min: 60%, flow rate: 3.5 ml/min, RT: 38 min, temperature 40°C, column: see 2.7.2).

This compound was already reported in cultures of *Phomopsis oblonga* and was given the name of Phomopsolide B[62]. It was also isolated in our group by Dr. M.-L. Leroux from another strain of *Phomopsis* sp.

The ^{13}C and DEPT NMR spectra showed the presence of three methyl groups, nine CH and three quaternary carbons whereas the ^{1}H spectrum gave 12 signals. Protons at 5.91 and 6.03 ppm are on the same double bond in a *trans* configuration, the coupling constant being of 15.7 Hz. The long-range HMBC experiment shows the correlation of these two protons with C-6 (78.9 ppm) and C-4' (76.6 ppm) (Figure 3.30). It can also be seen in the COSY spectrum (Figure 3.31) the correlation between protons 2', 3', 4' and 5'. Carbons C-3' and C-4' are linked to OH moiety as their chemical shifts suggest (71.0 and 76.7 ppm respectively).
The HMBC spectrum (Figure 3.30) also shows the correlation between H-3 and C-5
.
These values correspond to what has been reported in the literature for the structure and configuration of the compound[62].

Table 3.8 Chemical shifts for compound **7** in $CDCl_3$ as compared to literature (^{13}C: $CDCl_3$, 360 MHz) **[62]**

Position	Compound **7**		Literature[62]	
	^{13}C NMR	^{1}H NMR	^{13}C NMR	^{1}H NMR
1	-	-	-	-
2	162.8 (C)	-	162.6	
3	125.4 (CH)	6.26 (d, J = 9.6 Hz)	124.8	6.23
4	141.3 (CH)	7.03 (dd, J = 9.6 & 5.5 Hz)	141.1	7.00
5	63.8 (CH)	5.40 (dd, 5.5 & 2.9 Hz)	63.4	5.37
6	78.9 (CH)	5.10 (m)	78.7	5.1
1'	135.1 (CH)	5.91 (ddd, J = 15.7, 5.6 & 1.28 Hz)	135	5.89
2'	125.1 (CH)	6.03 (ddd, J = 15.7, 5.6 & 1.28 Hz)	124.6	6.01
3'	71.0 (CH)	3.90 (t, J = 6.0 Hz)	70.6	3.93
4'	76.6 (CH)	3.60 (dq, J = 6.2 Hz)	76.2	3.62
5'	19.2 (CH_3)	1.19 (d , J = 6.2 Hz)	18.8	1.17
1"	167.1 (C)	-	166.7	-
2"	127.9 (C)	-	127.5	-
3"	140.2 (CH)	6.90 (m)	139.8	6.9
4"	15.0 (CH_3)	1.83 (s)	14.6	1.80
5"	12.4 (CH_3)	1.82 (m)	12.0	1.81

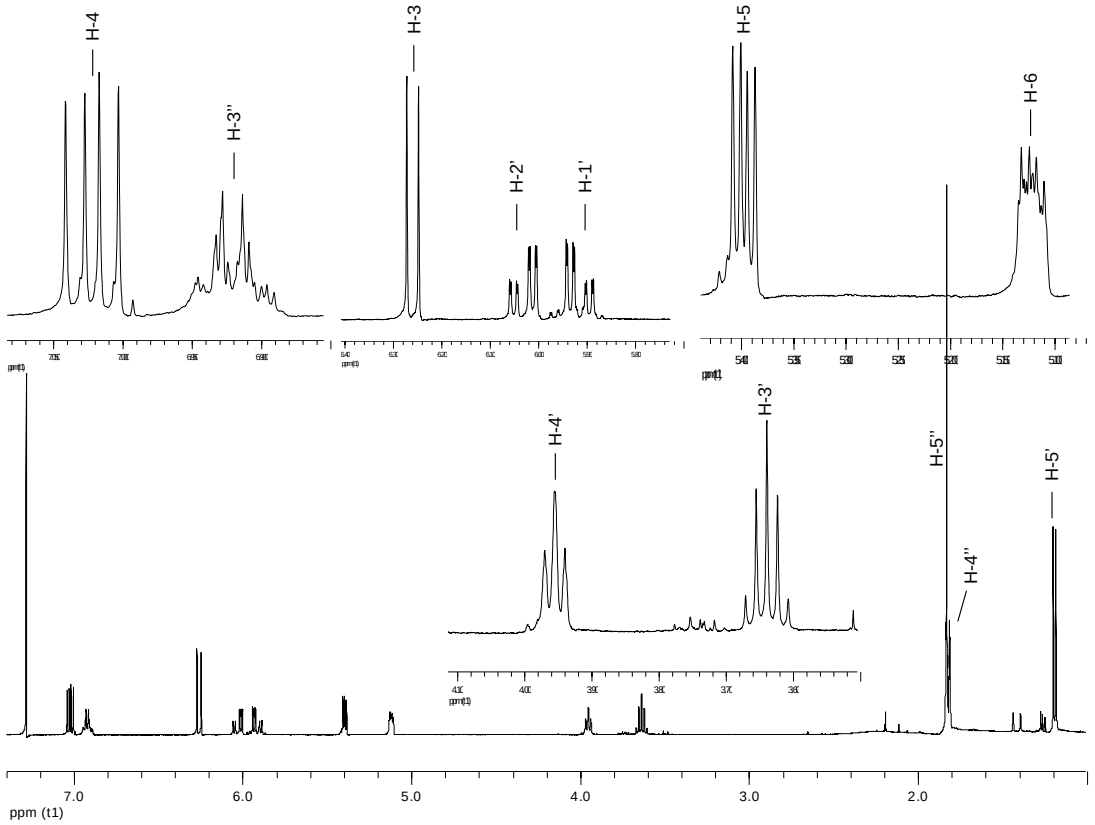

Figure 3.29 ^{1}H NMR spectrum of compound **7**

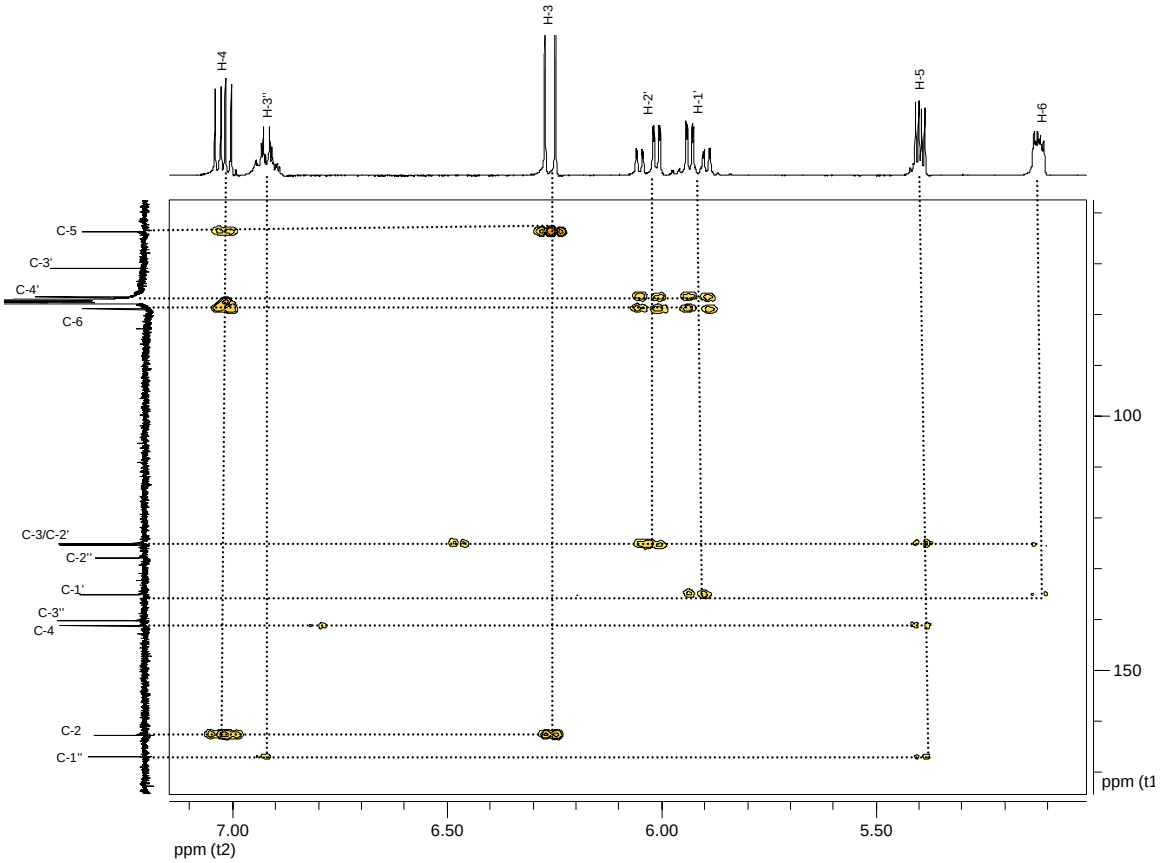

Figure 3.30 HMBC correlation spectrum of compound **7**

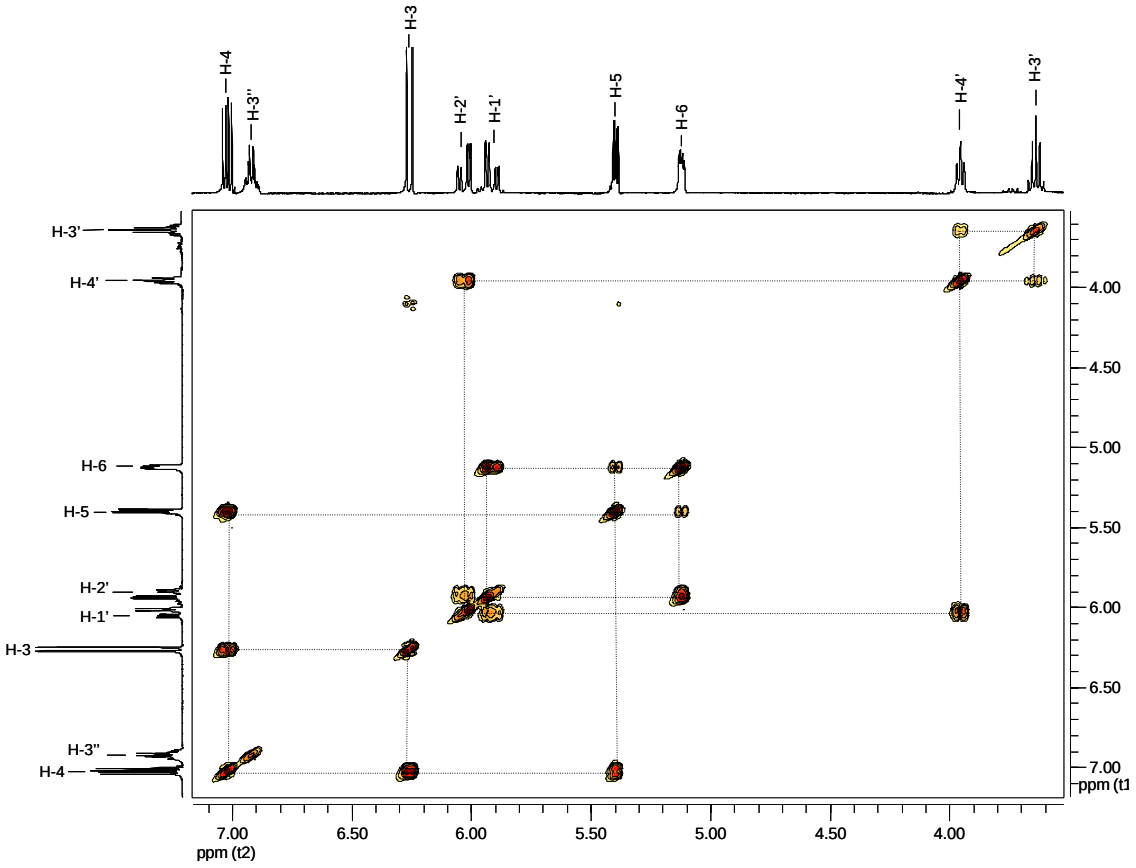

Figure 3.31 COSY NMR spectrum of **7** in the 3.8-7.1 ppm region

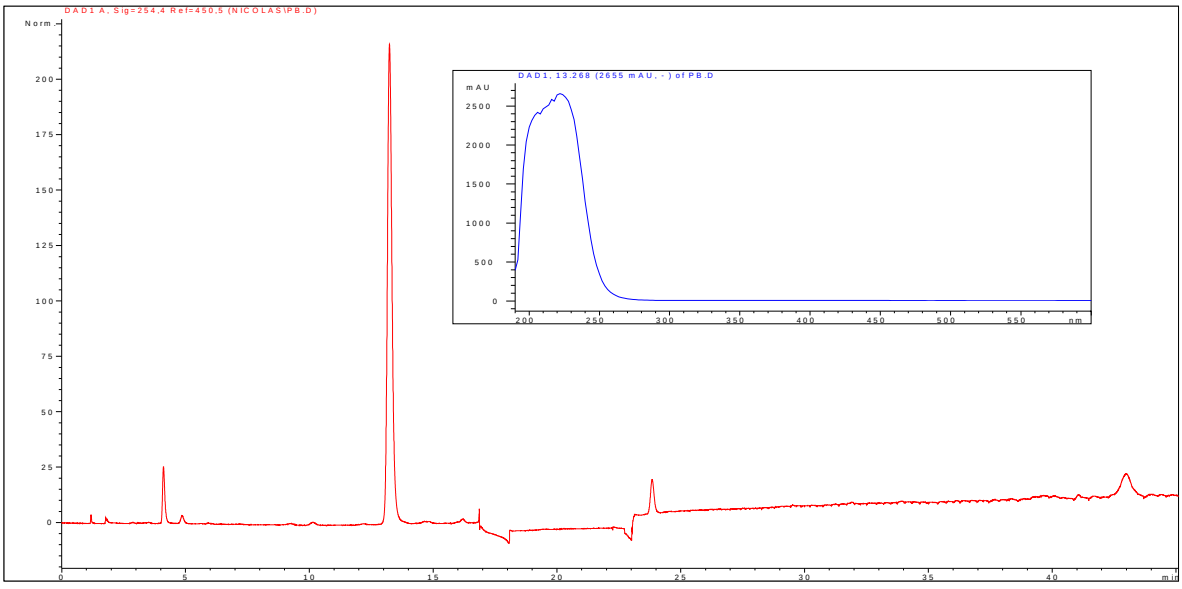

Figure 3.32 HPLC chromatogram of compound **7** (254 nm, standard run)

3.3.8. Compound 8: 5-[1'-(2''-methylbut-2''-enoate)-4', 5'-dihydrohex-2'-ene]-3, 4-dihydroxyfuran-2-one

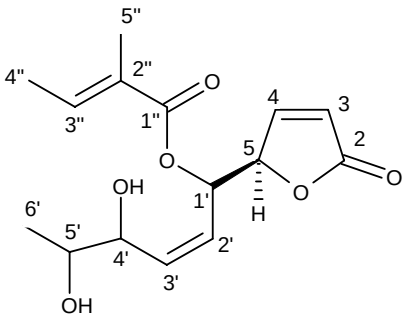

Compound **8** was purified from the same fraction as compound **7** using the same HPLC run and has a retention time of 12.6 min with the standard HPLC run. The chromatograms of both compounds are compared in Figure 3.36.

The main structural difference between the two comes from the cyclisation of the lactone. Whereas compound **7** has a six membered ring, this one has a five membered ring with the remaining carbon linking the two side chains to the furanone. The increased ring tension, due to the fact that it is 5-membered, results in a downfield chemical shit of the two protons on the double bond, H-3 and H-4.

Fukushima et al..[75] isolated from a culture broth of *Nigrospora sacchari* Phomalactone (A) and another compound, B, that possesses the same furanone ring than **8** with a sidechain on carbon C-5 (Figure 3.33). They determined its configuration as being 5S, 6S with coupling constants between protons C-5 and C-6 of 6.0 Hz and C-6 and C-7 of 7.3 Hz.

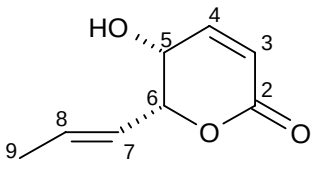

A
(Phomalactone)

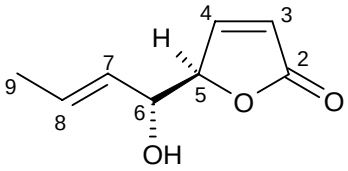

B

Figure 3.33 Phomalactone, A, and its co-metabolite, B, isolated from *Nigrospora saccharia*

These values being similar to those calculated for **8**, hence it can be deduced that its configuration is 5S, 1'S.

Table 3.9: Chemical shifts for compound **8** in $CDCl_3$ as compared to those of **7**

Position	Compound **8**		Compound **7** (Table 3.8)	
	^{13}C NMR	^{1}H NMR	^{13}C NMR	^{1}H NMR
1	-	-	-	-
2	172.72 (C)	-	162.8 (C)	-
3	123.84 (CH)	6.20 (dd, J = 5.7 & 1.9 Hz)	125.4 (CH)	6.26 (d, J = 9.6 Hz)
4	152.86 (CH)	7.45 (dd, J = 5.7 & 1.5 Hz)	141.3 (CH)	7.03 (dd, J = 9.6 & 5.5 Hz)
5	83.70 (CH)	5.21 (J = 1.9 & 5.5 Hz)	63.8 (CH)	5.40 (dd, 5.5 & 2.9 Hz)
1'	72.17 (CH)	5.64 (dd, J = 6.01 & 1.7 Hz)	78.9 (CH)	5.10 (m)
2'	135.99 (CH)	5.85 (J = 5.5 & 15.6 Hz)	135.1 (CH)	5.91 (ddd, J = 15.7, 5.6 & 1.28 Hz)
3'	126.22 (CH)	5.9 (J = 5.5 & 10.1 Hz)	125.1 (CH)	6.03 (ddd, J = 15.7, 5.6 & 1.28 Hz)
4'	76.68 (CH)	3.93 (J = 6.3 Hz)	71.0 (CH)	3.90 (t, J = 6.0 Hz)
5'	70.83 (CH)	3.68 (dq, J = 5.7 & 1.9 Hz)	76.6 (CH)	3.60 (dq, J = 6.2 Hz)
6'	19.34 (CH_3)	1.2 (d, J = 6.4 Hz)	19.2 (CH_3)	1.19 (d , J = 6.2 Hz)
1"	166.98 (C)	-	167.1 (C)	-
2"	128.21 (C)	-	127.9 (C)	-
3"	139.64 (CH)	6.89 (m)	140.2 (CH)	6.90 (m)
4"	14.9 (CH_3)	1.81 (m)	15.0 (CH_3)	1.83 (s)
5"	12.42 (CH_3)	1.82 (s)	12.4 (CH_3)	1.82 (m)

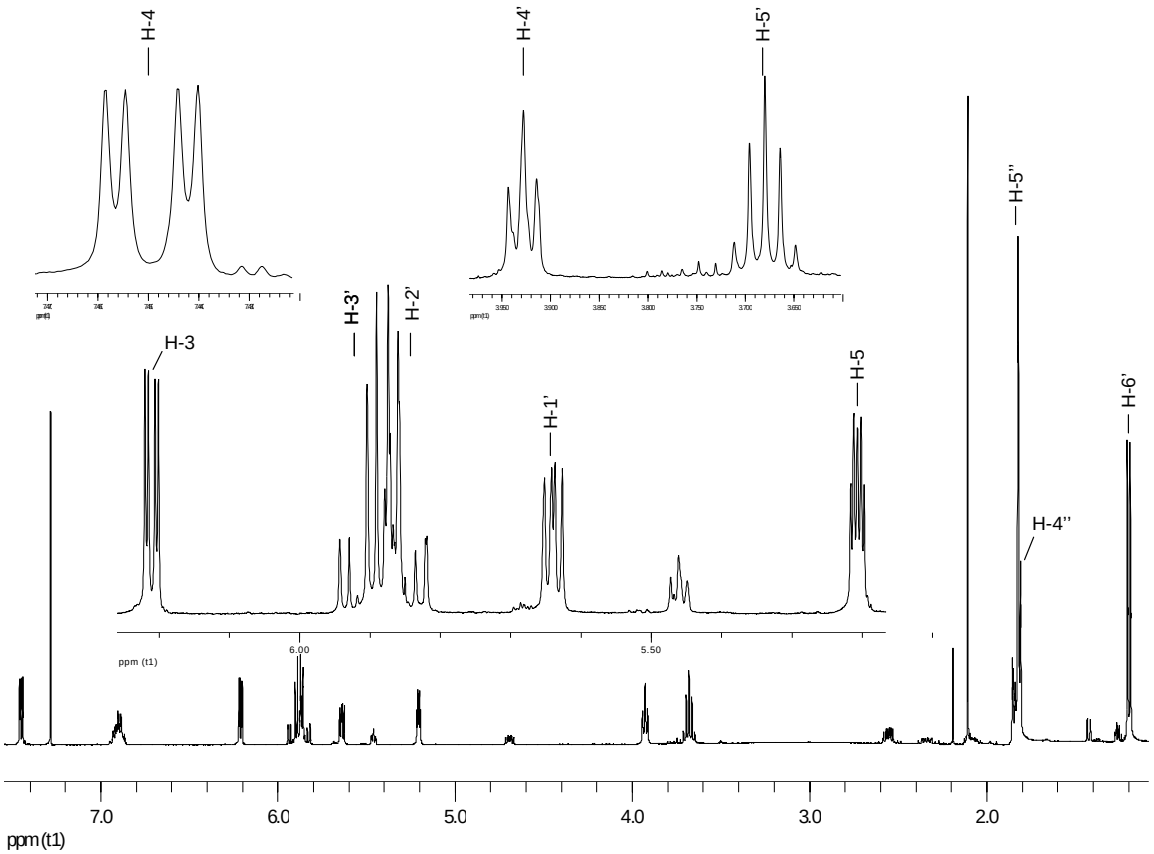

Figure 3.34 ^{1}H NMR spectrum of compound **8**

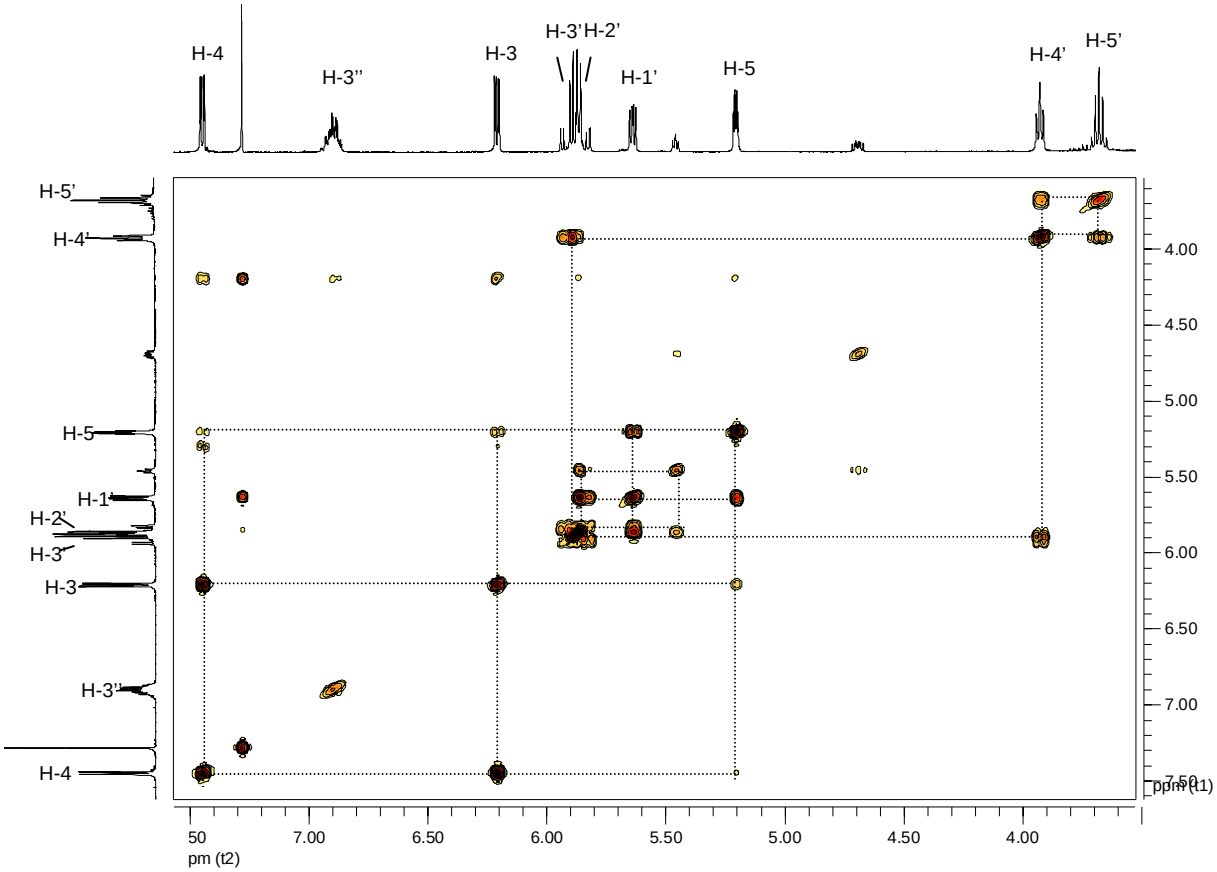

Figure 3.35 ^{1}H-^{1}H COSY spectrum of **8**

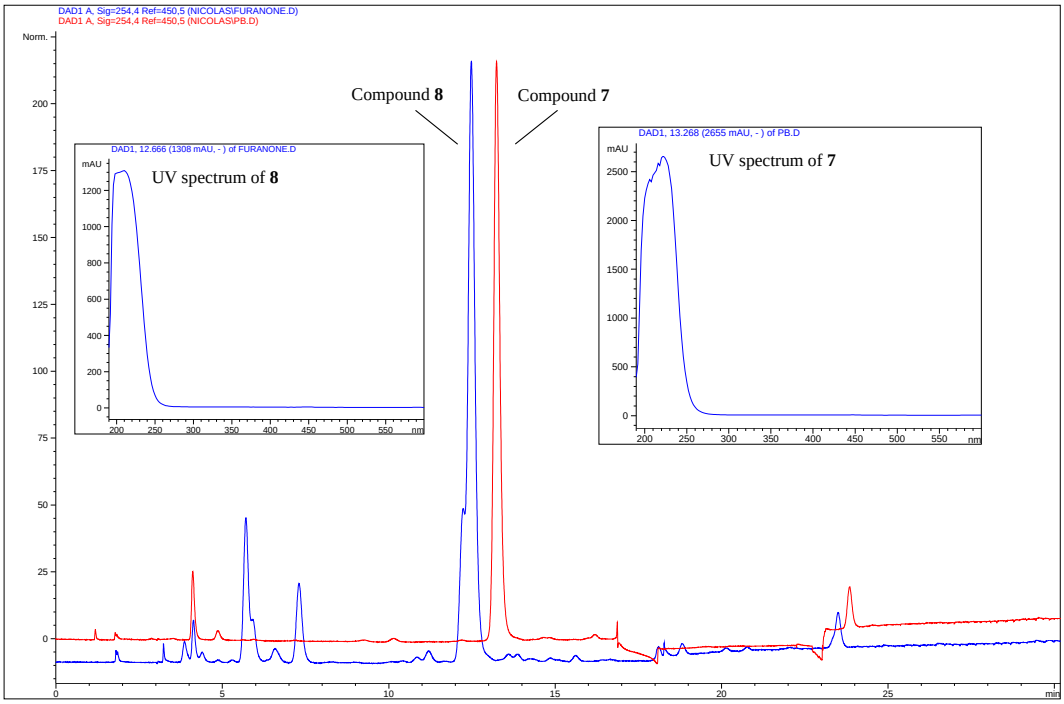

Figure 3.36 HPLC chromatogram of compound **8** compared to compound **7**, Phomopsolide B (254 nm, standard run) and their UV spectra

3.3.9. Compound 9: 4-methyl-5-hydroxyethyl-thiazole

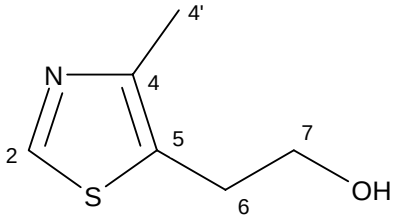

Compound **9** is an heterocycle with a thiazole ring system. It has a retention time of 5.7 min with the standard HPLC run (Figure 3.39).

The ^{13}C NMR spectrum showed five signals: two aromatics carbons at 149.80 and 149.70 ppm, two secondary carbons at 62.99 and 29.66 ppm and one methyl at 14.95 ppm. The chemical shift of carbon C-7 indicates the presence of a hydroxyl group.
The COSY spectrum showed a correlation between protons H-6 and H-7 at 3.0 and 3.8 ppm respectively.
The ^{1}H- ^{13}C HMBC spectrum revealed the presence of a second quaternary carbon at 128.0 ppm. The relatively high shift of C-2 and its proton (8.57 ppm) indicated the presence of a heteroatom. This was confirmed by the ESI-(+) mass spectrum which showed a peak at m/z 144.1 Da corresponding to the $[M+H]^+$ ion. The fragmentation pattern obtained with the EI (m/z 143.10 $[M]^+$ (30%), 112.15 $[M-CH_2OH]^+$ (100%), 85.15 $[M-CH_2OH-HCN]$ (56%)) spectrum (Figure 3.37) confirmed the structure. The postulated fragmentation pathway is given in Figure 3.38[62;76;77].

Table 3.10 NMR chemical shifts for compound **9** in $CDCl_3$

Position	^{13}C NMR	^{1}H NMR
2	149.80	8.57 (s)
4	149.70	-
5	128.0	-
6	29.66	3.00 (t, J = 6.3 Hz)
7	62.99	3.82 (t, J = 6.3 Hz)
4'	14.95	2.40 (s)

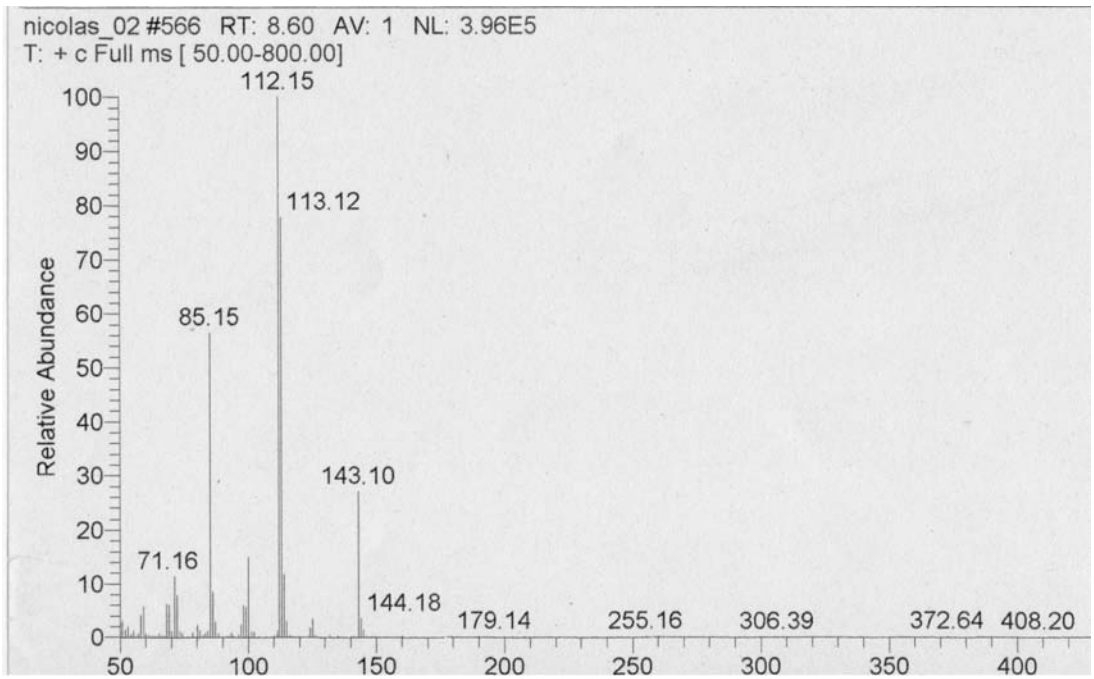

Figure 3.37 EI spectrum of compound **9**

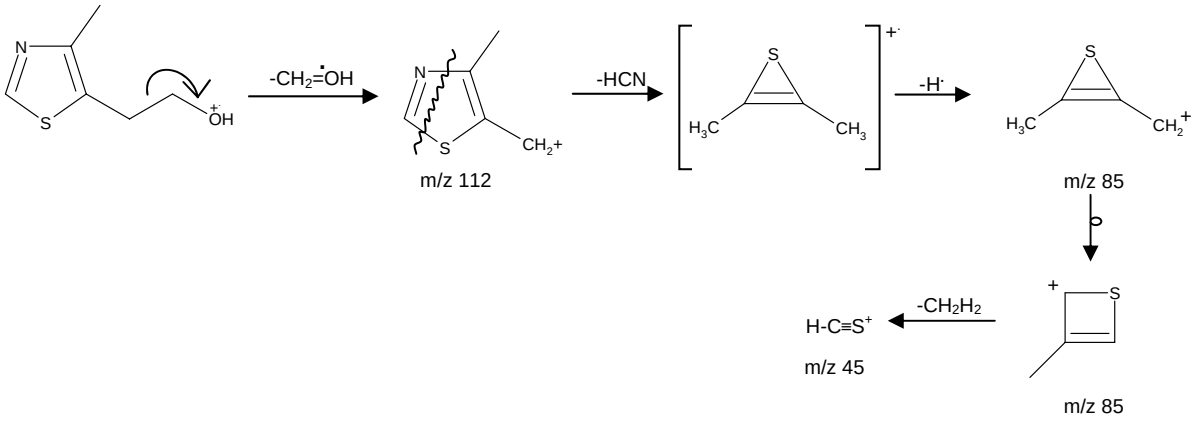

Figure 3.38 Proposed fragmentation pathway for compound **9**

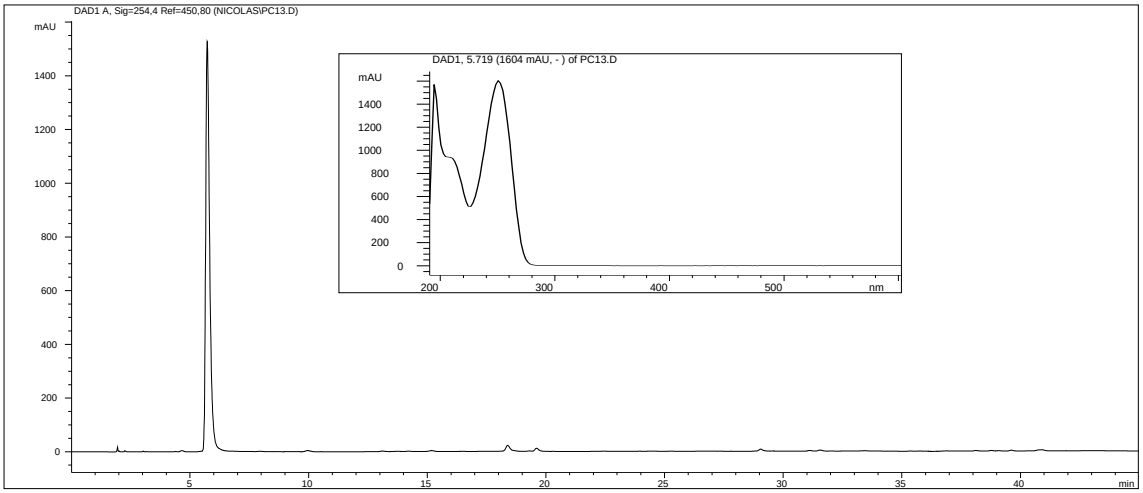

Figure 3.39 HPLC chromatogram (254 nm) of compound **9** and its UV spectrum

3.4. Bioassays

In order to evaluate the phytotoxicity of the isolated compounds they were tested using the leaf-disk bioassay. This technique has the advantage of requiring small amounts of products, which is the main limitation with the metabolites isolated during this work.

Compound **6**, the sterol, was not tested. Compounds **7**, phomopsolide B, and **8**, the furanone, were also tested together to see if any synergistic effect took place. For this, two mixtures were made, one with 100 μg of each compounds and the second one with 200 μg of each. Necrosis could be seen as brownish bands on the outer perimeter of the leaves.

Leaf necrosis was assed after 24 hours. Results are given in Table 3.11 and photos of the leaves in Tables 3.12 and 3.13. Values are given as the mean of the 3 replicates. These had to be evaluated since necrosis was not regular, as can be seen in Table 3.13. After 6 hours, necrosis was observed only at 500 μg for compounds **4**, **7** and eutypine. It is only after 12 hours that necrosis appeared for the other compounds **1**, **2** and **8**.

After 24 hours, the results showed that the xanthones **1** and **2** (reminder: compound **2** is mixed with compound **1**, see 3.3.2) show relatively similar necrosis of the leaves. At 100 μg, no necrosis was observed, at 200 μg the edges of the leaves started to become brown and at 500 μg, the discoloration extended to a distance of 0.10 mm. Compound **3**, *para*-

hydroxybenzaldehyde, shows only a very weak activity at 500 μg with the edge of the leaves starting to turn brown.

Table 3.11 Necrosis percentage after 24 hours for the leaf-disk bioassay. * 100 μg of each compound, **200 μg of each compound, n.a. : not available

Quantity [μg]	Compound									
	1	**2**	**3**	**4**	**5**	**7**	**8**	**7 + 8**	**9**	Eutypine
100	-	-	-	-	30	-	-	-*	-	35
200	30-35	30-35	-	-	80	60	-	30**	-	60
500	30-35	30-35	10	-	80	80	35	n.a.	-	80
	Concentration of each compound in μMol									
100	0.33	0.32	0.82	0.47	0.31	0.34	0.34	0.68	0.69	0.54
200	0.67	0.63	1.64	0.94	0.62	0.68	0.68	1.36	1.39	1.08
500	1.67	1.58	4.10	2.36	1.55	1.69	1.69	n.a.	3.47	2.69

With compound **5**, the cytosporone, the leaves show strong discoloration. At 100 μg, the perimeter of the leaves becomes brown on 0.05 to 0.1 mm. At 200 μg, the browning extends to 0.15 mm and at 500 μg it is superior to 0.15 mm. After 48 hours, approximately 80% of the leaves surfaces are discoloured (Table 3.13).

Compound **7** shows also strong activity, however mostly at 500 μg (Table 3.13). At 100 μg necrosis starts on the edge of the leaves. At 200 μg this necrosis extends only slightly to approximately 0.1 mm. However at 500 μg, extension of the necrosis reaches 0.15 to 0.20 mm with some portions of the leaf disks completely necrosed. For compound **8**, there is only a slight necrosis, reaching less than 0.1 mm, even at 500 μg. Compounds **7** and **8** in mixture show the same effect than when they were tested seperately. Compound **4** and **9** show no activity, even at 500 μg.

Table 3.12 Photos of the leaf-disk bioassay with the tested compounds at three different concentrations after 24h

Quantity	Compound								
	Blank	**1**	**2**	**3**	**4**	**5**	**7**	**8**	**9**
100 µg									
200 µg									
500 µg									

Table 3.13 Blown-up photos of selected leaves and compounds at 200 and 500 µg/mL after 24h

Quantity	Compound				
	(**1**)	(**5**)	(**7**)	(**7**) & (**8**)	Eutypine
200 µg	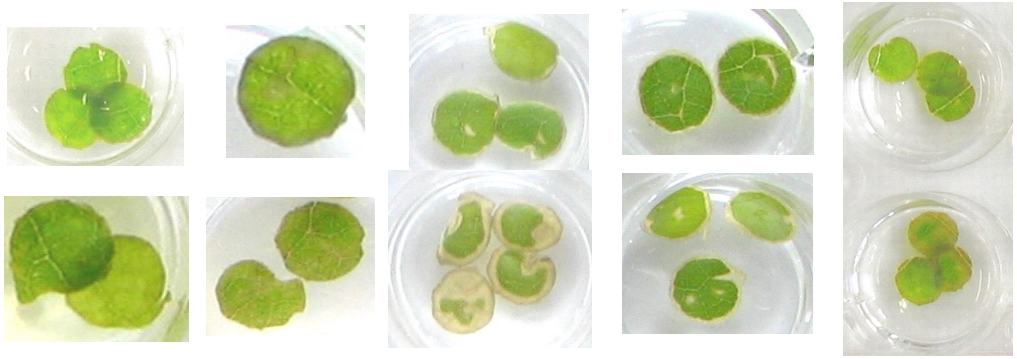				
500 µg					

In conclusion, this test showed that cytosporone and phomopsolide B have similar activities as eutypine at 500 µg and thus could be responsible for excoriosis or at least one of the factors participating in it.

The two xanthones, the *p*-hydroxybenzaldehyde and the furanone showed only a weak acitivity, with just the edges of the leaves turning brown.

3.5. LC-MS/MS analysis of strains 180 and 239 at different growth times

The two strains were grown for 14, 21, 28 and 35 days in order to asses which metabolites are produced when. The results are given in Table 3.14. Some of the compounds were not detected at all in the crude extracts used for this analysis. This shows the evolution of metabolite production in the fungus since the crude extracts the metabolites were isolated from were not the same that were used for this analysis.

Table 3.14 Detected compounds in strains 180 and 239 according to the growth time (n.d.: not detected)

Compound	RT (min)	Strain 180				Strain 239			
		Number of days				Number of days			
		14	21	28	35	14	21	28	35
1	23.5	n.d.	n.d.	n.d.	n.d.	n.d.	APPI	n.d.	n.d.
2	19.5	ESI	n.d.	n.d.	n.d.	n.d.	APPI/ESI	APPI	APPI/ESI
3	7.4	ESI	n.d.	n.d.	n.d.	n.d.	APPI	ESI	APPI/ESI
4	10.6	n.d.	ESI	ESI	n.d.	n.d.	n.d.	n.d.	n.d.
5	29.1	n.d.	APPI	n.d.	n.d.	n.d.	APPI/ESI	n.d.	APPI/ESI
6	38	n.d.	n.d.	n.d.	n.d.	n.d.	n.d.	n.d.	n.d.
7	13.5	n.d.	n.d.	n.d.	n.d.	n.d.	n.d.	n.d.	n.d.
8	11.5	n.d.	n.d.	n.d.	n.d.	n.d.	n.d.	n.d.	n.d.
9	5.7	n.d.	n.d.	n.d.	n.d.	n.d.	n.d.	n.d.	n.d.

It can be seen that, at 14 days, no compounds were produced by strain 239 and only **2** and **3** by strain 180. This is not surprising since it was shown previously (3.2) that very little was produced after 14 days.

It is of interest to notice that both xanthones and cytosporone continue to be produced after 21 days, indicating that they are not degraded by enzymes or that the metabolism does not change over the weeks.

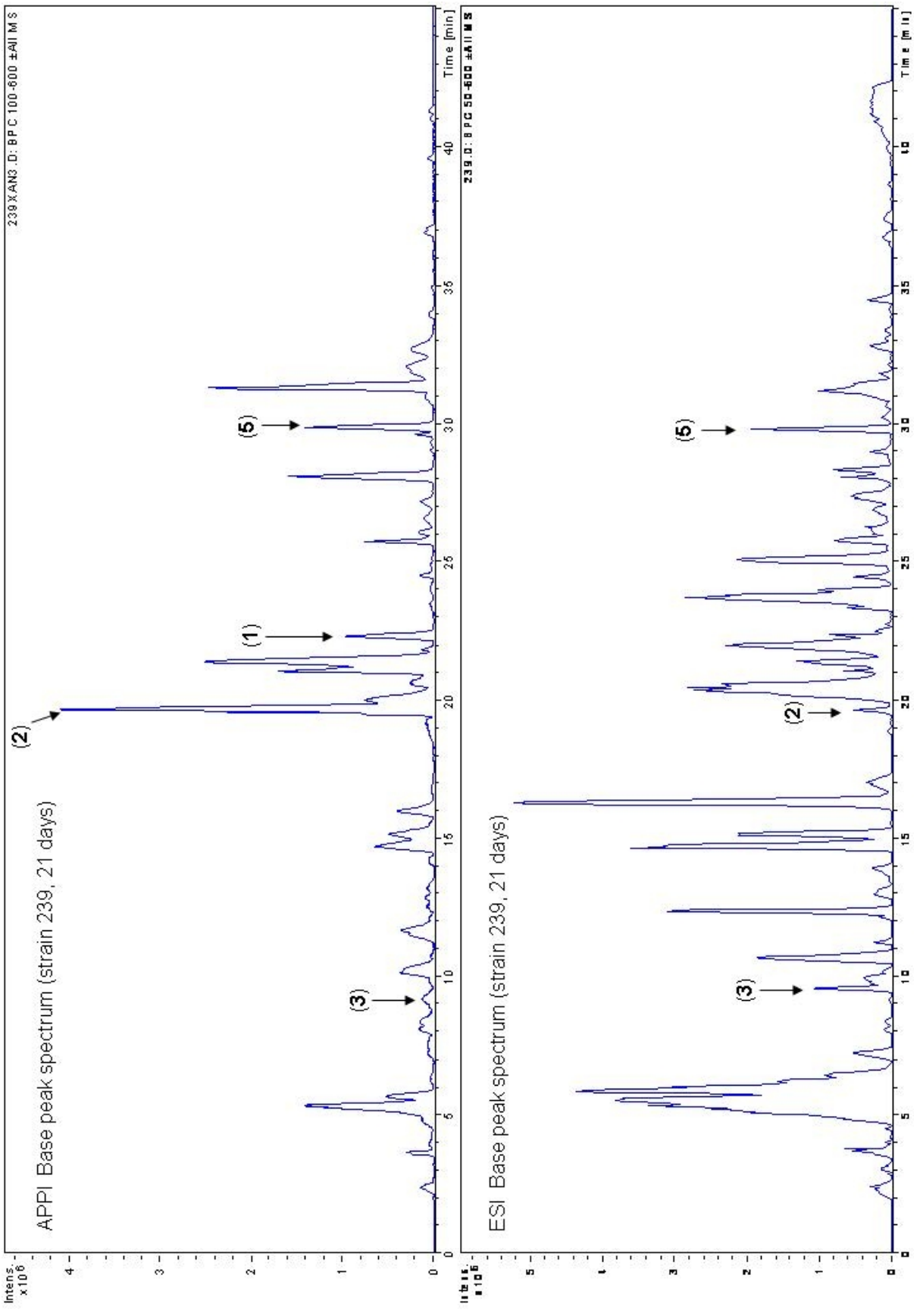

Figure 3.40 APPI and ESI base peak spectrums for strain 239 (21 days)

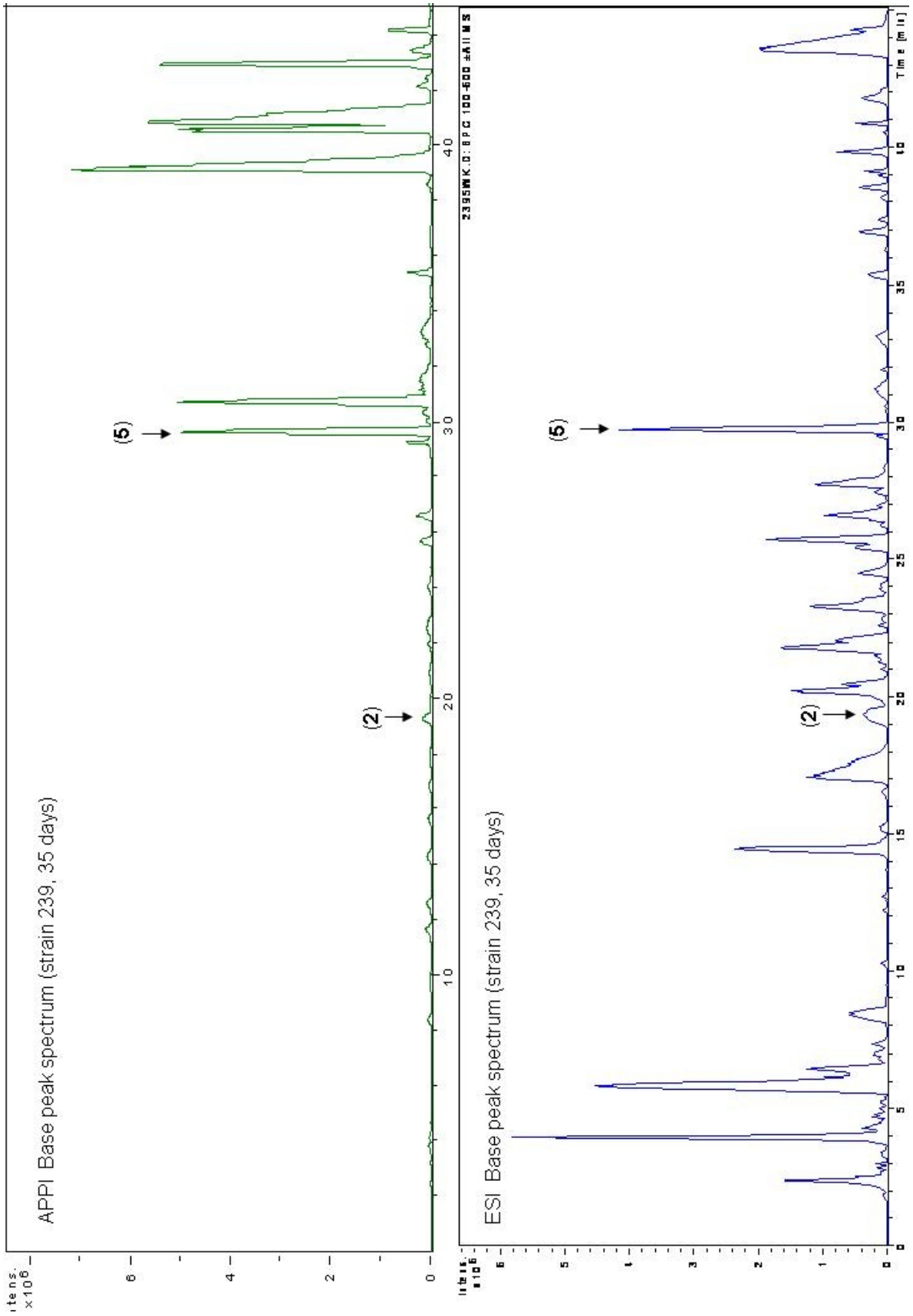

Figure 3.41 APPI and ESI base peak spectrums for strain 239 (35 days)

3.6. LC-MS/MS analysis of all studied strains

The metabolites that were found in strains 180, 239 and 283 were searched for in the crude extracts of the six other strains after growing them on PDA for 21 days: 00, 110, 279, 281, 282 and 301. This was done by using LC-MS. Since the nature of the analytes and the separation conditions have a strong influence on which technique provides the best results, both ESI and APPI interfaces were used. As the ionisation mechanisms differ, this allowed for the analysis of a wider range of compounds. Also, it appeared that the xanthones and the cytosporone were best detected using the APPI source whereas phomopsolide B and the furanone were best detected in ESI-(+) as sodium adducts. Consequently, the ionisation parameters for both sources were optimised using the pure compounds: the xanthone **1** for the APPI source and phomopsolide B for the ESI source. The HPLC method used was the standard run. The crude extracts of the six strains were obtained in the same manner as for strains 180 and 239 and were dissolved in methanol and filtered prior to injection. Detection of the compounds was based on retention time, mass spectrum and fragmentation. Table 3.15 gives the results of the investigation with the detection technique.

Table 3.15 Detected compounds in the crude extracts of the strains after 21 days (n.d.: not detected).

Compound	RT (min)	Strain number									
		00	110	180	239	275	279	281	282	283	301
1	23.5	n.d.	n.d.	n.d.	APPI	n.d.	n.d.	n.d.	n.d.	n.d.	n.d.
2	19.5	n.d.	n.d.	n.d.	APPI/ESI	n.d.	n.d.	APPI/ESI	n.d.	n.d.	n.d.
3	7.4	n.d.	n.d.	n.d.	APPI/ESI	n.d.	APPI/ESI	APPI/ESI	APPI/ESI	n.d.	ESI
4	10.6	ESI	n.d.	ESI	n.d.	n.d.	n.d.	n.d.	n.d.	n.d.	n.d.
5	29.1	n.d.	n.d.	APPI	APPI/ESI	n.d.	APPI/ESI	APPI/ESI	APPI/ESI	n.d.	n.d.
6	38	n.d.	n.d.	n.d.	n.d.	n.d.	n.d.	n.d.	n.d.	n.d.	n.d.
7	13.5	ESI	ESI	n.d.	n.d.	ESI	n.d.	n.d.	n.d.	ESI	ESI
8	11.5	ESI	ESI	n.d.	n.d.	ESI	n.d.	n.d.	n.d.	ESI	ESI
9	5.7	n.d.	n.d.	n.d.	n.d.	ESI	n.d.	n.d.	n.d.	n.d.	n.d.

The xanthone **2**, the cytosporone **5** and the *p*-hydroxy-benzaldehyde **3** were detected using both ESI and APPI techniques. Phomopsolide B **7** and the furanone **8** were only detected as sodium adducts by ESI in the positive ion mode. Phomopsolide B and the furanone were the

metabolites detected in most strains (6 of them). The cytosporone was detected in five strains and the *p*-hydroxybenzaldehyde in four.

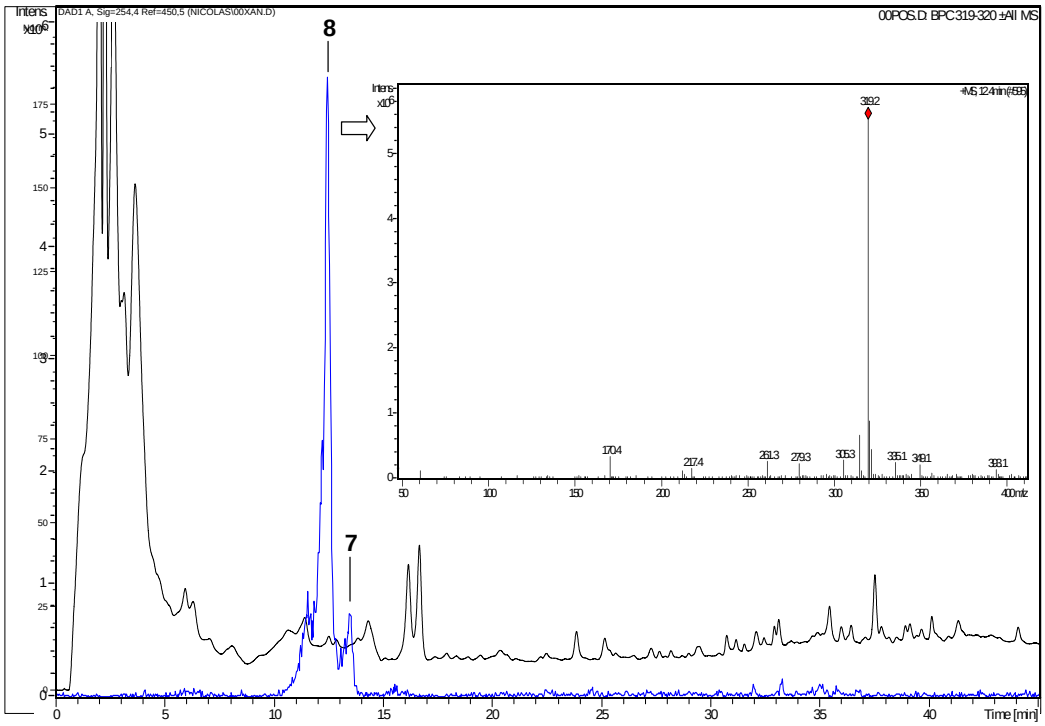

Figure 3.42 Superimposition of the UV chromatogram (254 nm) with the ESI-(+) extracted ion chromatogram m/z [319-320] of compounds **7** and **8** in strain 00 with, inset, the mass spectrum of **8**

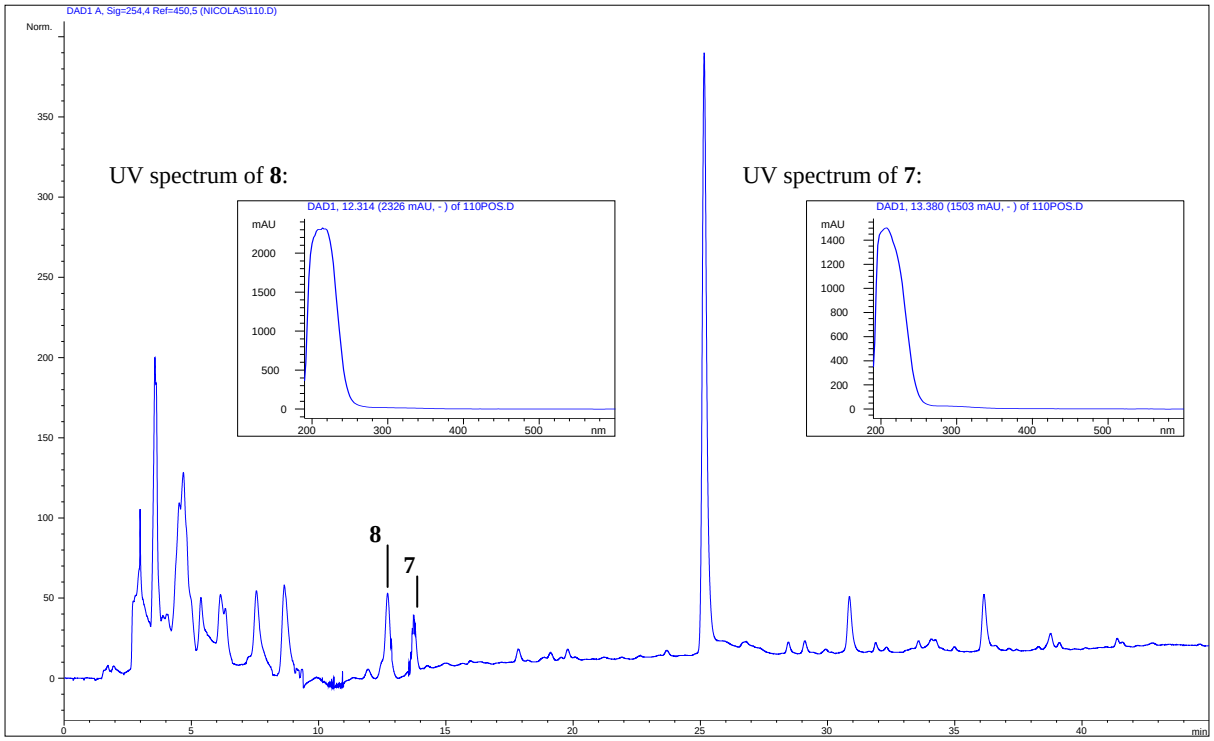

Figure 3.43: HPLC-UV spectrum (254 nm) of the crude extract of strain 110 and the detection of **7** and **8** and, inset, their UV spectra

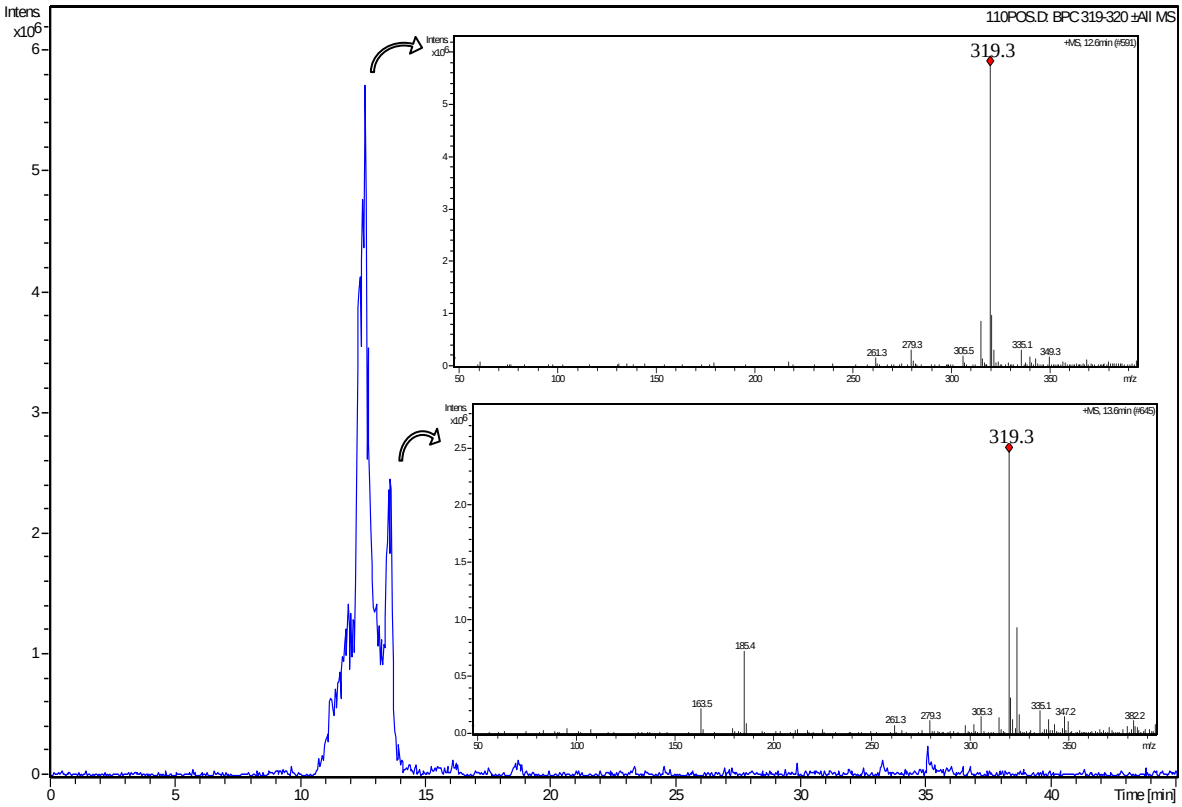

Figure 3.44 ESI-(+) extracted ion chromatogram of compounds **7** and **8**, with inset, the corresponding mass spectra in strain 110

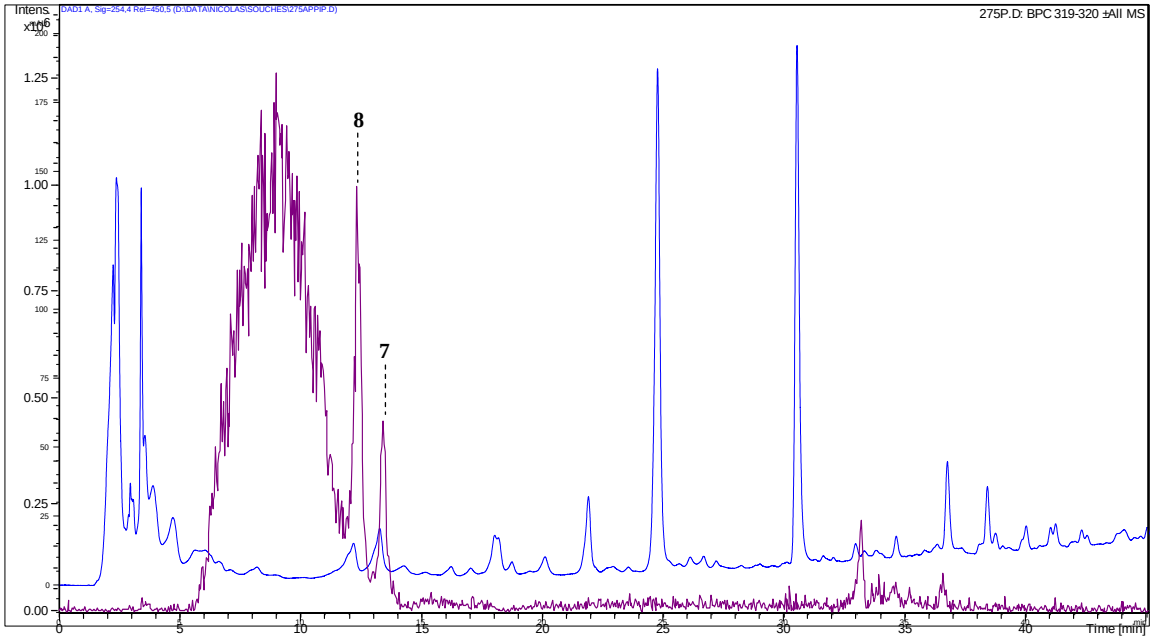

Figure 3.45 Superimposition of the UV chromatogram (254 nm) with the ESI-(+) extracted ion chromatogram m/z [319-320] of compounds **7** and **8** in strain 275

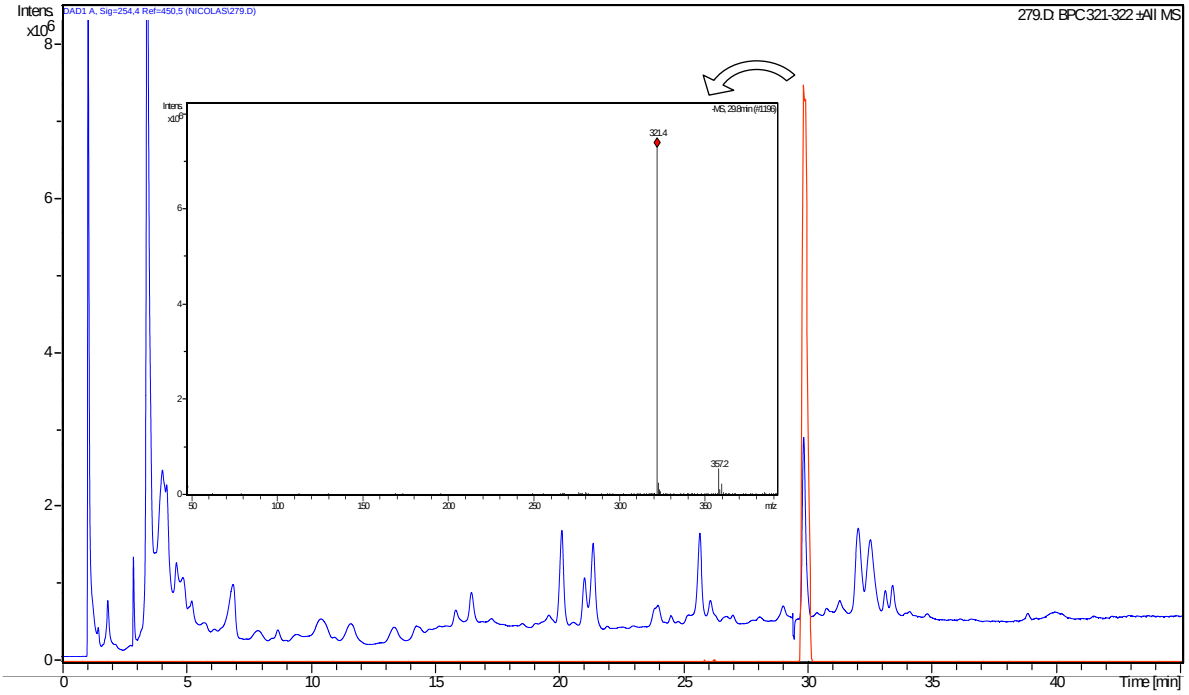

Figure 3.46 Superimposition of the UV chromatogram (254 nm) with the ESI-(-) extracted ion chromatogram m/z [321-322] of compound **5** with, inset, the corresponding mass spectra in strain 279

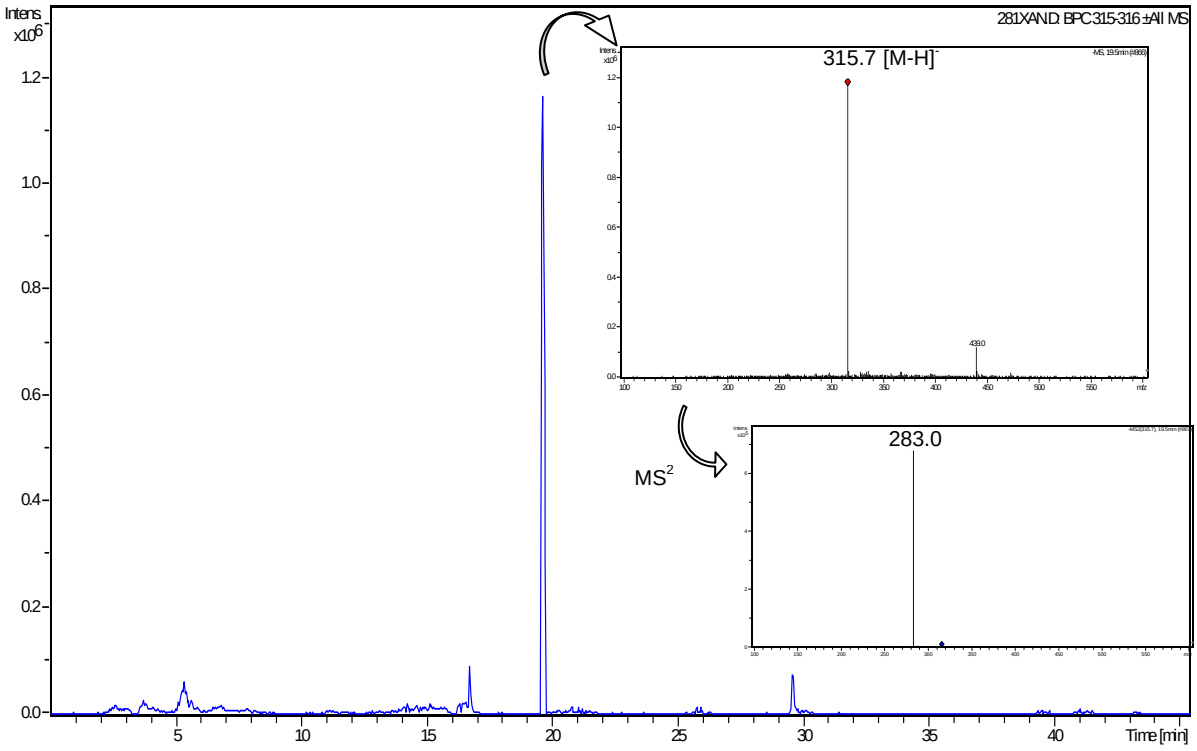

Figure 3.47 APPI-(-) extracted ion chromatogram of compound **2** in strain 281, with, inset, the corresponding MS and MS^2 mass spectra

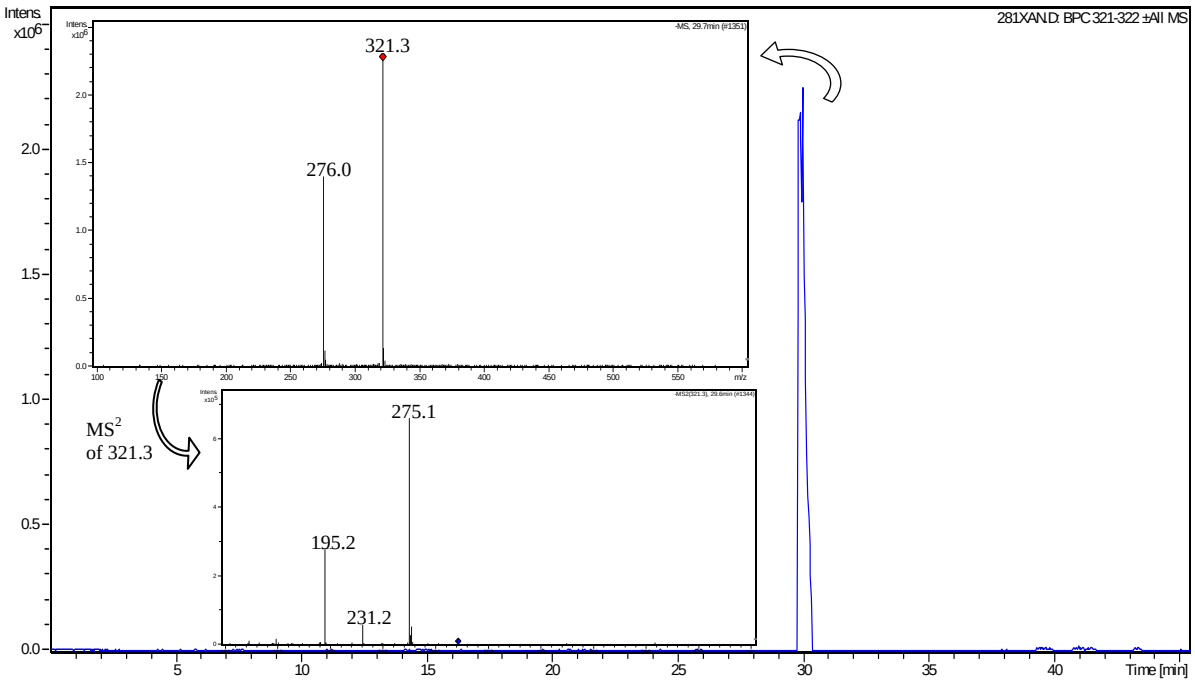

Figure 3.48 Appi-(-) base peak ion chromatogram of compound **5** of strain 281 with, inset, the corresponding MS and MS^2 mass spectra

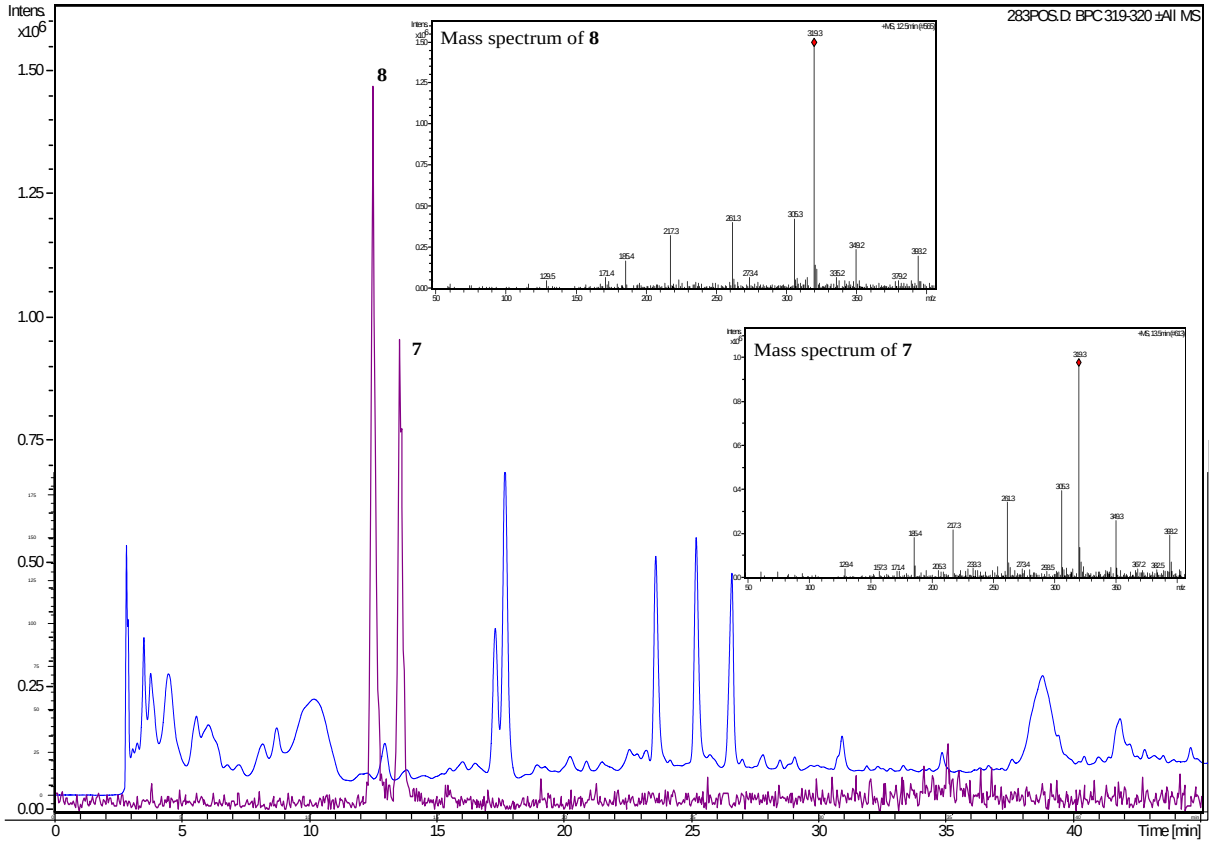

Figure 3.49 Superimposition of the UV chromatogram with the ESI-(+) extracted ion chromatogram m/z [319-320] of compounds **7** and **8**, with, inset, their respective mass spectra in strain 283

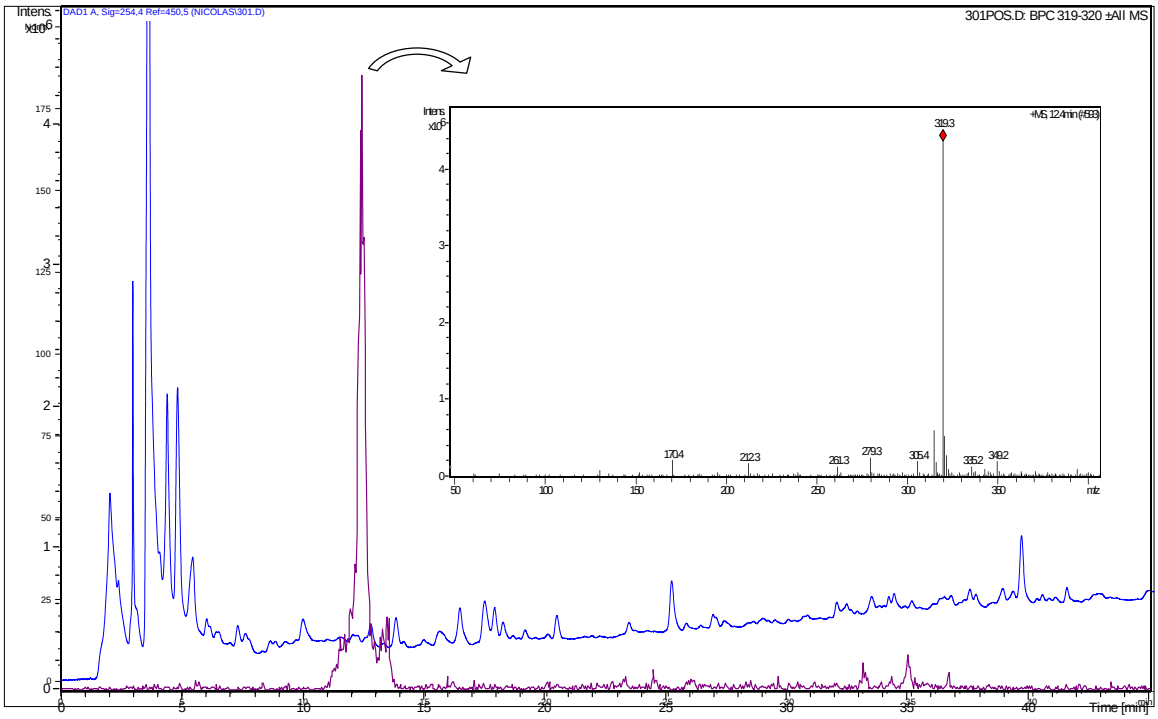

Figure 3.50 Superimposition of the UV chromatogram (254 nm) with the ESI-(+) extracted ion chromatogram m/z [319-320] of strain 301

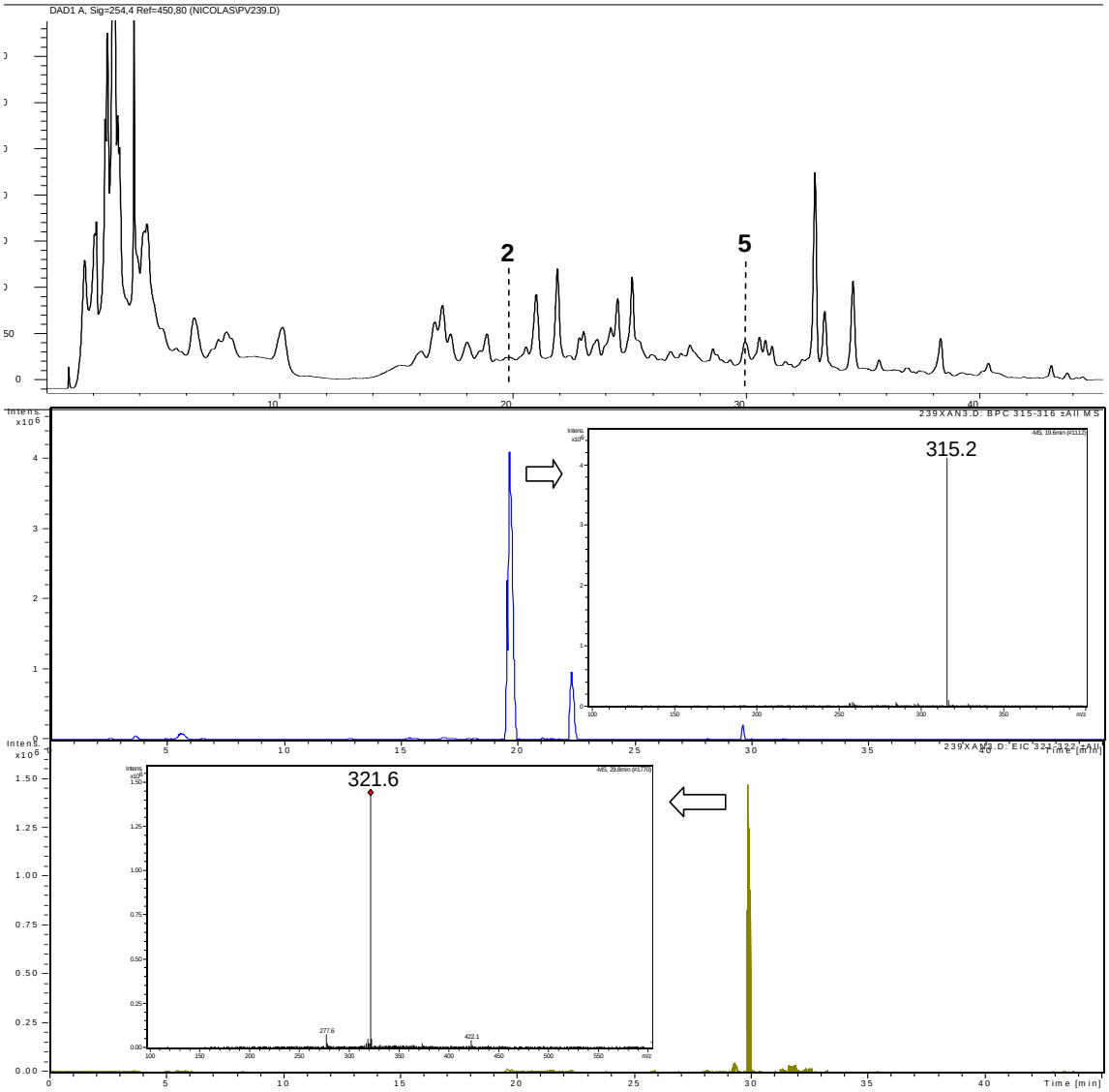

Figure 3.51 HPLC UV chromatogram (254 nm, top) with the extracted APPI-(-) ion chromatograms of compounds 2 (middle) and 5 (bottom) with, inset, their respective MS spectra in strain 239.

3.7. Fungal cultures on grapevine wood

The metabolites we found came from extracts of the fungus grown on an artificial medium, potato dextrose agar. However, it is known biochemical pathways active in fungi can vary depending on the nutrients available. Because of this, an experiment was made to see if the metabolites were also produced on grapevine plants. The fungus was grown on pruned grapevine canes, which is close enough to natural conditions without having the inherent problems that might arise when using healthy sentient canes like the coexistence of several

other fungi on the canes, or a purely practical problem such as the detection of the metabolites since they are produced in such small quantities. Thus, with this method, the contact surface of the fungus with the wood is high, hopefully promoting a high production of metabolites.

Figure 3.52 The grapevine wood infected by the fungus in the bag, 21 days after inoculation

The strain used for this experiment was the 239 as it not only provided most of the metabolites found but also in large quantities. Once the wood was inoculated with the fungus, it was left for 21 days and then extracted. Figure 3.50 shows the wood invaded by the mycelium of the fungus after 21 days. Two extracts were obtained, the "water extract" and the "ethyl acetate" extract (see Material and Methods, 2.2).

This experiment showed the limitations of the UV detector (Fgure 3.50) as none of the compounds were detected with it. However, three of the metabolites were detected by MS in the wood extract: **1**, **2** and **3**.

The LC-MS/MS analysis of the water extract showed the presence of compounds **2** and **3** which were detected by using the APPI interface. In the ethyl acetate extract, the two

xanthones **1** and **2** along with compound **3** were detected, this time by both APPI and ESI techniques. The fact that phomopsolide B was not detected is not surprising since it was not found in the PDA cultures of strain 239. The cytosporone **5** was also not detected despite the fact that it was produced on PDA. It seems unlikely that it remained undetected: the pure compound was used to optimise the APPI-(-) ionisation parameters and it still remained undetected. It is more likely that, as the wood used for the experiement is a relatively poor media compared to PDA, where glucose is readily available, the beginning of the synthesis of **5** could be delayed. Possibly, 28 days after the inoculation it would have been possible to isolate **5**. For the xanthones however, the situation is different since we showed that they were already produced after only two weeks on PDA.

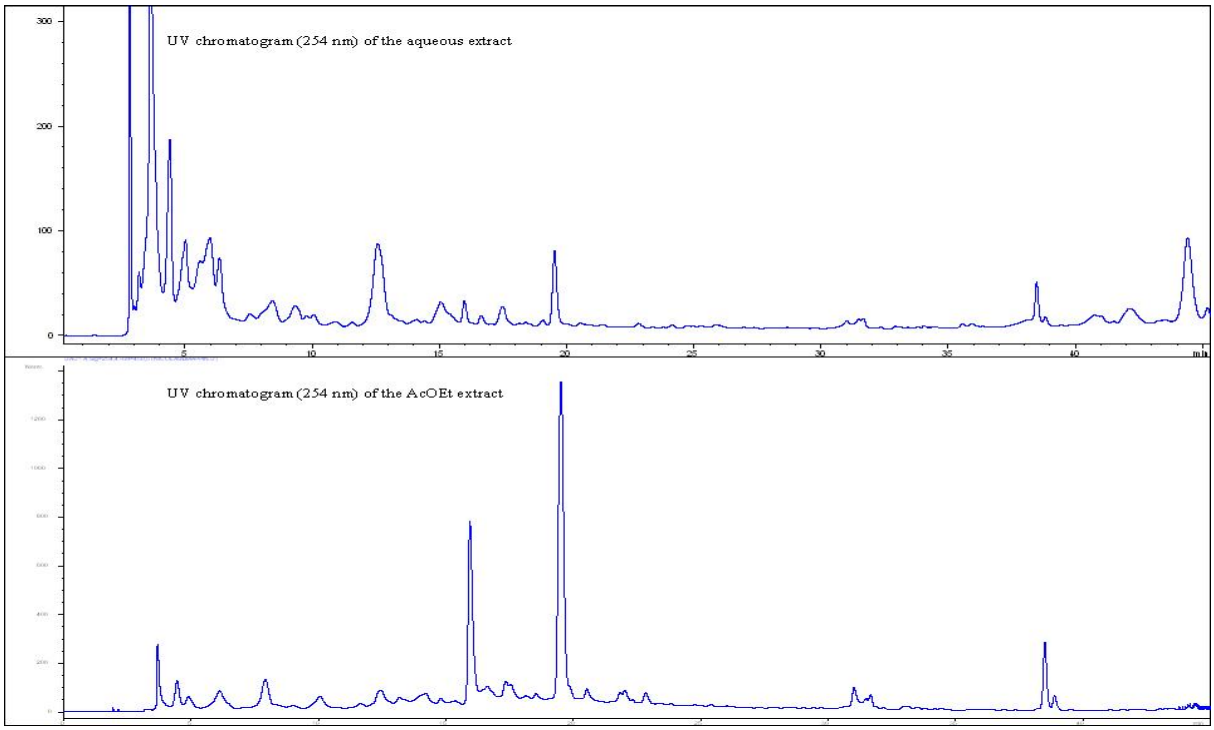

Figure 3.53 HPLC-UV chromatograms of the aqueous (top) and EtOAc extracts of the infected wood

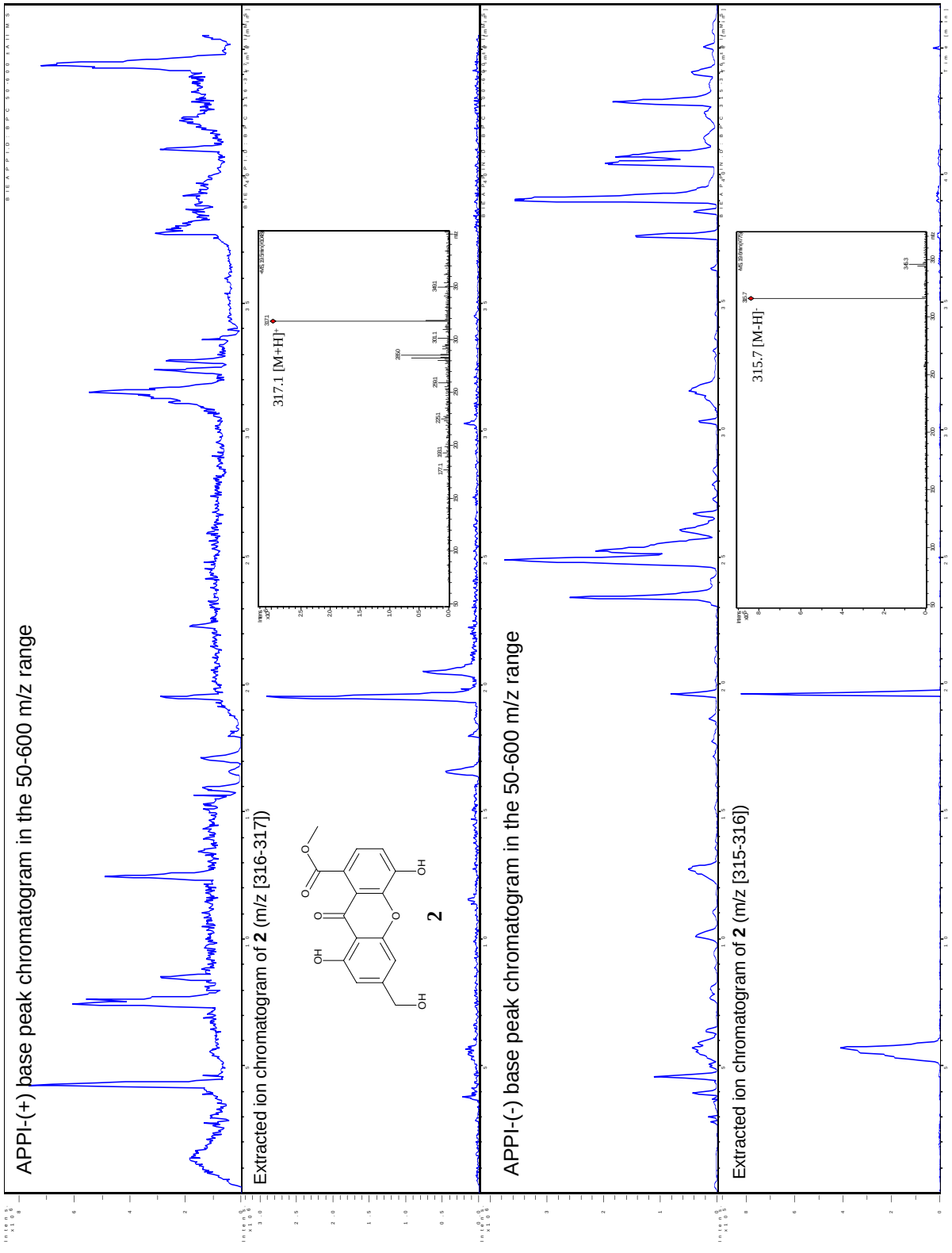

Figure 3.54 APPi-(+) & (-) base peak and extracted ion chromatograms with MS spectrum of **2** (Water extract)

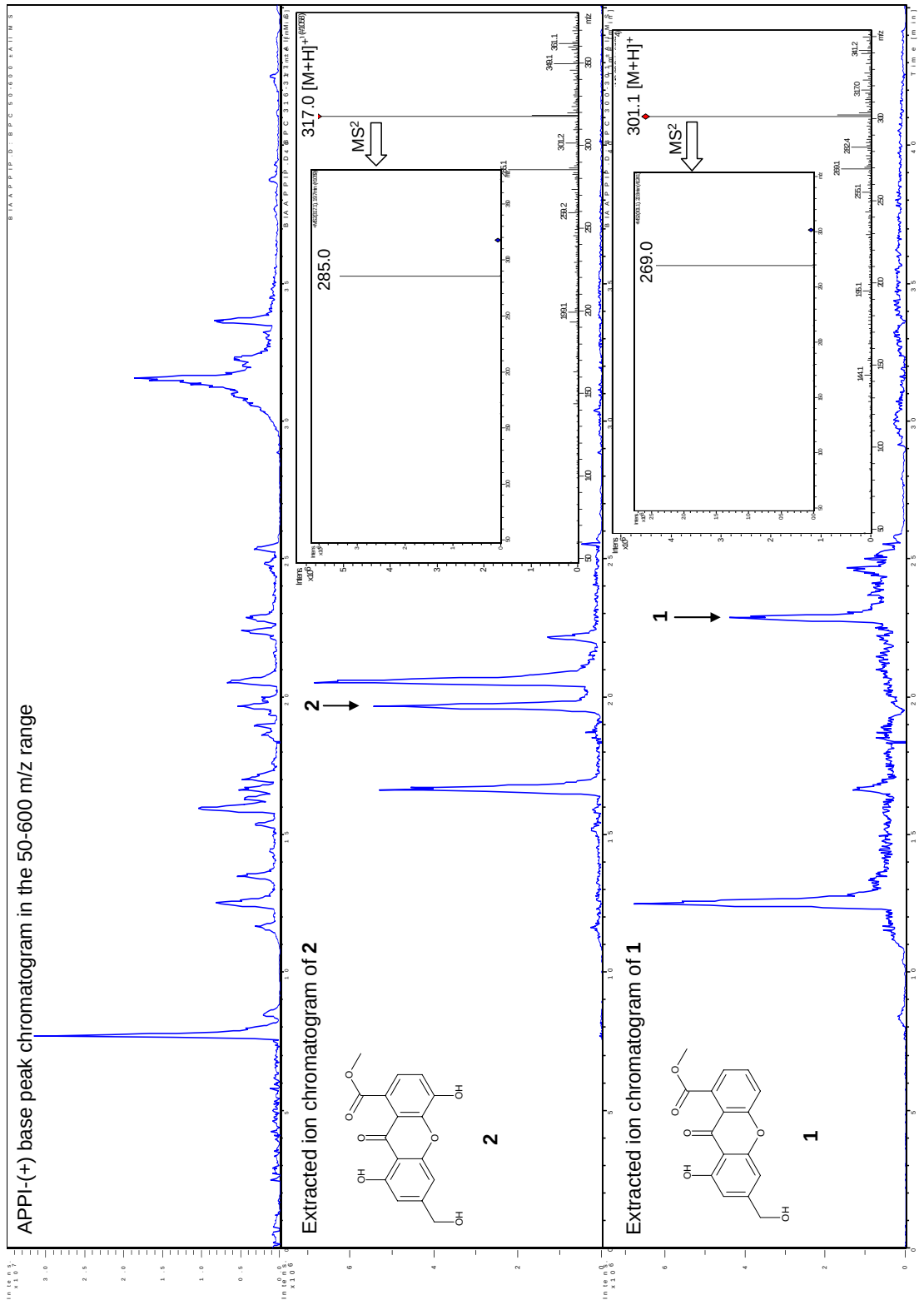

Figure 3.55 APPI-(+) base peak and extracted ion chromatograms of **1** and **2** with, inset, MS and MS^2 spectra (EtOAc extract)

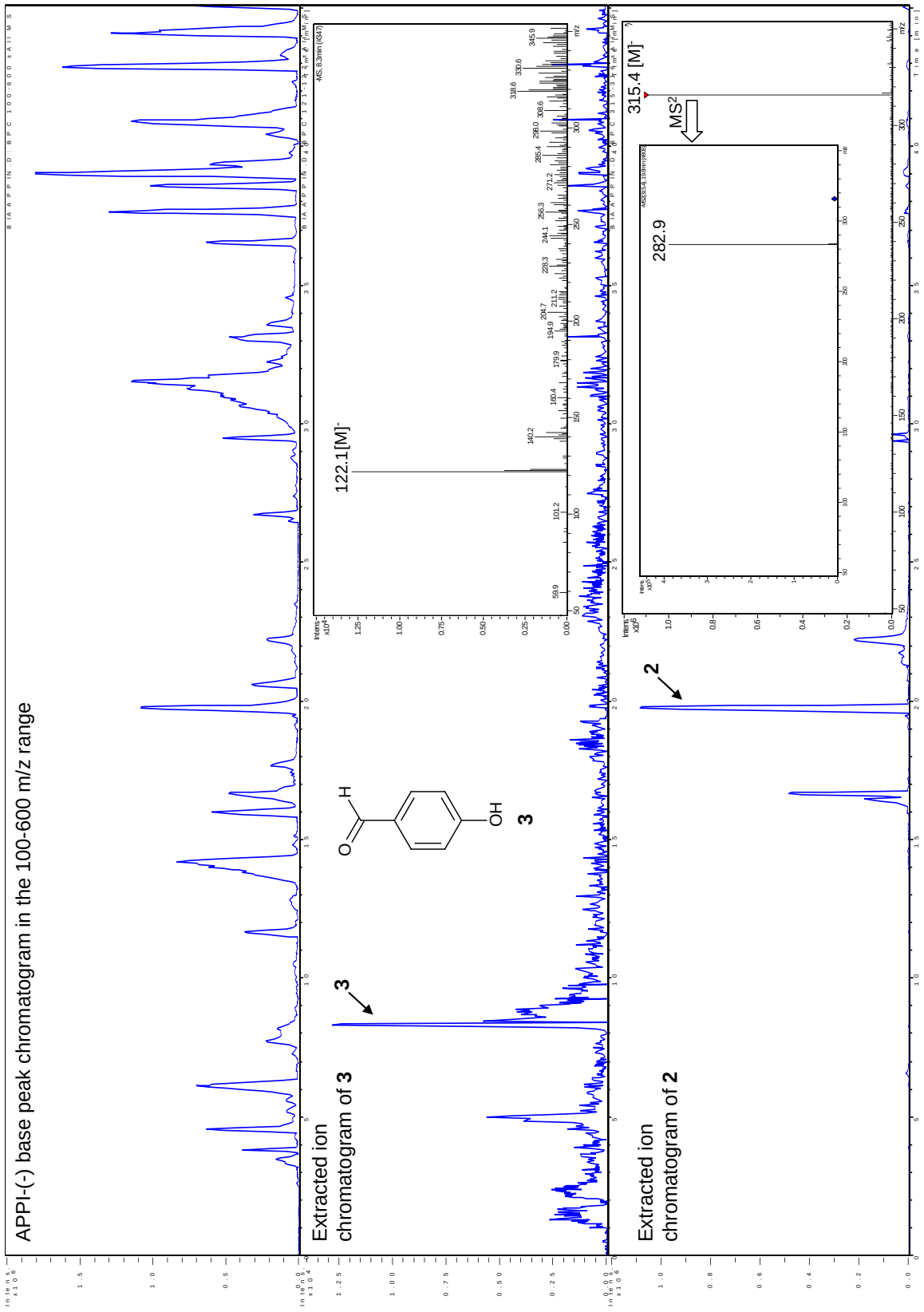

Figure 3.56 APPI-(-) base peak and extracted ion chromatograms of **2** and **3** with, inset, MS spectra (EtOAc extract)

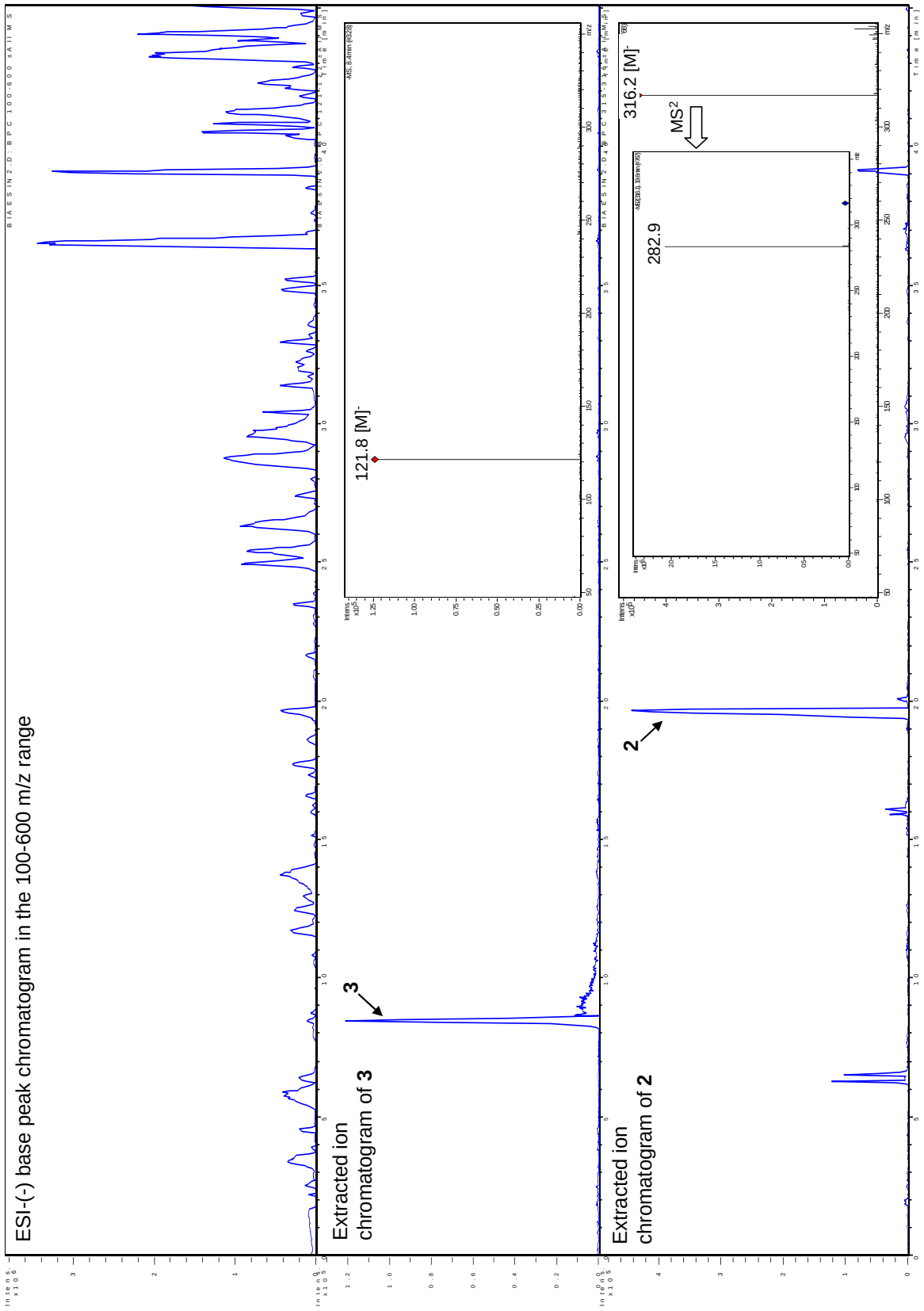

Figure 3.57 ESI-(-) base peak and extracted ion chromatograms of **2** and **3** with, inset, MS and MS^2 spectra (EtOAc extract)

4. Discussion

4.1. Primary metabolism

The purpose of the primary metabolism of an organism is to provide it with energy, synthetic intermediates and macromolecules such as proteins or DNA via a series of complex enzyme-catalysed chemical reactions. Generally speaking the reactions encountered in the primary metabolism are the same for all living organisms. It is thus not specific and neither are the metabolites produced by primary metabolism.

The main source of carbon comes from glucose or carbohydrates. A long sequence of biosynthetic processes is used to oxidise the sugar to water and CO_2 with the production of energy, in the form of 38 molecules of ATP. A succinct scheme with the various reactions is shown in Figure 4.1. The most important intermediate is the acetyl coenzyme A (acetyl CoA) which comes from the conversion of glucose into triose, then pyruvate. Carboxylation of acetyl CoA gives malonyl CoA which, in turn, can undergo a linear condensation with, again, acetyl CoA, to give either fatty acids or to polyketides. Alternatively, three molecules of acetyl CoA can condensate to give mevalonic acid, the intermediate to the synthesis of terpenes, sterols and carotenoids. Finally, condensation of acetyl CoA with oxaloacetate via the tricarboxylic acid ring results in the complete oxydation of glucose and also in the synthesis of amino acids, organic acids and secondary metabolites. There are three routes the fungi can use to convert glucose to pyruvate: the Embden-Meyerhof, the pentose phosphate and the minor Entner-Douderoff pathways[60].

The secondary metabolism uses synthetic pathways whose end products role are not established[60;78] but are characterised by low molecular weight (< 1500 Da), have no function in growth and have unusual and varied chemical structures[31]. The boundary between both metabolisms is not really clear; however, secondary metabolites are usually characteristic of the family or genus studied[31;60;78]. This specificity is also a means to classify organism according to their chemical composition and has been termed chemotaxonomics[31].

The diversity in secondary metabolites is enormous and ranges from amino acids derivatives, to terpenoids, flavonoids, phenolic compounds, etc.

Figure 4.1 shows the different branchings the secondary metabolism can take. In fungi, the polyketide family is the largest group of compounds. They are synthesised by mechanisms

analogous to those used for the biosynthesis of fatty acids but differences, such as oxidations, cyclisation, occur during chain elongation[78].

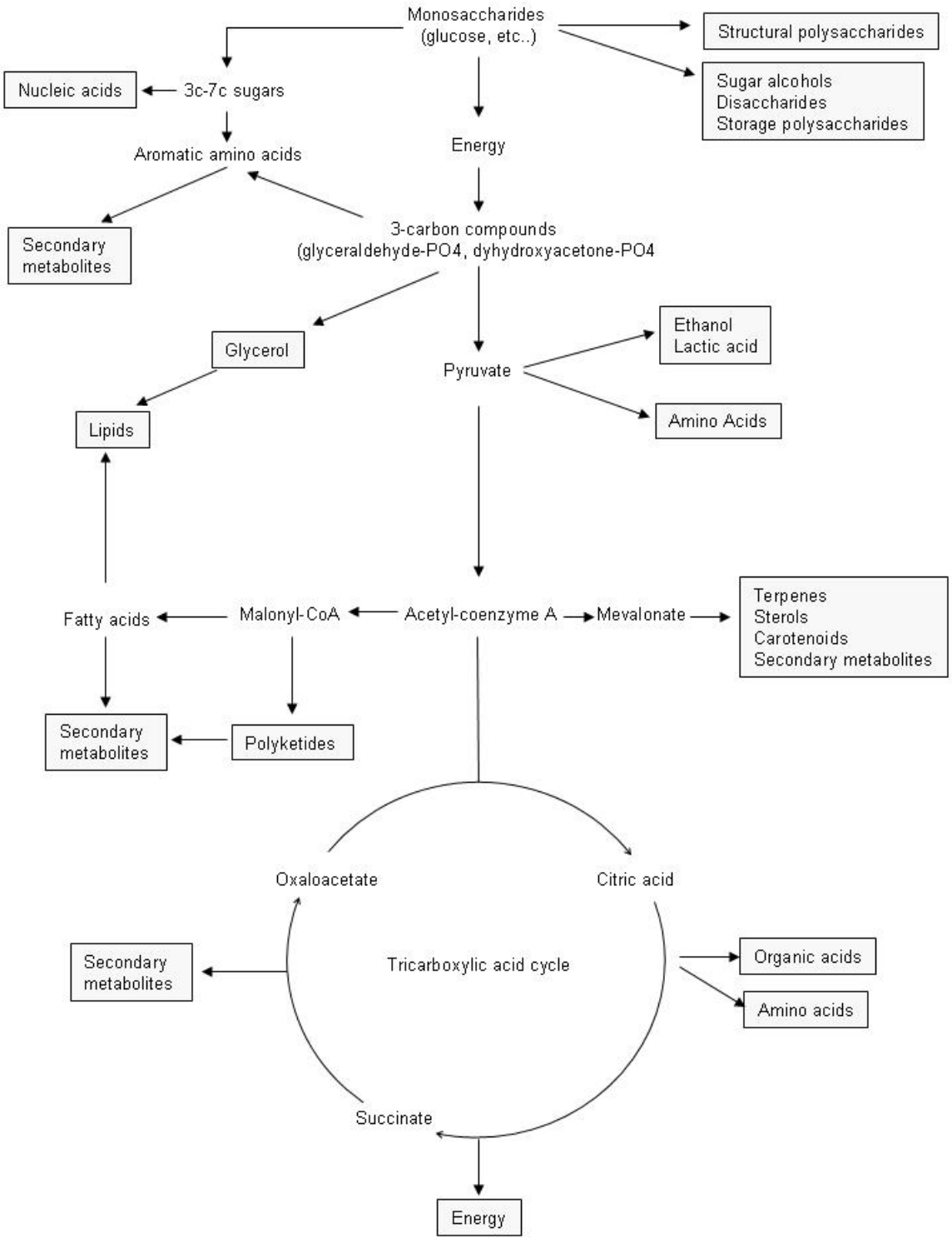

Figure 4.1 The primary metabolism in fungi[60]

Several hundreds of thousands of metabolites have been described over the last 60 years and some of them have become well-known like the antibiotics penicillin and cephalosporin C[31;78]. The mycotoxins, toxic substances produced by fungi, have a broad range of chemical structures and include aflatoxins (produced by *Aspergillus* sp.), trichothecenes (*Fusarium* sp.), zearalone (*Fusarium* sp.) and Ochratoxin A (*Penicillium verrucosum*)[79;80].

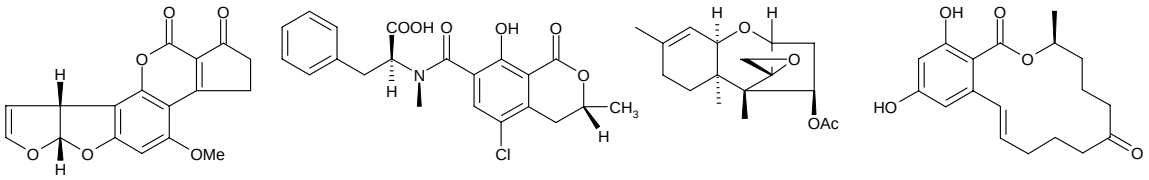

Figure 4.2 The structures of some well-known mycotoxins

4.2. The shikimic acid pathway: *p*-hydroxybenzaldehyde biosynthesis

The shikimic acid pathway converts simple carbohydrate precursors derived from glycolysis and the pentose phosphate pathway to the aromatic amino acids without intervention of the acetate[81]. Its main role is to provide the organism with the essential aromatic amino acids that are tryptophan, tyrosine and phenylalanine[60;81]. One of the pathway intermediates is shikimic acid, which has given its name to this whole sequence of reactions.

This pathway is present in plants, fungi, and bacteria but is not found in animals. Animals have no way to synthesize the three aromatic amino acids which are therefore essential nutrients in animal diets.

The shikimic acid pathway begins with the condensation of erythrose-4-phosphate (derived from the pentose phosphate pathway) with phosphoenolpyruvate (derived from the Embden-Meyerhof pathway) to give 3-deoxy-7-phospho-D-arabinoheptulosonate which will then be converted to shikimate.

As well as leading to the amino acids, it also provides the intermediates for the biosynthesis of aromatic secondary metabolites which can either be benzene derivatives,

diphenylbenzoquinones or miscellaneous compounds. Among the benzene derivatives, one can find *para*-hydroxybenzaldehyde that was isolated from *P. viticola*.

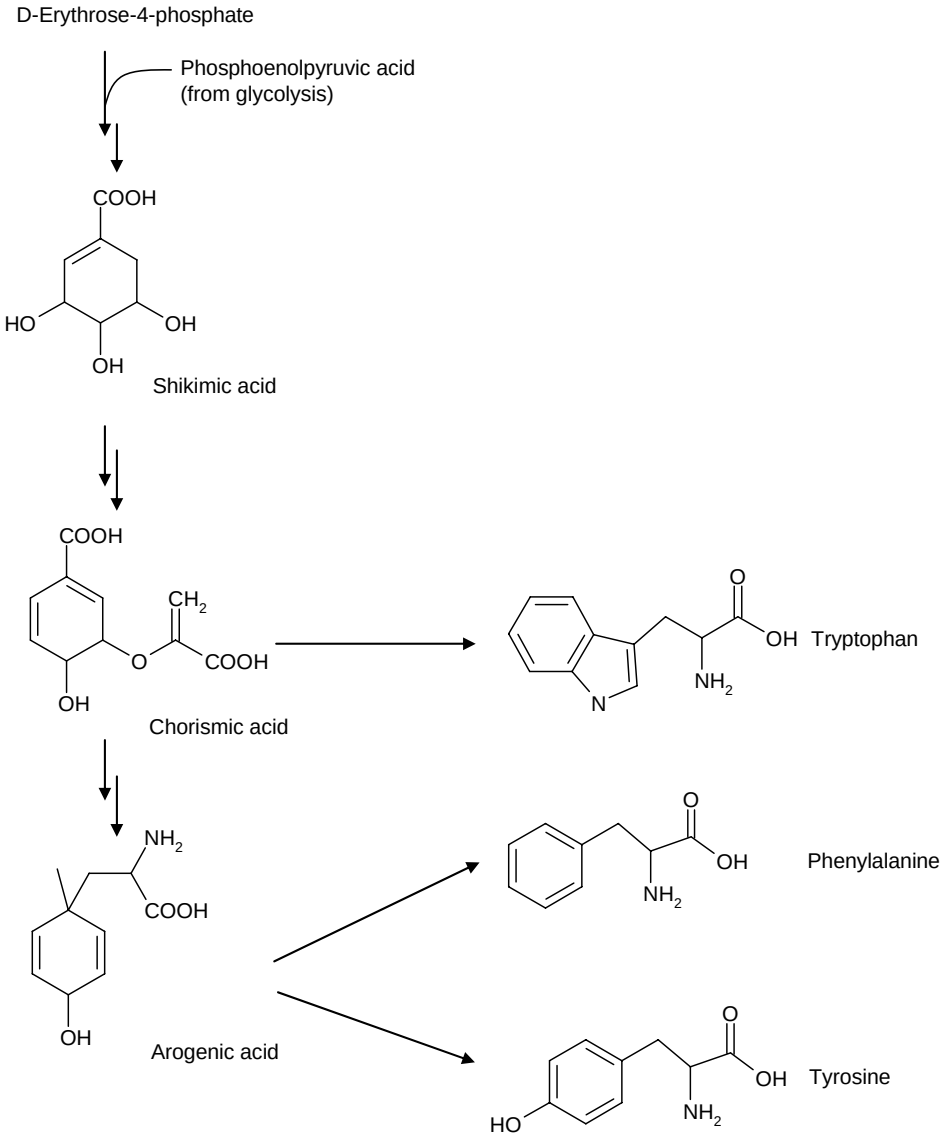

Figure 4.3 The shikimic acid pathway

Bonnarme et al.[82] proposed the following biosynthetic pathways (Figure 4.4) for the degradation of L-phenylalanine in the white rot fungus, *Bjerjkandera adusta*, in oxidative and non-oxidative fashions. One of the degradation products is *p*-hydroxybenzaldehyde which could explain its isolation from *P. viticola*.

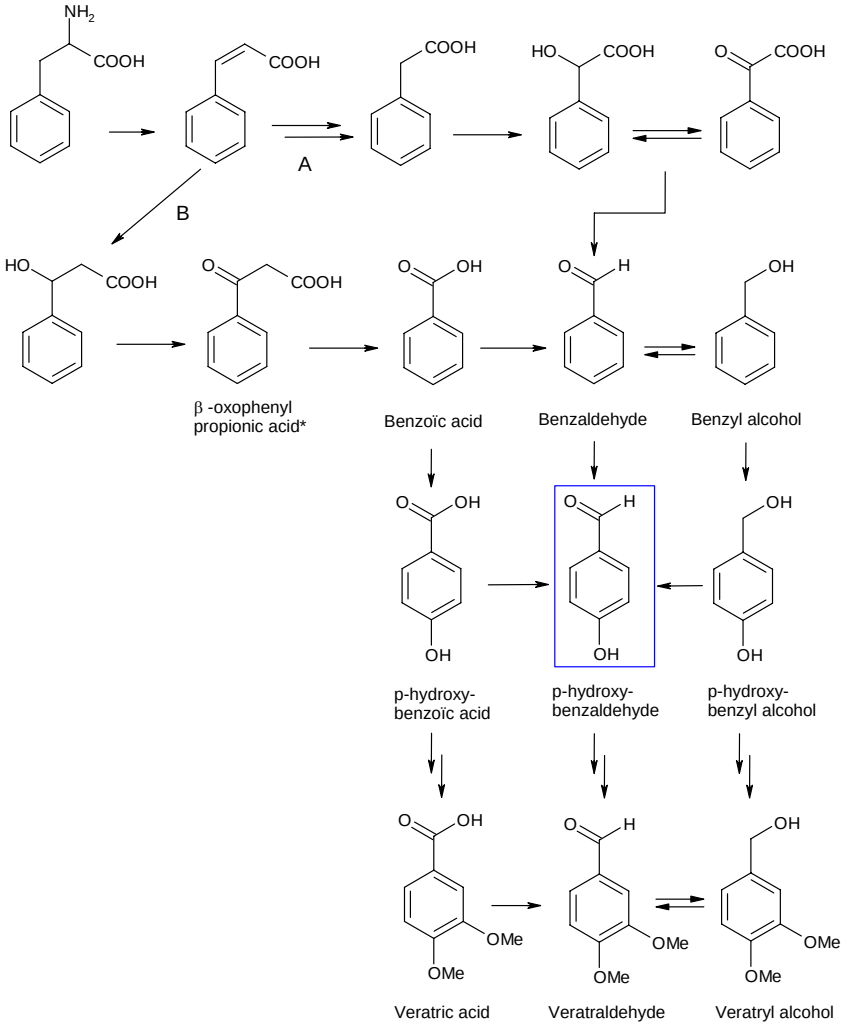

Figure 4.4 The two supposed pathways (A: non-oxidative B: β-oxidation) for the degradation of phenylalanine in *B. adusta* (adapted from Bonnarme et al..[82])

4.3. The polyketide pathway

The polyketide pathway starts with the condensation of an acetyl unit with malonyl units with a decarboxylation step to result in a poly-β-ketomethylene moiety which possesses activated methylene groups which can react internally by aldol-type condensations to give aromatic compounds, i.e. secondary metabolites. As chains with different lengths can be used, a great variety of cyclisations are possible. Further diversity can be obtained by different reactions.

4.3.1. Biosynthesis xanthones 1 and 2

As reported in the introduction, it is not surprising to find xanthones in the current study as the species from the *Phomopsis* genus are well-known producers of this type of compound.

It is generally accepted that xanthones are formed in plants by cyclisation of hydroxylated benzophenones deriving from shikimate but their biogenesis usually differs in fungi[83-85]. In plants, the central xanthone ring partly comes from oxidative coupling of benzophenone derived from shikimate. In fungi (and lichens) benzophenones are totally acetate-derived and ring closure is done by an addition-elimination process. Two types of cyclisation processes can take place with the fungal polyketide chain, either a circular folding (Figure 4.5) or a looped folding (Figure 4.6) [84].

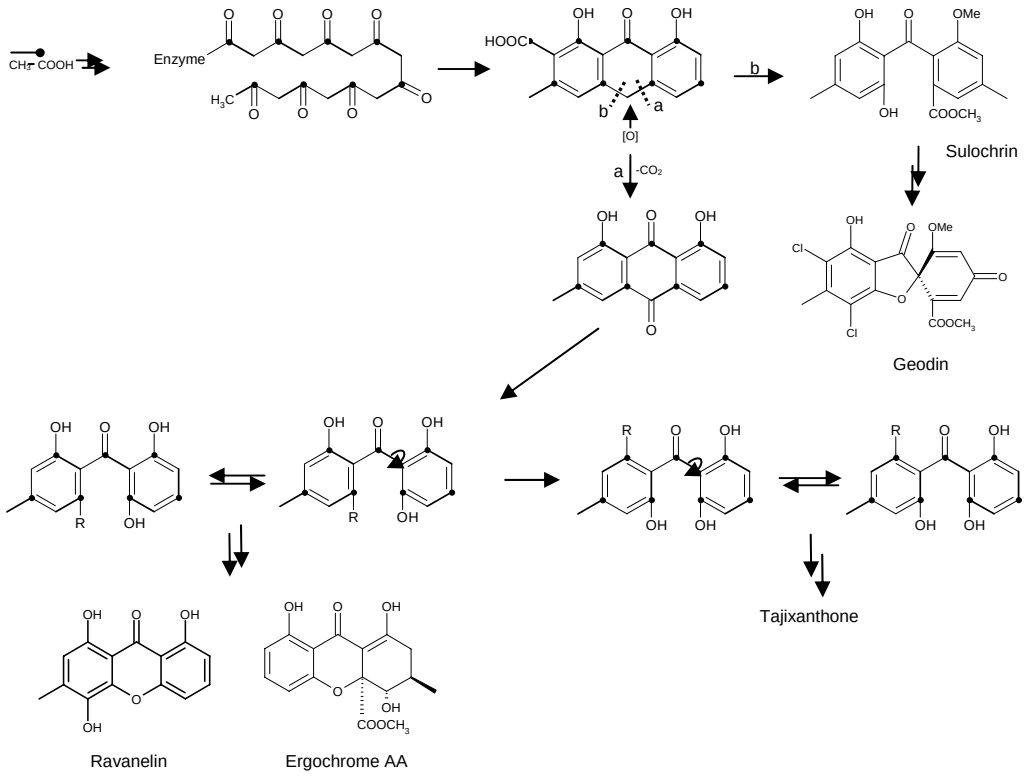

Figure 4.5 The circular folding encountered in xanthones biosynthesis

The looped folding leads directly to the precursors of griseoxanthones (Figure 4.6).

The circular folding requires the oxidative cleavage of an intermediate, an anthraquinone (such as chrysophanol[83;84;86-89]) or an anthrone, to lead directly to the formation of benzophenones or directly to metabolites, for example sulochrin, which was discovered in *Aspergillus terreus* [83;84].

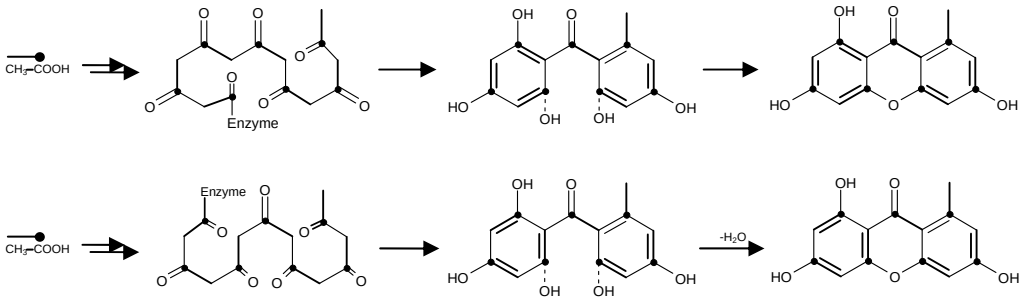

Figure 4.6 The two types of looped folding encountered in xanthone biosynthesis

The fission of the central ring is believed to follow a Bayer-Villiger mechanism[84;89]. Each of the ortho hydroxyl groups of the benzophenones is capable of an electrophilic attack on the adjacent ring to yield the xanthones by an addition-elimination mechanism which is yet still not understood. The benzophenones often possess two rotation axes around which the aromatic rings can rotate thus affording different xanthones (Figure 4.7).

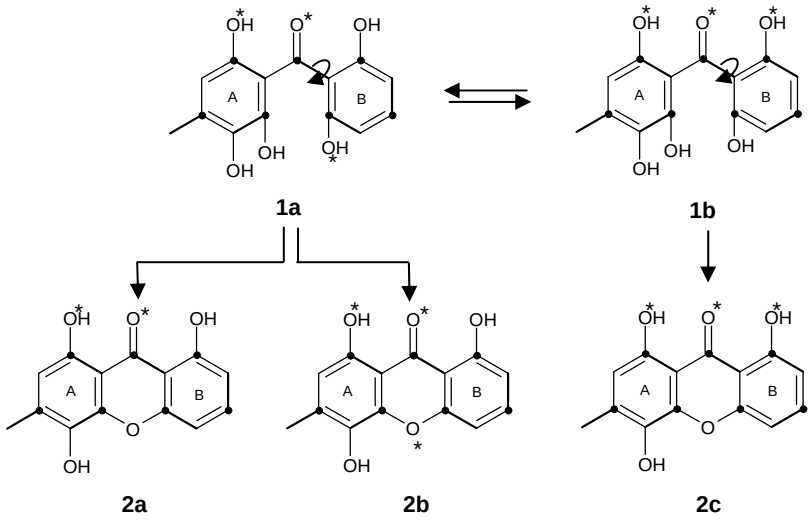

Figure 4.7 The three possible rotamers 2a, 2b, 2c

Labelling experiments with ^{18}O and the detection of induced chemical shift changes in ^{13}C NMR spectra for the biosynthesis of ravanelin showed different labelling patterns in the xanthones, thus demonstrating this possibility[84]. Theoretically, from the rotamers 1a and 1b, three different xanthones should be formed: **2a**, **2b** and **2c** (Figure 4.7). However, **2b** and **2c** represent the majority of formed molecules thus suggesting that ring closure is done by the nucleophilic attack of ring B on the ortho position of ring A.

Given this, the biosynthesis of sydowinin A, compound **1**, and of compound **2** should follow one of these pathways, probably starting by a circular type folding to form chrysophanol **3a**. Then the formation could follow two paths, A and B (Figure 4.8). Pathway a comes from the mechanism proposed by Hamasaki *et al*.[63] that suggested chrysophanol was the precursor of sydowinol **3b**, by an oxidative cleavage of the anthraquinone, which was in turn dehydrated to form **1**. This is supported by the fact that they isolated **3b** along with **1** in the culture medium. An alternative, pathway b, comes from the biosynthetic study on chloromonilicin that was isolated from a culture filtrate of *Monilinia fructicola*, a fungus responsible of brown rot on rosaceous fruit trees[90]. It showed that chrysophanol **3a** was the intermediate to the synthesis of moniliphenone **3c** which was in turn transformed to chloromonilicin (Figure 4.8)[90]. However, an interesting fact is that they also isolated the xanthone **4a** which is the reduced version of **1**.

.

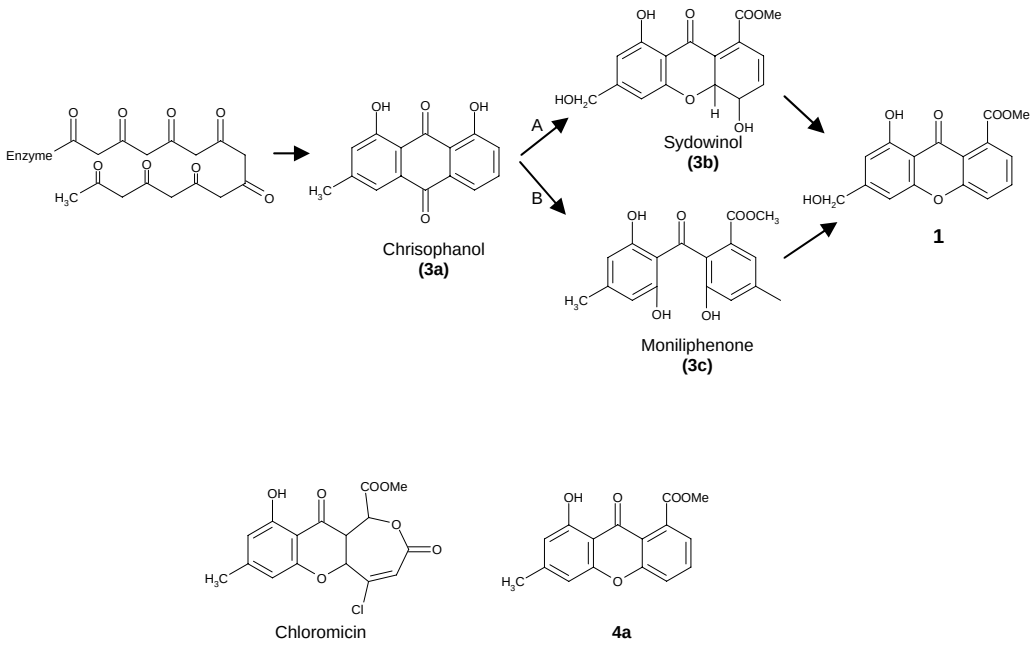

Figure 4.8 The proposed biosynthetic route for **1** and the structures of chloromycin and **4a**

4.3.2. The cytosporone (5) biosynthesis

Brady et al.[61] who isolated, amongst others, cytosporone A, B and C (Figure 4.9), suggested that their biosynthesis could come from the polyketide pathway. Isocoumarins and coumarins are common natural products but the type of cyclisation seen for the formation of these lactones not so. However, a closely related compound could be curvularin. Although the structures seem different, they might possess the same precursor, the difference being the way

they cyclicise. Thus, Brady suggested that cytosporone A could be this precursor and that, while curvularin would close the lactone ring at C-15, cytosporone C would be formed by the reduction of C-15 followed by ring closure[61].

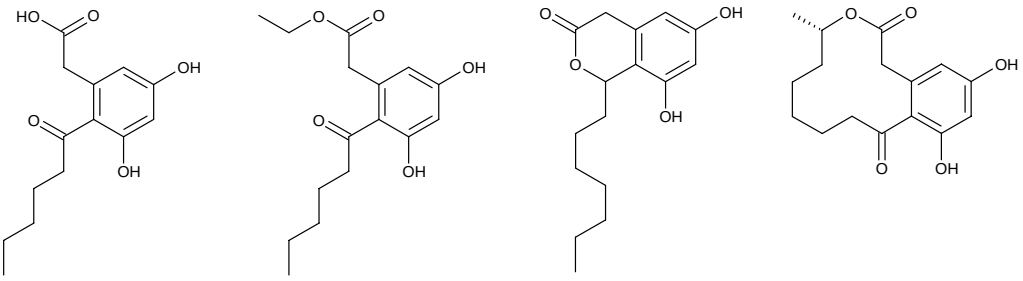

Figure 4.9 The structure of cytosporones A, B, C and curvularin

The following pathway can be proposed for the formation of the cytosporones, starting with a circular type of folding of the polyketide to form the dihydroxybenzene ring (Figure 4.10). Then the acid is esterified to give the final compound, **5**.

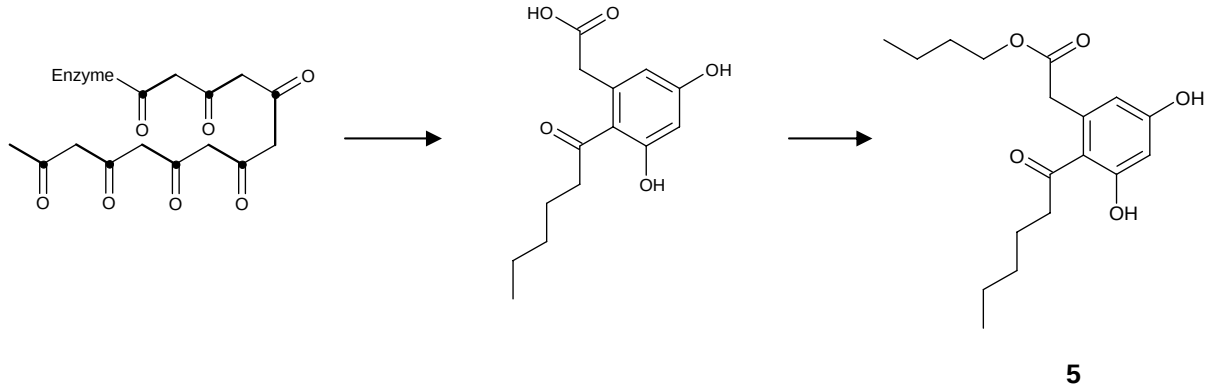

Figure 4.10 The proposed biosynthetic route for **5**

4.3.3. Phomopsolide B (7) and the furanone (8) biosynthesis

Secondary metabolites possessing a pyran-2-one moiety are found in a large number of fungi and are responsible for a wide range of biological effects, for example antibiotic, cytotoxic, neurotoxic activity, etc. Among these compounds, there are aspyrone and asperlactone two co-metabolites deriving from the polyketide pathway and that were isolated from strains of

Apergillus species. Several feeding studies with labelled ^{13}C and ^{18}O have shown that they came from a common intermediate and excluded the possibility of an aromatic precursor. Incorporations studies with ^{13}C labelled acetate also proved that the C-2 and C-8 originated from the same acetate units and thus a Favorskii-type of rearrangement occurred during the biosynthesis[91].

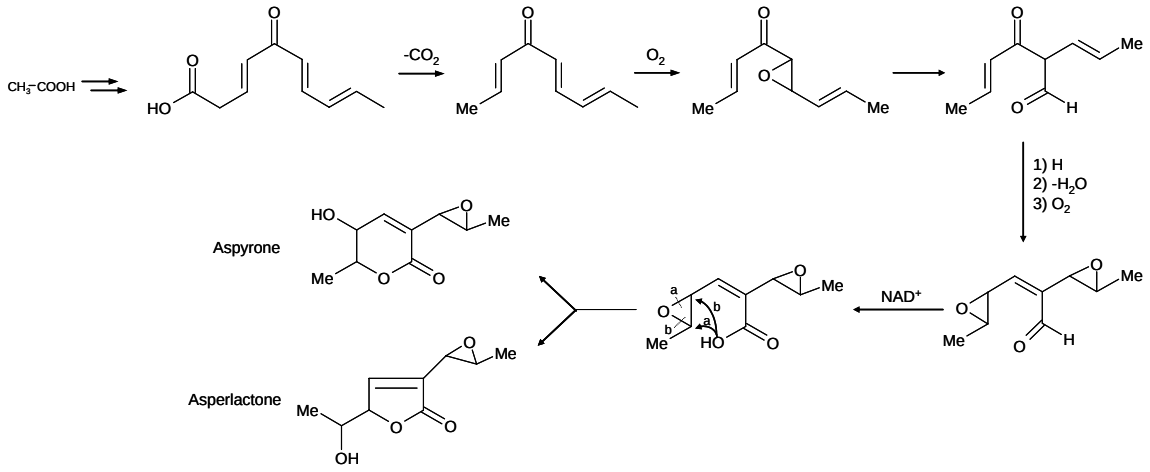

Figure 4.11 The probable biosynthesis pathway of aspyrone and its co-metabolite aspelactone[92;93]

The intervention of an aromatic intermediate was ruled out by tritium labelled acetate incorporation studies. Indeed, in the formation of mellein, a co-metabolite, or other aromatic metabolites, all three hydrogens would have been removed in the formation of the ring whereas in this case, two acetate derived hydrogens were retained[88;91].

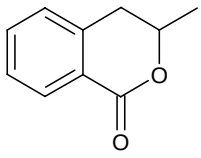

Figure 4.12 The structure of mellein

It was also established that the oxygens of the epoxy and the C-5 hydroxy came from O_2 of the atmosphere and were not acetate-derived. Investigations with [1-^{13}C, $^{18}O_2$] acetate showed that no ^{18}O isotope induced shifts in the ^{13}C NMR spectrum occurred. However, incorporation of ^{18}O at the epoxy and C-5 was done when the fungus was grown under an atmosphere of $^{18}O_2$.

Taking into consideration these results, it can be postulated that compounds **7** and **8** are not only co-metabolites but also derive from the polyketide pathway in a similar fashion to that proposed for aspyrone and asperlactone. A hypothetical biosynthetic pathway for phomopsolide B and its co-metabolite the furanone can be proposed.

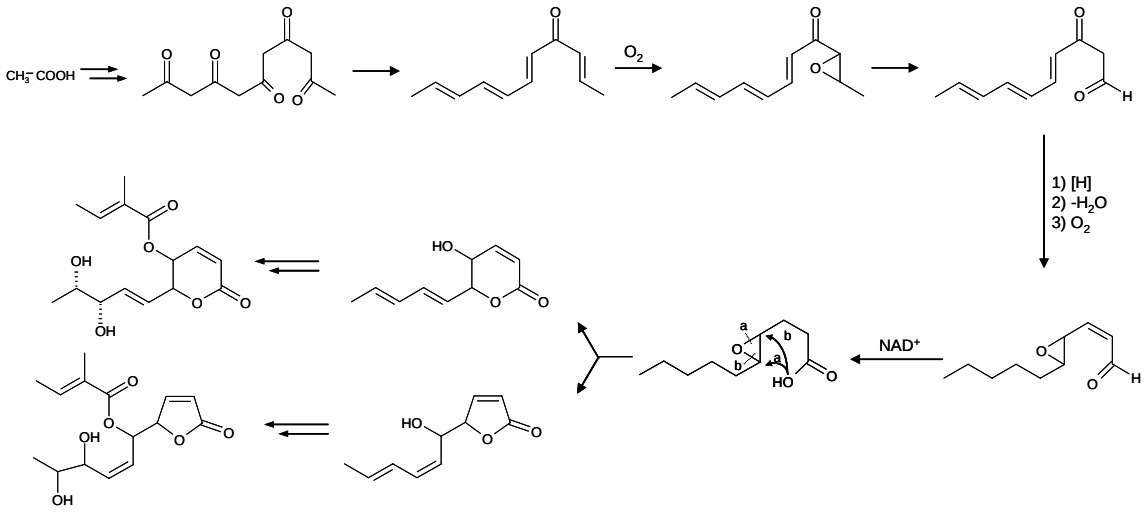

Figure 4.13 The proposed biosynthetic route for the synthesis of **7** and **8**

4.3.4. The biosynthesis of 4

It seems likely that **4** should come from the polyketide pathway although no references to similar compounds were found. Also, the fact that it was found in extremely small quantities (less than 1 mg) and in only one culture extract makes us believe that it could be either an artefact (such as a fragment of a metabolite) resulting from the use of some solvents (such as MeOH) or due to the acidity of the silica columns. Further studies should be made to confirm the production of this compound.

4.4. The mevalonic acid pathway: the sterol (6) biosynthesis

Terpenes and steroids are compounds that are widely distributed in nature and their biosynthesis has been studied extensively over the years. One of the most widespread sterols in fungi and yeasts is ergosterol, which was first isolated from ergot (*Claviceps purpurea*). The skeleton of terpenoids is acetate based, with mevalonic acid as the main precursor. The

biosynthesis of sterols starts by the condensation of two molecules of acetyl CoA to form acetoacetate. A third molecule of acetyl CoA followed by a reduction step with NADPH gives mevalonic acid. After phosphorylation, decarboxylation and elimination of phosphate, it gives isopentenyl pyrophosphate, the precursor of monoterpenes. It is reversibly isomerised into dimethylallyl pyrophosphate. Further condensations leads to the formation of squalene, via geranyl pyrophosphate and farnesyl pyrophosphate and the intervention of NADPH as a proton supplier (Figure 4.14).

Cyclisation of squalene is initiated by the formation of squalene epoxide. Depending on the conformation on the enzyme surface and how the backbone is rearranged upon cyclisation, a number of subgroups can de formed. A multiple cyclisation process then takes part to give lanosterol. Next, a series of reactions occur, with the loss of three methyl groups, two of which by oxidation and decarboxylation, to give zymosterol. It ends with the addition of the methyl group in C_{24} and the formation of the double bond at C_{22} to give ergosterol (Figure 4.15).

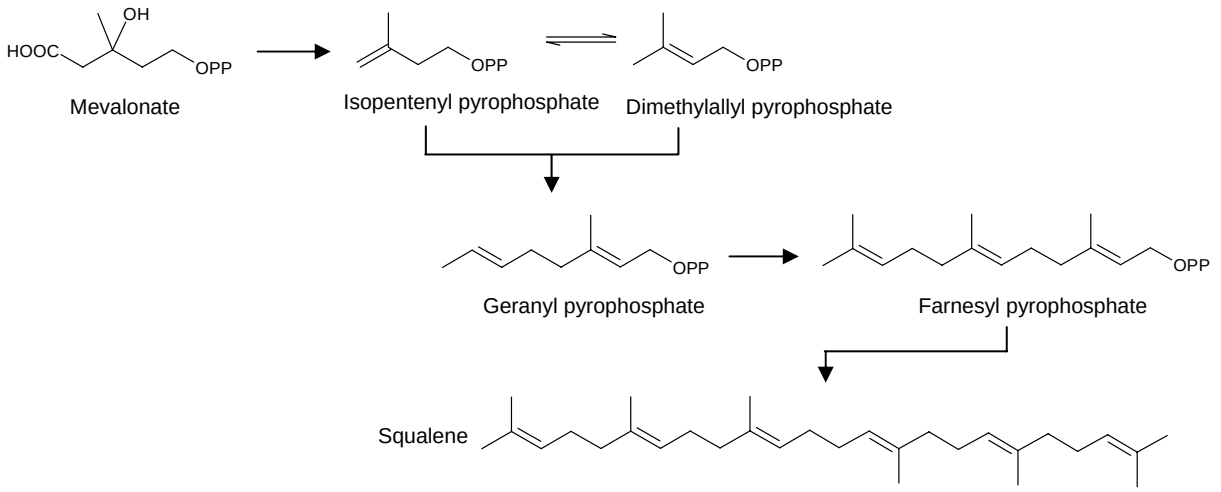

Figure 4.14 The biosynthesis of squalene

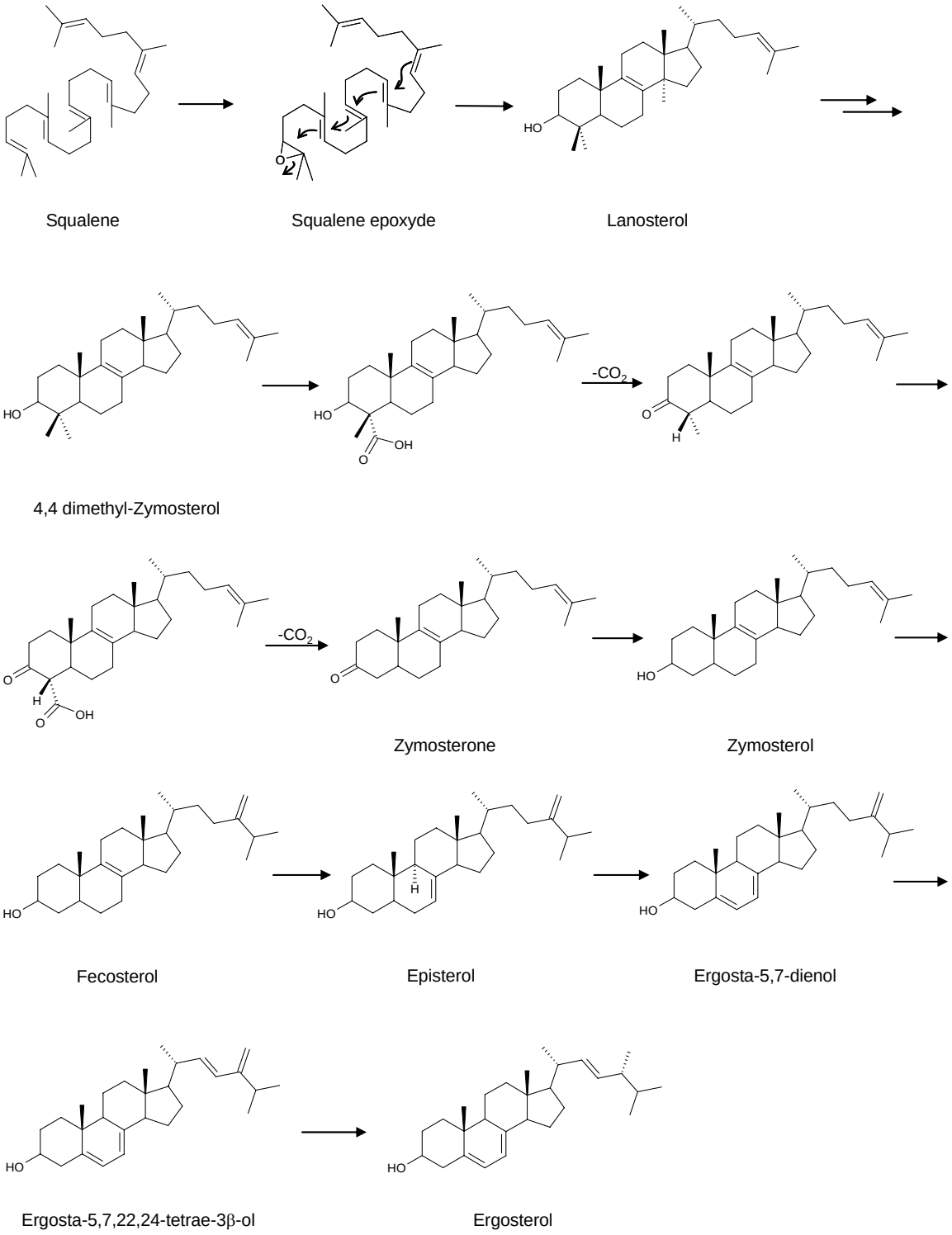

Figure 4.15 The biosynthetic pathway of ergosterol

Introduction of additional hydroxyl or olefin groups, oxidation of alcohols into carbonyl functions are all common secondary modifications the sterols have. Hence, it could be due to these additional modifications that compound **6** was biosynthesised.

4.5. The biosynthesis of 9

The isolation of compound **9** could be explained by the biosynthesis by the fungus of thiamine (vitamin B1). It was first reported in 1869 that *Aspergillus niger* excreted growth-promoting substances into its medium. Since then, much has been discovered in this field especially with bacteria and yeasts. It is generally accepted that the biosynthesis occurs by the initial separate synthesis of the pyrimidine and thiazole moieties before being linked [92;94-97]. The precursor of the thiazole part is glycine in yeasts (tyrosine in bacteria) which supplies the nitrogen and the adjacent CH carbon (C-2) while the remaining C_5 unit comes from a pentose intermediate generated by glucose or fructose by either the non-oxidative or the oxidative pentose phosphate pathway[94;98].

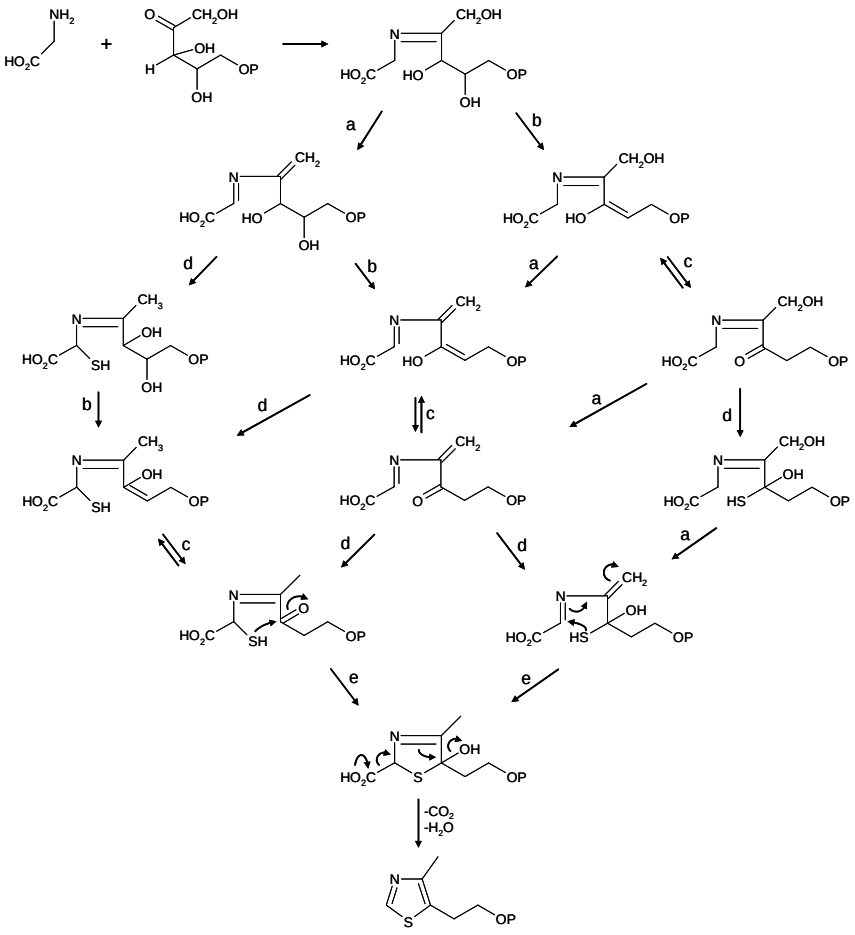

Figure 4.16 The proposed biosynthesis pathway for thiazole in yeasts a: dehydration or elimination of P, b: dehydration, c: tautomerisation, d: sulphur addition, e ring closure

This was put into evidence by White and Spenser[94;95] with *Saccharomyces cerevisiae* by radioactive experiments with D-[1-^{14}C], D-[2-^{14}C] and D-[6-^{14}C] glucose, from D-[1-^{14}C] fructose and [1-^{14}C] glycerol that showed incorporation patterns in the C_5 chain (Carbons C-4', 4, 5, 6, 7) of the thiazole unit. Other possible sources for the C_5 moiety such as polyketides, glutamate, pyruvate or lactate were discarded by White and Spenser by different labelling experiments[94;95]. Thus, they proposed the biosynthethic pathway shown in Figure 4.16 which comprises a series of steps with dehydrations, decarboxylation and sulphur addition.

4.6. Biological activities of the compounds

Five of the isolated metabolites showed biological activities in the leaf-disk assays at high concentrations. These were the two xanthones, cytosporone F, phomopsolide B and the furanone. It is interesting to note however that the aspect of the necrosis promoted by the phomopsolide B and the cytosporone is quite different. Indeed, with phomopsolide B the leaves become beige-white whereas with eutypine they become brown and with the cytosporone they not only become brown but the green part of the leaf becomes darker. It would be interesting to further study the toxicity of these compounds for vine plants and also to other types of biological assays, such as antibacterial or antiviral.
Previous reports have been made regarding the biological activity of such compounds but the quantities isolated here did not allow us to perform in-depth biological tests (e.g. paper disk diffusion tests, bioautography on thin plates or grapevine calli assays[2;99]).

Phomopsolide B (±) was previously isolated from another fungus of the *Phomopsis* genus, *P. oblonga*, frequently found in the outer bark of elm trees[62]. It has shown antiboring/antifeeding activity against the elm bark beetle (Scolytid beetle, *Scolytus* sp.)[62;100;101]. This insect is the vector of the fungus *Ceratocystis ulmi*, the responsible of Dutch elm disease, a pandemic disease that has killed over 40 million trees in North America (and Europe) since its propagation there.
The co-metabolite isolated with phomopsolide B, the furanone (**8**), displayed weaker activity in our leaf-disks test than compared to **7**. This could be caused by the fact that the ring is five membered. Indeed, Fukushima et al. isolated phomalactone (A) and a co-metabolite (B) (Figure 4.17) from a fungus showing herbicidal activity, *Nigrospora sacchari*[75]. Whereas

phomalactone displayed strong phytotoxic activity in leaf-puncture assays, the co-metabolite with the furanone ring was not so active. By applying a droplet of each compound to a puncture wound in leaves, 5 μg of phomalactone produced a 10 mm diameter necrotic lesion and B a 5 mm lesion both after 72 h. In whole plant assays, with barnyardgrass (*Echinochola crus-galli var. crus-galli),* green foxtail (*Setaria viridis*), slender amaranth (*Amaranthus virids*) and velvetleaf (*Abutilon theophrasti*), phomalactone caused rapid chlorosis and dessication. Fukushima et al..[75] postulated that, since B (Figure 4.17) was not so toxic and if both compounds opened by a C-O bond cleavage they would give the same chain, the ring structure of the metabolite played an important role in its phytotoxicity activity. It was also suggested that A (Figure 4.17) killed plants through cellular disruption resulting in an electrolytic leakage, in the same manner as dipyridinium and p-nitro-diphenyl ether herbicides do.

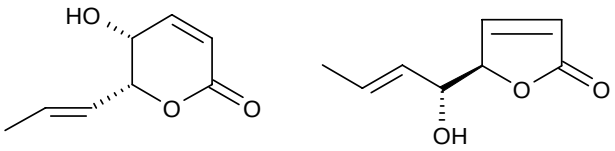

A
(Phomalactone)

B

Figure 4.17 Phomalactone (A) and its co-metabolite (B) isolated from *Nigrospora sacchari*

Therefore, although further studies should be made in order to verify this, the difference in necrosis that was observed in the leaf-disks assays with phomopsolide B and the furanone could be the result of a similar mode of action.

Sydowinin A (**1**) had already been isolated from a malt agar extract of a mould found in foodstuffs, *Aspergillus sydowi* [63], however no toxicity tests had been made. Despite the fact that the two xanthones showed slight activity, with approx. 30% of the leaves surface showing necrosis, previous studies have shown the potential of xanthones as active compounds from a pharmacological point of view[102]. However, it should be pointed out, that, to our knowledge, none produced by fungi have been reported to display phytotoxic effects.

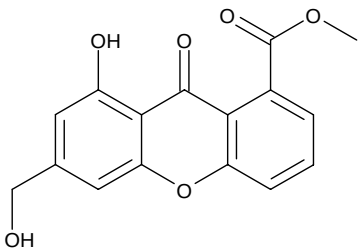

Figure 4.18 Sydowinin A (**1**)

Some xanthones have already been isolated from different *Phomopsis* species, like Phomoxanthones and dicerandrols produced by a *Phomopsis* sp. BC1323 and *Phomopsis longicolla* respectively.

Here is a short review of some of the pharmacological activities of some xanthones. They can possess antidepressant action and antitubercular activity, while xanthone glycosides exhibit depressant action[102]. The choleretic, diuretic, antimicrobial, antiviral and cardiotonic action of some xanthones has also been established[102]. Some xanthones are reported to possess antileukaemic, antitumour, antiulcer, antimicrobial, antihepatotoxic activities and their derivatives have also been shown to be effective as allergy inhibitors and bronchodilators in the treatment of asthma [102].

A series of isoprenylated xanthones isolated from Moraceous plants show interesting biological activities such as hypotensive effect, anti-rhinoviral activity, inhibition of the formation of some prostanoids and anti-tumour promoting activity. In a study of structure/activity relationships, it was found that some tetraoxygenated xanthones possess antiplatelet effects, and that the mechanism of action of 1,3,6,7-tetraoxygenated xanthones is due to both inhibition of thromboxane formation and phosphoinositide breakdown[102]. Recently, various bioactivities of xanthones including cytotoxic and antitumour activities, anti-inflammatory activity, antifungal activity, enhancement of choline acetyltransferase activity and inhibition of lipid peroxidase have been described[102].

Cytosporones D and E (Figure 4.19) isolated by Brady et al..[61] were reported to show antibacterial activity against *Staphylococcus aureus* (that can cause sepsis, meningitis, arthritis, pneumonia, etc), *Enterococcus faecalis* (a frequent cause of nosocomial infections), *Escherichia coli* and a fungus *Candida albicans*.

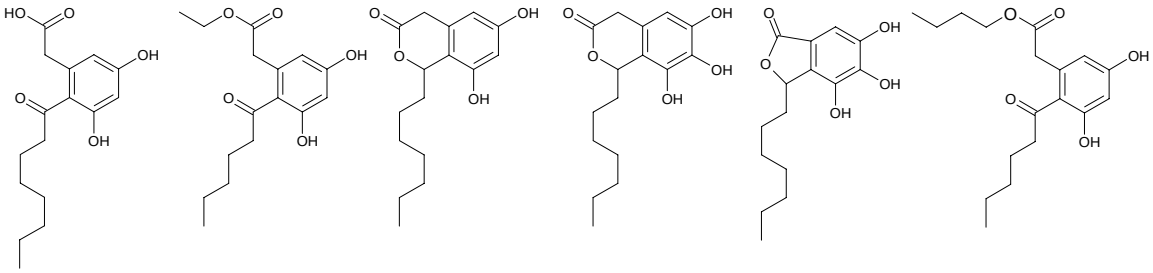

Figure 4.19 Cytosporones A-F

The importance of discovering new antibiotic compounds is even bigger if we take into account the fact that bacteria have been developing resistance to the available antibiotics. However two groups, Ohzeki et al..[103] and Hall et al..[104], synthesised cytosporones D and E and found only very weak activities for both compounds, cytosporone only showing effective antimicrobial activity against Gram-positive bacteria.
Further studies should be made with cytosporone F to assess if it is also toxic towards other grapevine parts (e.g. fruits, trunk) and also to check if it is produced by the fungus on grapevine.
The remaining metabolites that were isolated from our strains showed weak activity.

In conclusion, some of the isolated metabolites showed biological acitivity in leaf-disks assays, however at high concentrations. This is not enough to assume they are responsible for the excoriosis symptoms. The symptoms could be a reaction of the plant to the fungus. On green wood, *Ph. viticola* provokes necrosis (by a reaction of the plant) but does not sporulate or develop. On pruned wood, the fungus develop in and under the bark which whitens and pycnides are formed. Thus the plant reacts against the fungus and inhibits its growth.

4.7. *Phomopsis* chemotaxonomics

Traditionally, the taxonomy of fungi, lichens and plants has been based on morphology with other criteria coming into account also such as colour, toxins, volatiles profile, etc[105]. Secondary metabolite profiling has also been used as a complement to this as they were thought to be species-specific. Furthermore, it is also of interest for biotechnological reasons

as filamentous fungi are used as sources of chemicals for food ingredients, pharmaceuticals or enzymes. This type of work had been done for example by Frisvad et al.[106] by thin-layer chromatography (TLC) where strains of *Penicillium* were distinguished thanks to the different mycotoxins they produced, such as roquefortine C, ochratoxin A, chaetoglobosine, penicillic acid, etc.

Then metabolite profiling by HPLC-UV was also done by Frisvad in the 1980's[32;33;107]. However, since it has been possible to couple mass spectrometers to HPLC, this has proved to be a much more efficient technique. Now *Penicillium* species of the series *Viridicata* (*Penicillium* subgenus *Penicillium*) can be differentiated by direct infusion mass spectrometry [35;47;105] which shows how powerful the techniques have become.

As we have shown in the current work, detection limits are greatly reduced thanks to the very low detection limits achieved with mass spectrometers as compared to UV detectors. In the fungal cultures on wood, the metabolites were only detected by MS and not by UV since the signals of the compounds was too low to be detected.

Variations in *Phomopsis* isolates has been reported for various species, e.g. *P. oblonga*[108] and *P. viticola*[6;8;9;12;109]. In the case of the former, two distinct groups have been made (termed 'group one' and 'group two') based on morphological characteristics[108]. In the case of group one, isolates varied in colony colour, abundance and shape and size of conidiophores whereas in group two, the colony morphologies were uniform. Moreover, the mating systems were different and it was not possible to cross-fertilize the two groups. In short, the two groups could be regarded as different taxa.

As for *P. viticola*, we reported in the introduction (point 1.1) the taxonomic problems encountered with the identification of this fungus. Because of the character's plasticity, isolates show differences, in particular in cultural morphology and spore formation. These latter can be with or without guttules and can vary in shape and size.

Four of our strains were sent to the Belgian Co-ordinated Collections of Micro-organisms (BCCM) of the Catholic University of Louvain-la-Neuve in Belgium for identification (see also Material and Methods 2.1).

The strains were identified according to Moster et al.[8] as follows:

- Strain 180: *Phomopsis viticola* (Sacc.) Sacc.
- Strain 239: *Phomopsis viticola* complex

- Strain 281: *Phomopsis viticola* complex
- Strain 275: *Phomopsis* sp.

Strain 180 was identified as the typical type of strain found on *Vitis*, i.e. *P. viticola.*
Strains 239 and 281 were described as being "very similar, with the dimensions of α-conidia slightly bigger than those described for the typical *viticola* strain. The molecular biological analysis and sequencing of the ITS and 28S zones make it possible to note that the two samples have a succession of bases similar to that described by *Mostert* et al..[8] called *Phomopsis* sp. 2 and taken up in the *Phomopsis viticola* complex".
Strain 275 showed smaller α-conidia and shorter β-conidia than those described for the *viticola* species but molecular biological study did not give results that allowed for further identification of the strain.
The remaining strains could only be identified as being species belonging to the *Phomopsis* genus by D. Christen of the ETH in Zürich.

The following table briefly summarizes the strains in which these 5 metabolites were found and the strains species.

Table 4.1 The relationship between strains and some metabolites

Strain	Species	Metabolite				
		1 (Xanthone)	**2**	**5** (Cytosporone)	**7** (Phomopsolide B)	**8** (Furanone)
00	*Phomopsis* sp.				x	x
110	*Phomopsis* sp.				x	x
180	*Phomopsis viticola (Sacc.)*			x		
239	*Phomopsis v. complex*	x	x	x		
275	*Phomopsis* sp.				x	x
279	*Phomopsis* sp.			x		
281	*Phomopsis v.* complex		x	x		
282	*Phomopsis* sp.				x	x

283	*Phomopsis* sp.	x	x
301	*Phomopsis* sp.	x	x

It appears that the strains seem to be divided into two groups: the ones that produce the phomopsolide and the furanone (strains 00, 110, 275, 283, 301), those that produce either the cytosporone or the xanthones (180, 239, 279, 281). Thus, it would seem that two different biosynthetic pathways exist for the strains, leading to distinct groups of compounds. This variability in metabolite production could reflect the observation made by Crous et al.[12] regarding the diversity in *Phomopsis* isolates found on grapevines.

It would be interesting if further analyses by LC-MS of *Phomopsis* isolates could establish a relationship between the metabolites produced by the strain, the strain species and the eventual phytotoxicity of the strain. Indeed, usually classification is primarily based on morphology but the use of HPLC provides an effective system for a precise identification based on chemotaxonomic data[32;33;36]. Moreover, the coupling of HPLC to mass spectrometry greatly enhances the detection limits and thus the amount of information available greatly improves. This correlation could be established by using the simple experimental procedure used by Rawnsley[5;10] with grapevines canes (described in the introduction) to determine the virulence of the strains with also the LC-MS/MS method we employed here for the detection of the metabolites. However, there would be a limitation in the determination of the chemotaxonomics of a strain which is the variation in metabolite production by the strains. This point is discussed in the following section.

4.8. Variations in metabolite production

One of the problems when working with fungi can be the variation in metabolites production from one culture to another or even from one culture flask to another [60]. This has been the case with various fungi [60;110;111], with *Phomopsis* species[59;108], and also for *Phomopsis viticola* as found by Rawnsley et al.[5] and for the current study. As was mentioned earlier, not all metabolites were found in the ten strains and only three were found in the fungal grapevine wood cultures. Moreover, differences between culture batches at several months interval appeared with some metabolites lacking from the crude extracts of the fungus. This could be

due to a problem of adaptation of the fungus to the artificial medium and to mutations that can occur[2;31;60].

These chromatograms show evident dissimilarities which could be due to the fact that these are different species belonging to the *P. viticola* complex. This situation where strains of the same fungal species show very different biosynthetical pathways is not surprising as it is well documented that different isolates of a same fungus can be very different in the production of metabolites, even when collected from the same host plant [59;60]. Variability of metabolite production for one single isolate can also vary under a given set of fermentation conditions [59]. This could be the result of portions of the mycelium having different biochemical pathways and thus producing different compounds [60].

An example in variations in metabolite production was given by Horn et al. who investigated the production of phomopsolide B and phomodiol by *Phomopsis* isolates from willow trees (*Salix spp.*) and non-willow trees (*Heliconia mariae, Quercus prinus, Platanus occidentalis, Myrica pensylvanica, Liriodendron tulipiferae*) [59]. By collecting the isolates from different trees, in the US and in the UK (sometimes up to 27 isolates from one tree), they demonstrated how they produce different amounts of these two metabolites. The isolates were grown on millet and in malt extract broth. HPLC analysis of the strains showed that, out of the 52 isolates tested, 42% produced phomodiol (35% for the US isolates and 67% for the UK ones) from 1.0 to 125.0 μg/mL. Isolates from the same tree showed also variability. In the case of phomopsolide B, 92% of the isolates produced it, in quantities ranging from 0.1 to 289.18 μg/mL. A flask to flask experiment showed that the production of phomopsolide B by one single isolate varied from 4.37 to 34.19 μg/mL.

The importance of the medium on which the fungus was grown was also demonstrated since phomodiol was only produced on corn and millet media but not in a malt extract broth. A similar observation was made by Stierle et al. who noted that production of Phomopsolide B and other metabolites isolated from a *Penicillium* sp. varied when grown either in a glucose-soytone broth or in a glucose-soytone-$Mg_3(PO_4)_2$ broth[111]. The difference was only of 1.5 times for phomopsolide B but 11 times for another metabolite.

Nicolet[110] isolated from a strain of *Stagonospora* sp. leptosphaeradione when it was grown on a potato dextrose broth and elsinochrome A when grown on V8 media.

These examples show the importance and limitations of artificial culture media when growing fungi as they can influence not only the amount of metabolites produced but also the biosynthetic pathways. As the goal is to discover which compounds are responsible for the symptoms observed for excoriosis, it seems natural to employ media that are as close as possible to the natural conditions in order to be sure that the same ones are produced on the plant[3]. This is why we performed tests by growing the fungus on grapevine wood and indeed three of the compounds isolated from the PDA medium were detected in the wood extracts.
Nonetheless, further studies using sentient plants are still necessary in order to verify if the secondary metabolites production is unchanged compared to the cultures on artificial media.
This can be problematic since the lack of predictability in metabolite production can have implications for programs that screen fungi for biological activity. Indeed, some metabolites could be missed in flasks that have an unusually small production [59;107].

These variations explain the difficulties encountered during this work when trying to re-isolate compounds, in order to have sufficient quantities for NMR analysis, from different culture batches of the strains.
However, this might not be too much of a problem for a LC-MS screening programm since only one culture batch would be needed and the strain would not have to be grown on artificial media for several months by subcultures, thus reducing the risks of eventual changes in the metabolic pathway of the strain.

5. Summary and conclusions

During our study of the pathogenic fungus *P. viticola*, nine metabolites **1-9** were isolated, all for the first time for this fungus. Among these, five of them, **2**, **4, 5, 6, 8** are new natural compounds.

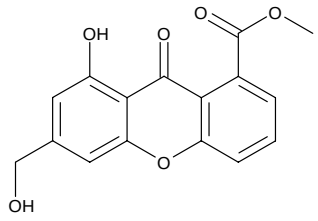

1

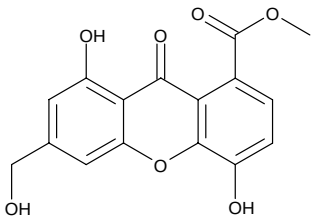

2

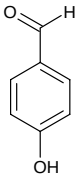

3

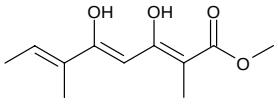

4

5

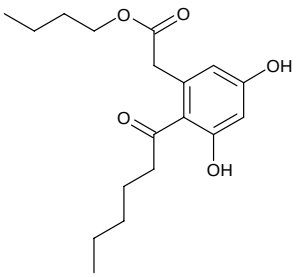

6

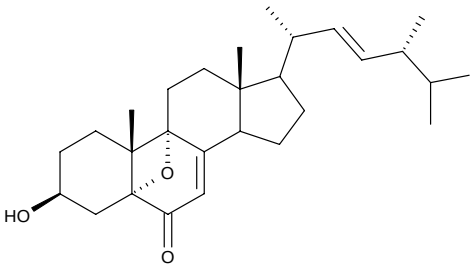

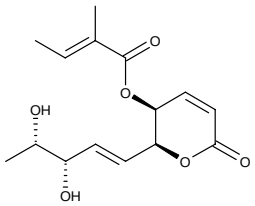

7

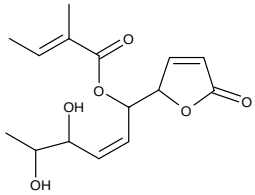

8

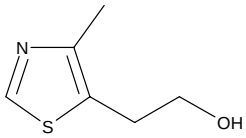

9

Future work could continue the investigation on isolation since more metabolites were isolated but their structure not elucidated due to the lack of quantity.

Leaf-disks assays showed that five compounds (**1**, **2**, **5**, **7**, **8**) were biologically active, two of them (**5** & **7**) showing necrosis of the leaves, however at high concentrations. Taking into account previous studies made on these compounds, or related compounds of the same families, they could show interesting biological and/or pharmaceutical activities. However, the quantities isolated here were not sufficient for in-depth study what should be done in further studies.

LC-MS analysis allowed for the detection of three compounds, **1**, **2** and **3,** in an experiment involving dry grapevine wood inoculated with a strain of the fungus. This showed that, despite the change in culture medium, the biological pathways of the fungus were the same so these metabolites will probably also be produced *in vivo* on grapevine plants. Compound **5** was not detected however it might be possible that it takes longer for the fungus to start producing it. A kinetic test showed that **2** and **5** were still produced on PDA Petri dishes after 5 weeks, so their toxicity could also be the result of an accumulation during summer when the fungus is latent.

LC-MS/MS analysis of all the studied strains showed that not all compounds were present suggesting that the different *Phomopsis* strains collected belonged to different species and therefore had different biological pathways. One of them leads to two groups of compounds, either **1**, **2** and/or **5** whereas the second one leads to **7** and **8**.
Hence, as the taxonomic classification of the different *Phomopsis* species found on grapevine plants is still the subject of debate, future work on this subject could use these compounds as chemical markers to help in differentiating them. Managing to differentiate the species would help grapegrowers and winemakers for control strategies of the fungi. An example is the fact that chemical sprays are not required to control *Diaporthe* (that belongs to the *P. viticola* complex) since it does not cause damage to the cultures.
Accumulating data with different isolates of *Phomopsis* species collected from different plants and from different geographical locations could hence help to clear up the taxonomic classification. This is not only important for biologists but also for grapegrowers and winemakers around the world. Indeed, it is important to know which fungi infects the plants in order to manage them adequately. This would prevent growers from unnecessary application of chemicals in the vineyards therefore reducing the chemicals in the industry, which would be economically and ecologically beneficial. Thus getting a clear view of the relationship fungus/symptoms caused is crucial in order to achieve better control strategies.

6. Bibliography

(1) Pearson, R. C.; Goheen, A. C. *Compendium of grape diseases* **1998**.

(2) Mendgen, K.; Deising, H. *New Phytologist* **1993**, *124*, 193-213.

(3) Grayer, R. J.; Kokubun, T. *Phytochemistry* **2001**, *56*, 253-263.

(4) Melanson, D. L.; Rawnsley, B.; Scheper, R. W. A. *Australasian Plant Pathology* **2002**, *31*, 67-73.

(5) Rawnsley, B.; Wicks, T. J.; Scott, E. S.; Stummer, B. E. *Plant Disease* **2004**, *88*, 1005-1010.

(6) Phillips, A. J. L. *Mycologia* **1999**, *91*, 1001-1007.

(7) Phillips, A. J. L. *Phytopathologia Mediterranea* **2000**, *39*, 341-356.

(8) Mostert, L.; Crous, P. W.; Kang, J. C.; Phillips, A. J. L. *Mycologia* **2001**, *93*, 146-167.

(9) Phillips, A. J. L. *Journal of Phytopathology-Phytopathologische Zeitschrift* **1998**, *146*, 327-332.

(10) Rawnsley, B. *PhD Thesis, University of Adelaide, South Australia* **2002**.

(11) Rawnsley, B.; Wicks, T. J.; Scott, E. S.; Stummer, B. E. *The Australian & New Zealand grapegrower & winemaker* **2002**, *464*, 30-35.

(12) van Niekerk, J. M.; Groenewald, J. Z.; Farr, D. F.; Fourie, P. H.; Halleen, F.; Crous, P. W. *Australasian Plant Pathology* **2005**, *34*, 27-39.

(13) Mendgen, K.; Hahn, M.; Deising, H. *Annual Review of Phytopathology* **1996**, *34*, 367-386.

(14) Pezet, R.; Pont, V. *Science* **1977**, *196*, 428-429.

(15) Pezet, R.; Pont, V. *Bulletin de la Société Botanique Suisse* **1977**, *87*, 154-162.

(16) Pezet, R. *Revue Suisse Viticole Arboricole et Horticole* **1976**, *8*, 19-26.

(17) Pezet, R.; Ducrot, V. *Revue Suisse Viticole Arboricole et Horticole* **1978**, *10*, 281-284.

(18) Jailloux, F.; Bugaret, Y.; Froidefond, G. *Crop Protection* **1987**, *6*, 148-152.

(19) Erincik, O.; Madden, L. V.; Ferree, D. C.; Ellis, M. A. *Plant Disease* **2001**, *85*, 517-520.

(20) Erincik, O.; Madden, L. V.; Ferree, D. C.; Ellis, M. A. *Plant Disease* **2003**, *87*, 832-840.

(21) Pezet, R. *Phytopathologische Zeitschrift* **1974**, *79*, 67-76.

(22) *Bulletin OEPP/EPPO Bulletin* **2002**, *32*, 371-392.

(23) Rodrigues, K. F.; Hesse, M.; Werner, C. *Journal of Basic Microbiology* **2000**, *40*, 261-267.

(24) Horn, W. S.; Schwartz, R. E.; Simmonds, M. S. J.; Blaney, W. M. *Tetrahedron Letters* **1994**, *35*, 6037-6040.

(25) Tsantrizos, Y. S.; Ogilvie, K. K.; Watson A.K. *Canadian Journal of Chemistry* **1992**, *70*, 2276-2284.

(26) Wagenaar, M. M.; Clardy, J. *Journal of Natural Products* **2001**, *64*, 1006-1009.

(27) Horn, W. S.; Simmonds, M. S. J.; Schwartz, R. E.; Blaney, W. M. *Tetrahedron* **1995**, *51*, 3969-3978.

(28) Namikoshi, M.; Kobayashi, H.; Yoshimoto, T.; Hosoya, T. *Journal of Antibiotics* **1997** , *50*, 890-892.

(29) Isaka, M.; Jaturapat, A.; Rukseree, K.; Danwisetkanjana, K.; Tanticharoen, M.; Thebtaranonth, Y. *Journal of Natural Products* **2001**, *64*, 1015-1018.

(30) Wrigley, S. K.; Sadeghi, R.; Bahl, S.; Whiting, A. J.; Ainsworth, A. M.; Martin, S. M.; Katzer, W.; Ford, R.; Kau, D. A.; Robinson, N.; Hayes, M. A.; Elcock, C.; Mander, T.; Moore, M. *Journal of Antibiotics* **1999**, *52*, 862-872.

(31) Demain, A. L.; Fang, A. *Advances in biochemical engineering/biotechnology 69*, 1-39.

(32) Frisvad, J. C.; Thrane, U. *Jourmal of Chromatography* **1987**, 195-214.

(33) Frisvad, J. C.; Filtenborg, O.; Thrane, U. *Archives of Environmental Contamination and Toxicology* **1989**, *18*, 331-335.

(34) Krohn, K.; Michel, A.; Romer, E.; Florke, U.; Aust, H. J.; Draeger, S.; Schul, B.; Wray, V. *Natural Product Letters* **1995**, *6*, 309-314.

(35) Smedsgaard, J.; Frisvad, J. C. *Journal of Microbiological Methods* **1996**, *25*, 5-17.

(36) Zhou, S.; Hamburger, M. *Journal of Chromatography A* **1996**, *755*, 189-204.

(37) Nielsen, K. F.; Thrane, U. *Journal of Chromatography A* **2001**, *929*, 75-87.

(38) Landreau, A.; Pouchus, Y. F.; Sallenave-Namont, C.; Biard, J. F.; Boumard, M. C.; Robiou du Pont, T.; Mondeguer, F.; Goulard, C.; Verbist, J. F. *Journal of Microbiological Methods* **2002**, *48*, 181-194.

(39) Thomson, B. A. *Journal of the American Society of Mass spectrometry* **1998**, *9*, 187-193.

(40) Hostettmann, K.; Wolfender, J.-L. *Pesticide Science* **1997**, *51*, 471-482.

(41) Cech, N. B.; Enke, C. G. *Mass Spectrometry Reviews* **2001**, *20*, 362-387.

(42) Herderich, M.; Richling, E.; Roscher, R.; Schneider, C.; Schwab, W.; Humpf, H.-U.; Schreier, P. *Chromatographia* **1997**, *45*, 127-132.

(43) Strege, M. A. *Jourmal of Chromatography B* **1999**, *725*, 67-78.

(44) Guilhaus, M. *Journal of Mass Spectrometry* **1995**, *30*, 1519-1532.

(45) Mamyrin, B. A. *International Journal of Mass Spectrometry* **2001**, *206*, 251-266.

(46) Amster, I. J. *Journal of Mass Spectrometry* **1996**, *31*, 1325-1337.

(47) Van Berkel, G. J. *Journal of Mass Spectrometry* **2000**, *35*, 773-783.

(48) Kebarle, P.; Peschke, M. *Analytica Chimica Acta* **2000**, *406* , 11-35.

(49) Cole, R. B. *Journal of Mass Spectrometry* **2000**, *35*, 763-772.

(50) Gaskell, S. J. *Journal of Mass Spectrometry* **1997**, *32*, 677-688.

(51) Ikonomou, M. G.; Blades, A. B.; Kebarle, P. *Analytical Chemistry* **1991**, *63*, 1989-1998.

(52) Kebarle, P.; Ho, Y. *Electrospray ionization mass spectrometry: Fundamentals, instrumentation and applications* ; John Wiley & Sons: New-York: 1997.

(53) Kebarle, P. *Journal of Mass Spectrometry* **2000**, *35*, 804-817.

(54) de la Mora, J. F.; Van Berkel, G. J.; Enke, C. G.; Cole, R. B.; Martinez-Sanchez, M.; Fenn, J. B. *Journal of Mass Spectrometry* **2000**, *35*, 939-952.

(55) Hanold, K. A.; Fischer, S. M.; Cormia, P. H.; Miller, C. E.; Syage, J. A. *Analytical Chemistry* **2004**, *76*, 2842-2851.

(56) Raffaelli, A.; Saba, A. *Mass Spectrometry Reviews* **2003**, *22*, 318-331.

(57) Robb, D. B.; Covey, T. R.; Bruins, A. P. *Analytical Chemistry* **2000**, *72*, 3653-3659.

(58) Syage, J. A. *Journal of the American Society for Mass Spectrometry* **2004**, *15*, 1521-1533.

(59) Horn, W. S.; Simmonds, M. S. J.; Schwartz, R. E.; Blaney, W. M. *Mycologia* **1996**, *88*, 588-595.

(60) Turner, W. B. *Fungal Metabolites*; 1971; p 446.

(61) Brady, S. F.; Wagenaar, M. M.; Singh, M. P.; Janso, J. E.; Clardy, J. *Organic Letters* **2000**, *2*, 4043-4046.

(62) Grove, J. F. *Journal of the Chemical Society-Perkin Transactions 1* **1985**, 865-869.

(63) Hamasaki, T.; Sato, Y.; Hatsuda, Y. *Agricultural and Biological Chemistry* **1975**, *39*, 2341-2345.

(64) Hamasaki, T.; Sato, Y.; Hatsuda, Y. *Agricultural and Biological Chemistry* **1975**, *39*, 2337-2340.

(65) Ayer, W. A.; Browne, L. M.; Lin, G. *Journal of Natural Products* **1989**, *52*, 119-129.

(66) Carvalho, M. J.; Carvalho, L. M.; Ferreira, A. M.; Silva, A. M. S. *Natural Product Research* **2003**, *17*, 445-449.

(67) Fernandes, E. G. R.; Silva, A. M. S.; Cavaleiro, J. A. S.; Silva, F. M.; Borges, M. F. M.; Pinto, M. M. M. *Magnetic Resonance in Chemistry* **1998**, *36*, 305-309.

(68) Frahm, A. W.; ChaudhuriI, R. K. *Tetrahedron* **1979**, *35*, 2035-2038.

(69) Pickert, M.; Frahm, A. W. *Archiv der Pharmazie* **1998**, *331*, 177-192.

(70) Santos, L. C.; Piacente, S.; De Riccardis, F.; Eletto, A. M.; Pizza, C.; Vilegas, W. *Phytochemistry* **2001**, *56*, 853-856.

(71) Yang, S. P.; Xu, J.; Yue, J. M. *Chinese Journal of Chemistry* **2003**, *21*, 1390-1394.

(72) Aiello, A.; Fattorusso, E.; Magno, S.; Menna, M. *Steroids* **1991**, *56*, 337-340.

(73) Wright, J. L. C.; McInnes, A. G.; Shimizu, S.; Smith, D. G.; Walter, J. A. *Canadian Journal of Chemistry* **1978**, *56*, 1898-1903.

(74) Ishizuka, T.; Yaoita, Y.; Kikuchi, M. *Chemical & Pharmaceutical Bulletin* **1997**, *45*, 1756-1760.

(75) Fukushima, T.; Tanaka, M.; Gohbara, M.; Fujimori, T. *Phytochemistry* **1998**, *48*, 625-630.

(76) Budzikiewicz, H.; Djerrassi, C.; Williams, D. H. *Mass spectrometry of organic compounds*; Holden-Day, Inc: 1967.

(77) Porter, Q. N. *Mass spectrometry of heterocyclic compounds*; John Wiley & Sons: 1985.

(78) Bennett, J. W. *Canadian Journal of Botany* **1995**, *73*, S917-S924.

(79) Desjardins, A. E.; Hohn, T. M. *Molecular Plant-Microbe Interactions* **1997**, *10*, 147-152.

(80) Frisvad, J. C. *Archives of Environmental Contamination and Toxicology* **1989**, *18*, 452-467.

(81) Knaggs, A. R. *Natural Product Reports* **2001**, *18*, 334-355.

(82) Lapadatescu, C.; Ginies, C.; Le Quere, J. L.; Bonnarme, P. *Applied and Environmental Microbiology* **2000**, *66*, 1517-1522.

(83) Mannito, P. Biosynthesis of natural products; Wiley, J., ed. 1981; pp 200-202.

(84) Gordon Hill, J.; Nakashima, T. T.; Vederas, J. C. *Journal of the American Chemical Society* **1982**, *104*, 1745-1748.

(85) Bruneton, J. *Pharmacognosie - Phytochimie des plantes médicinales*; Technique et documentation - Lavoisier: 1993.

(86) Kachi, H.; Sassa, T. *Agricultural and Biological Chemistry* **1986**, *50*, 1669-1671.

(87) Henry, K. M.; Townsend, C. A. *Journal of the American Chemical Society* **2005**, *127*, 3724-3733.

(88) Simpson, T. J. *Natural Product Reports* **1991**, *8*, 573-602.

(89) Henry, K. M.; Townsend, C. A. *Journal of the American Chemical Society* **2005**, *127*, 3300-3309.

(90) Sassa, T. *Agricultural and Biological Chemistry* **1991**, *55*, 95-99.

(91) Brereton, R. G.; Garson, M. J.; Staunton, J. *Journal of the Chemical Society-Perkin Transactions 1* **1984**, 1027-1033.

(92) Evans, R. H.; Ellested, G. A.; Kunstmann, M. P. *Tetrahedron Letters* **1969**, *22*, 1791-1794.

(93) Dickinson, J. M. *Natural Product Reports* **1993**, *73*.

(94) White, R. L.; Spenser, I. D. *Journal of the American Chemical Society* **1982**, *104*, 4934-4943.

(95) White, R. L.; Spenser, I. D. *Journal of the American Chemical Society* **1979**, *101*, 5102-5104.

(96) Harris, D. L. *Archives of Biochemistry and Biophysics* **1955**, *57*, 240-251.

(97) Leonian, L. H.; Lilly, V. G. *Plant physiology* **1940**, *15*, 515-525.

(98) Young, D. W. *Natural Product Reports* **1986**, *3*, 395-419.

(99) Hadacek, F.; Greger, H. *Phytochemical Analysis* **2000**, *11*, 137-147.

(100) Begley, M. J.; Grove, J. F. *Journal of the Chemical Society Perkin Transaction 1* **1985**, 861-863.

(101) Claydon, N.; Grove, J. F.; Pople, M. *Phytochemistry* **1985**, *24*, 937-943.

(102) Peres, V.; Nagem, T. J.; de Oliveira, F. F. *Phytochemistry* **2000**, *55*, 683-710.

(103) Ohzeki, T.; Mori, K. *Bioscience Biotechnology and Biochemistry* **2003**, *67*, 2584-2590.

(104) Hall, J. D.; Duncan-Gould, N. W.; Siddiqi, N. A.; Kelly, J. N.; Hoeferlin, L. A.; Morrison, S. J.; Wyatt, J. K. *Bioorganic & Medicinal Chemistry* **2005**, *13*, 1409-1413.

(105) Smedsgaard, J.; Nielsen, J. *Journal of Experimental Botany* **2005**, *56*, 273-286.

(106) Frisvad, J. C.; Filtenborg, O. *Applied and Environmental Microbiology* **1983**, *46*, 1301-1310.

(107) Frisvad, J. C. *Botanical Journal of the Linnean Society* **1989**, *99*, 81-95.

(108) Brayford, D. *Mycological Research* **1990**, *94*.

(109) Mostert, L.; Crous, P. W.; Petrini, O. *Sydowia* **2000**, *52*, 46-58.

(110) Nicolet-dit-Felix, B. *PhD Thesis (University of Neuchâtel)* **1999**.

(111) Stierle, D. B.; Stierle, A. A.; Ganser, B. *Journal of Natural Products* **1997**, *60*, 1207-1209.